Water Transfer and Insulation Dynamic of Green Roofs with Coarse Recycled Materials

A Thesis Submitted in Partial Fulfillment of Requirements for the Joint Degree of Doctor of Philosophy in

ENGINEERING SCIENCE AND TECHNOLOGY (University of Liège)

by

Mostafa Kazemi

Jury Members:

Jacques TELLER	University of Liège (President of Jury)
Griet VERBEECK	Hasselt University (Jury Member)
Elodie PRUD'HOMME	INSA Lyon (Jury Member)
Frédéric COLLIN	University of Liège (Jury Member)
Shady ATTIA	University of Liège (Co-supervisor)
Luc COURARD	University of Liège (Supervisor)

Academic year 2023-2024

Author's contact details

Mostafa Kazemi

GeMMe Building Materials, Urban and Environmental Engineering (UEE), Faculty of Applied Sciences, University of Liège, 4000, Liège, Belgium

-1/434, B52 Quartier Polytech 1, Allée de la Découverte 9, 4000 Liège, Belgium

Email : mostafa.kazemi@uliege.be, kazemi.civil68@gmail.com

Acknowledgment

I would like to express my sincere gratitude to my supervisor, Prof. Luc Courard, for entrusting me with the responsibility and for his consistent support and precious guidance during the running of this project. Your knowledge, expertise and commitment have been truly inspiring. I also would like to give my special thanks to my co-supervisor, Prof. Shady Attia, without your valuable help and wise guidance this project would have not been the same!

I appreciate the effort and the spirit of teamwork among CityRoof's partners: Prof. Grégory Mahy, Prof. Jacques Teller, Lucie Rivière and Mitali Yeshwant Joshi. Thank you for your valuable support and fruitful collaborations. Additionally, I would like to acknowledge the jury and thesis committee members for their time, insightful criticism and remarks, which improved the thesis in various aspects.

During my research project at the University of Liège, I was surrounded by a team of pleasant colleagues, friends and lab members. I would like to mention Frédéric Michel, Amaury Daras, Pierre Illing, Julien Hubert, Philbert Nshimiyimana, Zengfeng Zhao, Sophie Grigoletto, Monique Denotte, Véronique Szepetiuk, Fabienne Libioulle, Yeakleang Muy, Imad Eddine Kanjo, Mousa Ka, Bao Minh Phuong, Yoan Van Puyvelde, Lucile Hennaut, Céline Van Puyvelde. Thank you so much for your valuable support through every step of my research work.

I would like to express my deepest and sincere gratitude to my beloved parents, Ali and Leila for their invaluable love, unwavering support and encouragement. I cannot thank you enough for everything you have done for me. I also would like to wholeheartedly thank my lovely sister, Maryam for her kindness and emotional support all through my life.

My sincere gratitude goes to my dear friends during my PhD in Belgium. I would like to mention Alireza (both), Ali, Hesam, Ramin and Enrico. Thank you for the kindness, support, humor and fun that you shared with me in my personal life. Every day's interactions with you made me not feel far from home. I also would like to thank my other best friends despite the long distance between us.

During my PhD study, I met many people and learned a lot from not only in my research work but also in my personal life. I would like to express my gratitude to them for their support, help and encouragement.

Thank you to you all!

Summary

Replacing natural materials with recycled and artificial materials for green roof systems with drainage and substrate layers can be considered as a potential solution to reduce the overuse of natural resources. However, assessing the thermal resistance, water permeability, water retention capacity and rainfall detention performance of green roof layers, including recycled and artificial materials has received less attention. Also, there is a lack of precise understanding of the performance of green roofs including artificial and recycled materials under future climate changes. Moreover, it is required to assess how the thermal resistance of green roof layers is sensitive to specific properties of artificial and recycled materials. To deepen the understanding of these critical issues, this thesis provides analytical, experimental and modeling studies on the use of recycled and artificial materials for substrate and drainage layers of green roof systems.

The thesis first presents selected materials for the green roof layers based on some criteria. The substrate with recycled coarse materials (SP) was proposed for the substrate layer and its results were compared with those of substrate without recycled coarse materials (SC). For the drainage layer, the results of Recycled Coarse Aggregate (RCA), Incinerated Municipal Solid Waste Aggregate (IMSWA) and Lightweight Expanded Clay Aggregate (LECA) were compared with those of Natural Coarse Aggregate (NCA). After that, three leading indicators as dependent variables are measured for green roof systems: Rc-value as heat resistance indicator, water permeability as water drainage indicator and water retention capacity as water holding indicator. The results of substrate materials showed that although the water permeability and water retention capacity of SC are more than that of SP, the results of both were within the range of FLL guidelines. Also, the thermal resistance of SC is marginally more than that of SP. Regarding the thermal resistance of drainage materials, LECA obtains the highest value and the results of NCA, IMSWA and RCA are nearly the same.

Further experimental research on the rainfall detention performance of green roof including coarse recycled materials is then presented. According to the results, the rainfall detention of green roofs without coarse recycled materials was marginally higher than that of green roofs containing coarse recycled materials.

The hygrothermal performance of green roof models including recycled coarse materials is then presented to assess the heat and moisture transfer within substrate and drainage layers. The results showed that 6-cm drainage layer and 18-cm substrate layer are the best designs to provide sufficient heat resistance for the green roof systems.

Further modeling research on the hygrothermal performance of green roof models under the temperate climate of Liège city is then presented, according to 3 weather scenarios: beginning, middle and end of the 21st century. Also, the heat flux sensitivity to the thickness and physical characteristics of green roofs with artificial and recycled materials is assessed. According to the results, the heat resistance of green roof models made of artificial and recycled materials increased for scenario 3 in comparison to scenarios 1 and 2 during the summer and the beginning of autumn due to a drop in the rainfall pattern till the end of the 21st century. The entire parameters change in the sensitivity analysis showed that the scatter of the thermal conductivity, layer thickness and density affects the dispersion of heat flux for the green roof layers.

Résumé

Le remplacement des matériaux naturels par des matériaux recyclés et artificiels dans les structures de toitures vertes peut être considéré comme une solution potentielle pour réduire la surutilisation des ressources naturelles dans les couches de drainage et de substrat. Cependant, l'évaluation de l'impact du remplacement sur la résistance thermique, la perméabilité à l'eau, la capacité de rétention d'eau et les performances de rétention des précipitations dans les différentes couches est peu étudiée. En outre, il existe un manque de compréhension précise des performances des toitures vertes, y compris avec des matériaux artificiels et recyclés, face aux futurs changements climatiques. Enfin, il est nécessaire d'évaluer dans quelle mesure la résistance thermique des couches de toiture verte est sensible aux propriétés spécifiques des matériaux artificiels et recyclés.

Pour approfondir la compréhension de ces questions critiques, cette thèse propose des études analytiques, expérimentales et de modélisation sur l'utilisation de matériaux recyclés et artificiels pour les couches de substrat et de drainage des systèmes de toitures vertes.

La thèse présente d'abord les matériaux sélectionnés pour les couches de toiture verte sur base de critères spécifiques. Des matériaux grossiers de béton recyclés (SP) ont été proposés pour la couche de substrat et les résultats ont été comparés à ceux d'un substrat sans matériaux grossiers recyclés (SC). Pour la couche de drainage, les granulats grossiers de béton recyclés (RCA), des granulats de déchets d'incinérateur d'ordures ménagères (IMSWA) et des granulats d'argile expansés légers (LECA) ont été comparés avec des granulats grossiers naturels (NCA). Ensuite, trois indicateurs (variables dépendantes) sont mesurés pour les systèmes de toitures vertes : la valeur Rc comme indicateur de résistance thermique, la perméabilité à l'eau comme indicateur d'évacuation de l'eau et la capacité de rétention d'eau comme indicateur de rétention d'eau. Les résultats sur les matériaux utilisés pour le substrat ont montré que, bien que la perméabilité à l'eau et la capacité de rétention d'eau du SC soient supérieures à celles du SP, les résultats se situaient pour les deux matériaux dans la plage des directives FLL. De plus, la résistance thermique du SC est légèrement supérieure à celle du SP. Concernant la résistance thermique des matériaux de drainage, LECA permet d'obtenir la valeur la plus élevée et les résultats de NCA, IMSWA et RCA sont presque les mêmes.

D'autres recherches expérimentales sur les performances de rétention des précipitations des toitures vertes incluant des matériaux grossiers recyclés sont ensuite présentées. Selon les résultats, la rétention des précipitations sur les substrats sans les matériaux grossiers recyclés était légèrement supérieure à celle des toitures vertes contenant des matériaux grossiers recyclés.

La performance hygrothermique des modèles de toitures vertes incluant des matériaux grossiers recyclés est ensuite présentée afin d'évaluer le transfert de chaleur et d'humidité au sein des couches de substrat et de drainage. Les résultats ont montré qu'une couche de drainage de 6 cm et une couche de substrat de 18 cm sont les meilleures conceptions pour fournir une résistance thermique suffisante.

Une modélisation des performances hygrothermiques des toitures vertes sous le climat tempéré de la ville de Liège est ensuite présentée, sur base de 3 scénarios météorologiques : début, milieu et fin du 21e siècle. En outre, la sensibilité du flux thermique à l'épaisseur et aux caractéristiques physiques des systèmes constitués de matériaux artificiels et recyclés est évaluée. Selon les résultats, la résistance thermique des toitures vertes réalisées à partir de matériaux artificiels et recyclés a augmenté pour le scénario 3, par rapport aux scénarios 1 et 2 pendant l'été et le début de l'automne

en raison d'une baisse du régime des précipitations jusqu'à la fin du 21e siècle. L'analyse de sensibilité a montré que la variation de la conductivité thermique, de l'épaisseur et de la densité affecte le flux thermique dans les différentes couches de la toiture verte et que les matériaux recyclés restent performants.

Forward

This thesis has been realized in the framework of ARC CityRoof project, funded by the University of Liège. CityRoof research project involves developing green roofs to provide ecosystem services in urban areas. The project contributes to the sustainable development of the built environment through the integration of recycled materials into green roofs. The potential impact of green roofs on the urban heat island effect as well as on water runoff is evaluated at the urban scale.

The results of the thesis have been completed by the investigations of other CityRoof's PhD researchers: Lucie Rivière and Mitali Yeshwant Joshi. The main objective of L. Rivière was to assess the capacity of extensive green roofs to develop analogous habitats for native dry grassland biodiversity. Also, L. Rivière aimed to evaluate the influence of functional traits of vegetation and substrate types including recycled materials on runoff from extensive green roofs. The main objective of M. Y. Joshi was to assess the potential of analogous green roofs at a city scale in Liège in regulating microclimate and strengthening the ecological networks.

Considering the aim of L. Rivière on the functional traits' effect of vegetation on runoff from extensive green roofs, this thesis evaluated the rainfall detention performance of green roof layers including coarse recycled materials without the presence of vegetation coverage. Also, the thermal performance, water retention capacity and water permeability of extensive green roof layers including recycled and artificial coarse materials were assessed in this thesis. On the other hand, along with the microclimate studies of M. Y. Joshi on analogous green roofs, this thesis assessed the influence of using artificial and recycled materials on green roof performance under the temperate climate of Liège city till the end of the 21st century.

Table of contents

List of Figures

List of Tables

List of Notations

A	cross-sectional area of specimen
A_1	water absorption coefficient
b_1	moisture-induced heat conductivity supplement
d_f	degrees of freedom
D_w	diffusion coefficients of water vapour in building materials
D_{ws}	liquid transport coefficient for suction
D_{ww}	liquid transport coefficient for redistribution
D_{w0}	diffusion coefficient of water vapour in air
D_v	water vapour permeability
k	water permeability
i	hydraulic gradient
L	thickness of green roof layers
m	minimum required measurement period
M	water vapour molecular weight
n	sample number
P	pressure
P_{in}	pressure inside of the container
P_L	ambient atmospheric pressure
P_{out}	pressure outside of the container
P_0	standard pressure
R	molar gas constant
R_A	water vapour resistance of the air gap between the specimen and the salt solution
S	area of the side immersed in water
S_p	pooled standard deviation
t	time interval
T	temperature
T_c	temperature in the thermal device's cooling side
T_h	temperature in the thermal device's heating side
q	heat flow rate
Q	flow rate
v	discharge velocity
W	water content
W_f	free water content
W_{max}	maximum water content
W_{80}	reference water content
$\bar{x}_1$	first group of material
$\bar{x}_2$	second group of material
$\frac{\Delta G}{\Delta t}$	water vapour permeability rate
Δh	water head difference
Δm	difference between the weight of dry specimen and wet specimens during testing
ΔP	difference in water vapour pressure between the ambient air and the salt solution
ΔT	difference between the top and bottom surfaces of specimen
θ	temperature
Λ	water vapour permeance
λ	thermal conductivity

$\lambda(w)$	thermal conductivity of materials in moist condition
λ_0	thermal conductivity of materials in wet condition
μ	water vapour diffusion resistance factor
μ_1	mean of the distribution
ρ_s	density
σ	standard deviation
φ	relative humidity

List of Abbreviations

COV	Coefficient Of Variation
IMSWA	Incinerated Municipal Solid Waste Aggregate
LECA	Lightweight Expanded Clay Aggregate
NCA	Natural Coarse Aggregate
RCA	Recycled Coarse Aggregate
RH	Relative Humidity
SC	Substrate without coarse recycled materials (Control Substrate)
SD	Standard Deviation
SP	Substrate with coarse recycled materials (Proposed Substrate)
T	Temperature
TMY	Typical Meteorological Year

Chapter 1: Introduction

1.1. Introduction

The use of green roofs has frequently been recommended for rooftops to make buildings more sustainable and reduce the detrimental environmental consequences of construction manufacturing industries (M. Zhao & Srebric, 2012). The green roof is renowned for being a sustainable ecosystem that can sometimes provide thermal resistance for rooftops and buffer surface stormwater runoff in urban areas (Fachinello Krebs & Johansson, 2021; Ma'bdeh et al., 2022; Ouldboukhitine et al., 2012; Schade et al., 2021; Vilar et al., 2021). According to the thickness of green roof systems, it can be classified into three categories: intensive, semi-intensive and extensive. Intensive and semi-intensive green roof systems are used for roof gardens, parks and free spaces in cites (Bianchini & Hewage, 2012). However, they can cause to overload buildings with low load bearing capacity because of their deeper substrate and drainage solutions compared to extensive green roof. Therefore, the extensive green roof has drawn the attention of researchers for rooftops of buildings and houses due to its shallower depth (about 20 cm) and lighter weight than other categories of green roofs (Oberndorfer et al., 2007). Generally, the possibility of using green roof systems depends on the load-bearing capacity of rooftops. For instance, the load-bearing capacity of 230 kg/m^2 is reported for some case studies in Liège city to use green roof systems (Rohon, 2017). As shown in Fig. 1.1, extensive green roofs include vegetation**,** substrate, thin filter, drainage and insulation layers (Tabares-Velasco et al., 2012).

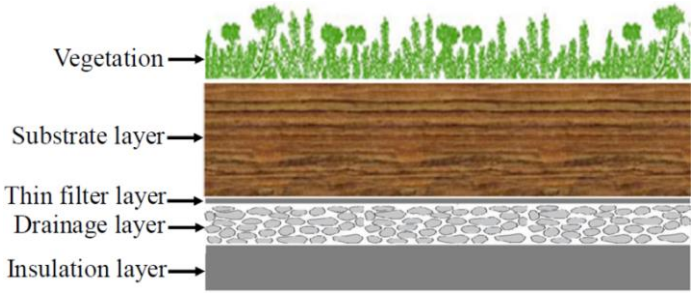

Fig. 1. 1. A cross-sectional view of green roof layers.

Normally, the Rc-value of green roof systems should be about 4 m^{2}K/W to provide the thermal resistance for rooftops (Becker & Wang, 2011). The insulation layer plays a key role in providing this resistance for green roof systems (Becker & Wang, 2011; D'Orazio et al., 2012; Meddage et al., 2022; Squier & Davidson, 2016). Also, the thermal resistance, the water retention[1] and the detention[2] of rooftops are substantially impacted by the materials used in the substrate and drainage layers of green roofs (Stovin et al., 2013; Szota et al., 2017; Vijayaraghavan, 2016). Also, climate conditions can have a significant impact on the effectiveness of green roofs made of various materials (Coma et al., 2016; Klein & Coffman, 2015; Pérez, Vila, et al., 2012). On the other hand, over the past few decades, the construction industry's excessive use of natural resources and aggregates has had devastating environmental effects by producing large quantities of Construction and Demolition Wastes (Vo et al., 2021). This issue can be somewhat solved by the partial replacement of natural aggregates with recycled and artificial aggregates in the green roof layers (Bisceglie et al., 2014; Coma et al., 2014). The use of recycled and artificial materials usually induces lower load to rooftops

[1] Water holding capacity of green roof layers
[2] Collected water after flowing across green roof layers

due to their lower weight and affects the thermal resistance, water permeability and water retention capacity owing to their higher porosity. In addition, the future climate change effect on the performance of green roofs with recycled and artificial materials is under question. That is why using alternative materials for green roof is becoming more common and it is required to assess the possibility of using recycled and artificial aggregates for the drainage and substrate layers of green roof systems.

1.2. State of art and motivation of the research

Long-term experimental work was performed by researchers to assess the thermal performance of green roof with the drainage layer made of rubber crumbs and volcanic gravel (Coma et al., 2014, 2016; Navarro et al., 2012; Pérez, Coma, et al., 2012; Pérez, Vila, et al., 2012; Vila et al., 2012). According to the results, the thermal insulation performance of the green roof was better than that of the typical flat roof. Also, compared to volcanic gravel as a drainage layer, a green roof with rubber crumb drainage layer provided more thermal resistance. Regarding the water passing ability of green roof materials, the water permeability for the substrate layer of a green roof is measured according to German FLL guidelines (FLL guidelines, 2008), which are widely accepted on a global scale. The substrate permeability is a crucial characteristic for stormwater reduction since it affects how much rainwater runs off of green roofs (De-Ville et al., 2018). In Gembloux Agro-Bio-Tech, Belgium, Rivière (Rivière, 2023) conducted an experimental study to investigate the effects of plant functional traits on the runoff of green roof including recycled materials under different levels of precipitation. The results showed that for shorter precipitation events (a two-year return time), the vegetated green roof retained 90% of the precipitation quantity; for longer precipitation events (a 20-year return period), it retained 30–40%. Furthermore, the root type, aerial biomass and vegetation height were found to affect the water runoff quantity, only during more intense precipitation events with higher runoff. More importantly, the variation of vegetation traits played only a marginal role in water runoff at low precipitation regimes. In contrast, under higher precipitation regimes, vegetation traits affected the runoff. Moreover, the type of substrate materials used should be considered in order to control water runoff during periods of intense precipitation. Olszewski and Young (Olszewski & Young, 2011) showed that by reducing the particle size of the materials utilized for the substrate layer, the water permeability of the green roof system decreased. Stovin et al. (Stovin et al., 2015) demonstrated that due to its high porosity, rounded shape and uniform size, using Lightweight Expanded Clay Aggregate (LECA) for the substrate layer improved the permeability and decreased the water retention time of the green roof system. The ability of substrate materials to retain water has been considered by several green roof guidelines and standards, including the German FLL guidelines (FLL guidelines, 2008), as another crucial indicator for green roof materials. Eksi and Rowe (Eksi & Rowe, 2016) showed that by reducing the recycled crushed porcelain particle size, the substrate layer's ability to retain water would presumably increased. Yang et al. (M. Yang et al., 2022) revealed that using coarse biochar improved water retention and lightened the substrate layer for green roofs. In general, it is clear that some studies have been done on thermal resistance, water permeability and water retention of green roof layers including granular aggregates; however, these parameters are required to be assessed for new materials suggested for green roof layers.

According to a study performed by Jim and Peng (Jim & Peng, 2012) in humid-subtropical climate conditions, due to the green roof effect, the daily maximum tile surface temperature was 5.2°C lower.

Typical sunny summer days with high solar radiation and low Relative Humidity (RH) boosted the passive cooling capacity of green roofs. The green roof fulfilled its role in energy saving when it rained, by slightly raising cooling load rather than lowering it. Finally, it was found that the installation of green roofs on public buildings had potential long-term environmental and economic benefits. Another study by Zhao and Srebric (M. Zhao & Srebric, 2012) during the winter showed that green roofs decreased heat transfer through the roof in cold weather, which reduced the need for heating energy. However, snow reduced the roof's thermal resistance and accelerated the heat transfer process, resulting in lower building energy savings. Joshi (Joshi, 2024) assessed the impact of green roofs on the local microclimate during a heatwave by introducing green roofs on buildings with flat roofs in all the realistic archetypes of Liège, Belgium. The center of Liège is largely covered with buildings, leaving few open green spaces. The city's summer time surface temperatures are noted to be high, leading a notable surface urban heat island influence. According to the results, while green roofs successfully lowered surface temperatures, their ability to reduce air temperature was limited in compact high-rise and semi-compact high-rise archetypes. Also, compact large low-rise and large low-rise archetypes, green roofs could be very useful in reducing surface and air temperatures. Getter et al. (Getter et al., 2011) evaluated the performance of green roofs and conventional gravel roofs in a Midwestern U.S. climate with hot, humid summers and cold, snowy winters. Green roof temperatures were consistently 5 °C lower than corresponding gravel roof temperatures in autumn and spring. Even in chilly and wet conditions, the green roof generated less heat from the building than the gravel roof. In brief, since the performance of green roofs made of various materials can be greatly influenced by climate factors (Coma et al., 2016; Klein & Coffman, 2015; Pérez, Vila, et al., 2012), their thermal performance and water retention capacity should be assessed in various weather scenarios.

1.2.1. Problem statement and identification of knowledge gaps

It is evident that the usability and performances of granular aggregates used in green roofs have already been studied. However, there is a need to assess whether the use of recycled and artificial materials is efficient for providing the same thermal resistance, water permeability and water retention for the green roof layers compared to the conventional green roof materials. Another gap that should be bridged is the modeling of the behaviour and the optimization of green roof layers when recycled and artificial materials are used. Moreover, climate conditions may have huge effect on green roof performances. Specially, the effect of climate changes till the end of the 21st century on the performance of green roofs including artificial and recycled materials has to be assessed. Finally, the thermal performance of green roofs is dependent on some materials' properties. In this sense, there is a need for determining how the thermal resistance of green roof layers is sensitive to specific properties of artificial and recycled materials.

1.2.2. Research novelties

In light of the foregoing background and knowledge gaps, the novelty of this research lies in assessing the water permeability, water retention capacity and thermal resistance of green roof layers designed with recycled and artificial aggregates. In addition, this work will help to evaluate the hygrothermal performance and the long-term weather condition effects of coarse artificial and recycled materials on the performance of green roof layers under the temperate climate of Liège city

till the end of the 21st century. A sensitivity analysis on green roof layers based on the properties of artificial and recycled materials will support the conclusions.

It is noteworthy that recycled and artificial aggregates can only be used for substrate and drainage layers of green roof systems. That's why the results of recycled and artificial aggregates will be compared with those of conventional materials for green roof systems in this work. Therefore, although green roof systems include different layers (Fig.1.1), this thesis will only focus on substrate and drainage layers.

1.2.3. Objectives

The thesis has the following objectives:

1. Proposing recycled and artificial materials for the drainage and substrate layers of green roof systems;
2. Verifying the thermal resistance, water permeability and water retention capacity of green roof layers including recycled and artificial materials;
3. Evaluating the rainfall detention performance of green roof layers including coarse recycled materials under high and low rainfall intensities;
4. Modeling the hygrothermal behaviour of materials and then optimizing the thickness of substrate and drainage layers;
5. Assessing the influence of using artificial and recycled materials on green roof performance under the temperate climate of Liège city till the end of the 21st century;
6. Evaluating the heat flux sensitivity to the thickness and physical characteristics of green roofs with artificial and recycled materials.

1.2.4. Research questions

To address research objectives, this thesis aims to answer the following five questions:

- To what extent can the presence of recycled and artificial materials provide thermal resistance, water passing ability and water retention capacity for substrate and drainage layers compared to conventional green roof materials?
- What is the influence of using coarse recycled materials on rainfall detention of green roof layers under high and low rainfall intensities?
- Whether are recycled and artificial materials able to provide nearly the same hygrothermal conditions for the green roof models as conventional materials or not?
- What is the influence of using artificial and recycled materials on green roof performance under the temperate climate of Liège city till the end of the 21st century?
- To what extent is green roofs' thermal resistance sensitive to drainage and substrate layer characteristics, including artificial and recycled materials?

1.3. Thesis outline

Based on the objectives, the main contribution of this thesis is assessing the possibility of using recycled and artificial materials for green roof layers. To fill research gaps, this thesis mainly focuses on substrate and drainage layers of green roof systems in which coarse recycled and artificial materials can be used. Fig. 1.2 presents the thesis outline, including 6 chapters.

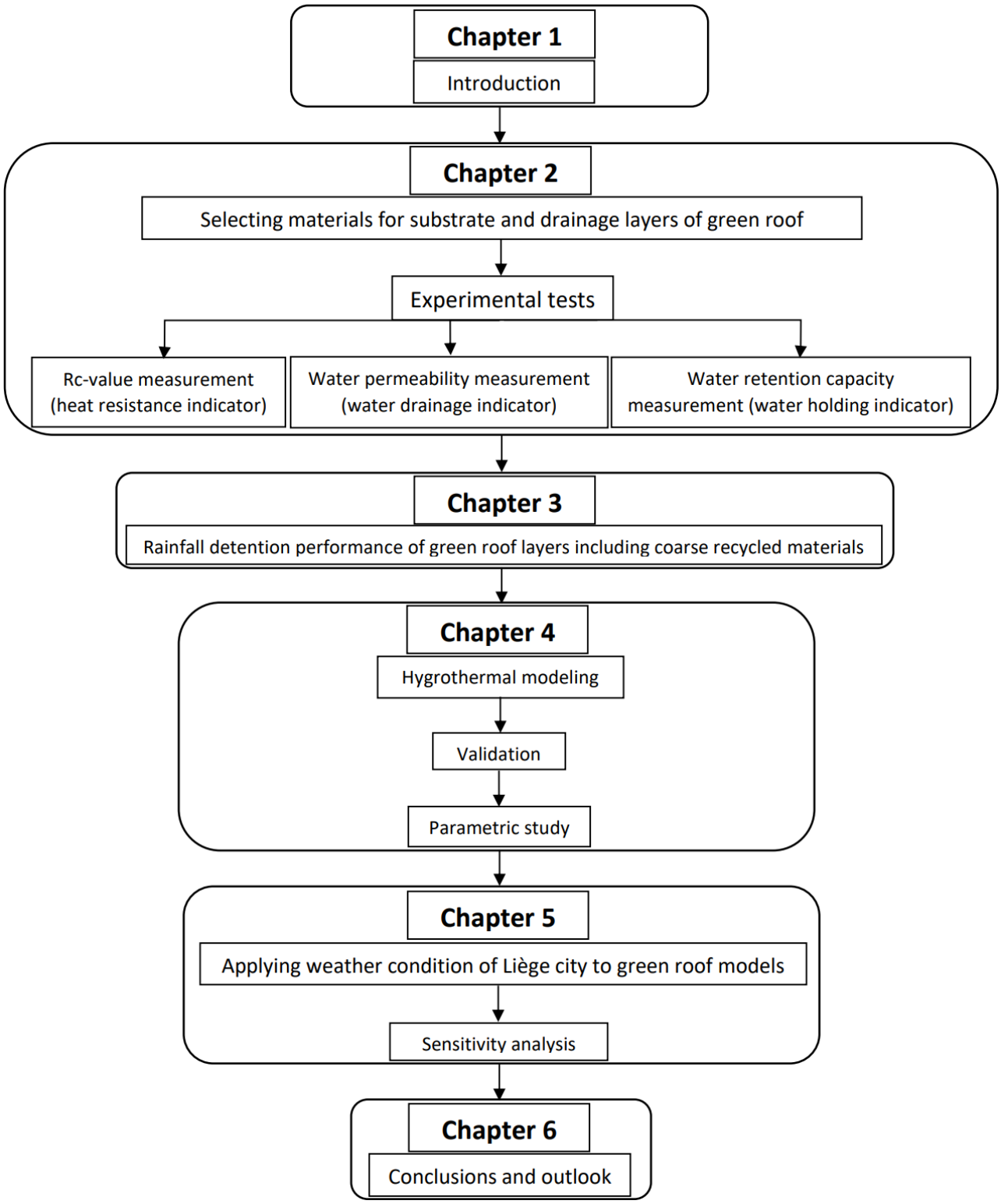

Fig. 1. 2. Research outline for meeting the thesis objectives.

To address the research outline, the chapters are organized as mentioned below:

- **Chapter 1:**

It is the current chapter as an introduction for the thesis in which the problem domain is first identified and then, the research background is critically presented. After that, the knowledge gaps and research novelties are provided. In the next step, objectives and research questions are presented. In the end, the thesis outline is determined to meet the thesis objectives.

- **Chapter 2:**

Chapter 2 is paper based. The first objective of this chapter is to propose recycled and artificial materials for the drainage and substrate layers of green roof systems. The second objective is to verify the thermal resistance, water permeability and water retention capacity of green roof layers including recycled and artificial materials. Considering this, the coarse recycled and artificial materials are considered as independent variables and are chosen for the substrate and drainage layers according to specific selection criteria. After that, three leading indicators as dependent variables are measured and analyzed for green roof systems: Rc-value as heat resistance indicator, water permeability as water drainage indicator and water retention capacity as water holding indicator. The Rc-value measurements are conducted following ISO 9869-1 (ISO 9869-1, 2014). The drainage and substrate materials' water permeability and water retention capacity are obtained and those for substrates are controlled using the German FLL guidelines (FLL guidelines, 2008).

- **Chapter 3:**

The main objective of chapter 3 is to evaluate the rainfall detention performance of green roof layers including coarse recycled materials under low and high rainfall intensities. Chapter 3 presents the construction process of a mini-experimental green roof in a lab-scale. Then, the rainfall detention performance of green roof layers including coarse recycled materials is assessed under high rainfall intensity (100 mm/h) and low rainfall intensity (50 mm/h).

- **Chapter 4:**

Chapter 4 is paper based. The main objective of this chapter is to model the hygrothermal behaviour of green roof materials and optimize the thickness of substrate and drainage layers. In order to shed some light on heat and moisture transfer within green roof layers including recycled materials, the hygrothermal performance is modeled using WUFI software. The measured temperatures within green roof layers' depth are used to validate the modeling outputs with experimental results. Also, a parametric study based on temperature variations is proposed to obtain the optimum thickness for green roof layers.

- **Chapter 5:**

Chapter 5 is paper based. The first objective of this chapter is to assess the influence of using artificial and recycled materials on green roof performance under the temperate climate of Liège city till the end of the 21st century. Another objective is to evaluate the heat flux sensitivity to the thickness and physical characteristics of green roofs with artificial and recycled materials. Considering this, a sensitivity analysis and long-term weather condition effects on green roof models is realized. Three temperate weather scenarios of Liège city are applied to green roof models with artificial and recycled materials: the climatic conditions for the beginning, the middle and the end of the 21st century, as well as perspectives for future use are compared. In addition, since green roofs' thermal resistance is

sensitive to drainage and substrate layers' characteristics, the sensitivity of heat flux value to green roof layers' thickness and materials properties is assessed using analytical methods.

- **Chapter 6:**

  Chapter 6 will present conclusions and outlooks of this thesis.

Chapter 2: Water permeability, water retention capacity and thermal resistance of green roof layers made with recycled and artificial aggregates

Introduction

The extraction of natural aggregates for building envelopes such as green roof layers has imposed harmful impacts on the environment in recent years. Also, the polyethylene plastic modular panel (egg-carton-shaped panel) has commonly been used for the drainage layer of green roof which is harmful for the ecosystem. This has raised a demand for using appropriate materials for green roof applications to reduce the burden on the environment by saving natural aggregates and avoiding using plastic materials for the drainage layer. An eco-friendly way to lessen the load on rooftops and conserve natural resources is to replace natural aggregates in the drainage and substrate layers of green roofs with lightweight artificial and recycled coarse materials available in the market. Considering this, the main contribution of this chapter (paper based) is to select coarse recycled and artificial materials for green roof layers. This is also required to assess to what extent the presence of recycled and artificial materials can provide thermal resistance, water passing ability and water retention capacity for substrate and drainage layers compared to conventional green roof materials. Therefore, the first objective of this chapter is to propose recycled and artificial materials for the drainage and substrate layers of green roof systems based on specific criteria. The second objective is to verify the thermal resistance, water permeability and water retention capacity of green roof layers including recycled and artificial materials. Regarding this, the coarse recycled and artificial materials are considered as independent variables and are chosen for the substrate and drainage layers according to specific selection criteria. After that, three leading indicators as dependent variables are measured and analyzed for green roof systems: Rc-value as heat resistance indicator, water permeability as water drainage indicator and water retention capacity as water holding indicator. The Rc-value measurements are conducted following ISO 9869-1 (ISO 9869-1, 2014). The drainage and substrate materials' water permeability and water retention capacity are obtained and those for substrates are controlled using the German FLL guidelines (FLL guidelines, 2008).

Further experimental research on the rainfall detention performance of green roof including coarse recycled materials is presented in the next chapter (chapter 3).

Abstract

Substituting natural aggregates in the green roof substrate and drainage layers with lightweight artificial and recycled coarse materials is an eco-friendly alternative for applying lower load to the rooftops and preserving natural resources. However, a lack of precise understanding of the thermal resistance, water passing ability and water holding capacity of green roof materials, including recycled and artificial materials, has raised a demand for measuring their Rc-value, water permeability and water retention capacity as three main indicators for green roof systems. This study comparatively evaluated the thermal resistance, water permeability and water retention capacity of green roofs with substrate and drainage layers, including coarse recycled and artificial materials. Different kinds of coarse granular aggregates were separately used for the drainage layer, including Natural Coarse Aggregate (NCA), Recycled Coarse Aggregate (RCA), Incinerated Municipal Solid Waste Aggregate (IMSWA) and Lightweight Expanded Clay Aggregate (LECA). The substrate layers were made with coarse recycled materials (SC) and without coarse recycled materials (SP) in wet and dry states. The outcomes revealed the highest thermal resistance and the lowest weight were obtained for 20-cm green roofs with a 15-cm substrate layer and 5-cm drainage layer of LECA. The water permeability of NCA was obtained 1.5 times more than that of LECA, whereas there was no significant difference between the result of the former, RCA and IMSWA. The water retention capacity of the LECA was two times higher than that of the NCA. SC and SP satisfied the water passing and retention criteria given for green roofs.

Keywords: Heat flow measurement; water permeability; water retention capacity; recycled and artificial aggregates; green roof.

Article: Kazemi, M., Courard, L., Attia, S. (2023). Water permeability, water retention capacity, and thermal resistance of green roof layers made with recycled and artificial aggregates, Building and Environment. 227, 109776. https://doi.org/10.1016/j.buildenv.2022.109776

Abbreviations:

LECA	Lightweight Expanded Clay Aggregate
NCA	Natural Coarse Aggregate
RCA	Recycled Coarse Aggregate
IMSWA	Incinerated Municipal Solid Waste Aggregate
SP	Substrate with coarse recycled materials (Proposed Substrate)
SC	Substrate without coarse recycled materials (Control Substrate)
SD	Standard Deviation

2.1. Introduction

Sustainable urban drainage systems have been increasingly developed for building envelopes such as rooftops to improve the energy efficiency of houses and reduce the high volume of runoff during stormwater events (Ávila-Hernández et al., 2020; Karczmarczyk et al., 2017; M. Kazemi & Courard, 2021b, 2022; La Roche et al., 2020; Norouziasas et al., 2022; Rahif, Hamdy, et al., 2022; Rahif, Norouziasas, et al., 2022; Wei et al., 2021; White & Alarcon, 2009). As a sustainable ecosystem system, the green roof is known for its ability to provide thermal resistance for rooftops in some cases and buffer the surface stormwater runoff in urban areas (Fachinello Krebs & Johansson, 2021; Hao et al., 2020; M. Kazemi et al., 2021; Ma'bdeh et al., 2022; Ouldboukhitine et al., 2012; Schade et al., 2021; Vilar et al., 2021; Zheng et al., 2022). The shape and type of materials used in green roof

drainage and substrate layers significantly impact energy efficiency and rooftop water evacuation (M. Kazemi & Courard, 2021a; Stovin et al., 2013; Szota et al., 2017; Vijayaraghavan, 2016).

The German FLL guidelines (FLL guidelines, 2008) are internationally recognized and widely used to measure the water permeability (estimating drainage) for the green roof substrate layer. These guidelines' targets for substrate performance are most relevant to green roof technologies in the European region's climate (Ampim et al., 2010; Dvorak, 2011; F. Kazemi & Mohorko, 2017). Regarding the water buffering capability, Kaczmarczyk et al. (Karczmarczyk et al., 2017) revealed that the water permeability depended on the porosity and shape of the materials used for the green roof substrate layer. Another study by Wong and Jim (Wong & Jim, 2014) revealed that using high porous materials such as rock wool for the substrate layer increased the porous nature and permeability of green roof systems. Ouldboukhitine et al. (Ouldboukhitine et al., 2012; Ouldboukhitine & Belarbi, 2015) measured the hydrological properties of the green roof components. According to the results, the green roof substrate's permeability was gained five times more than that of concrete materials owing to the higher porosity of the former (55.13%) than the latter (19.07%). Miller (Miller, 2003) demonstrated that increasing the number of tortuous paths for passing water through the substrate layer caused to increase in the detention times and decrease the water permeability of green roof systems. Stovin et al. (Stovin et al., 2015) assessed the hydrological performance of different types of green roof substrates. As per the results, the rounded shape, high porosity and uniformly-size LECA resulted in the most increased permeability and the lowest water detention time for the substrate layer.

Another important indicator for green roof materials is the water retention capacity of substrate materials, which has been taken into account by different green roof guidelines and standards, such as the German FLL guidelines (FLL guidelines, 2008). Since extensive green roofs require less maintenance and have shallower green roof layers, growing different types of plants and species is highly dependent on substrate and drainage layers (FLL guidelines, 2008; Graceson et al., 2013). In order to impose a lower load on buildings, the substrate layer should not be deeper than 20 cm. Hence, the maximum yearly water retention for green roof systems is approximately 65 % (FLL guidelines, 2008). Over the range of substrate depths associated with green roofs, substrate composition probably has a higher impact on a green roof's capacity to retain water than substrate depth does (FLL guidelines, 2008). Therefore, without considerably increasing the weight of green roofs, the substrate composition in green roof layers may be able to boost the green roof's ability to hold more water (Farrell et al., 2013).

Moreover, the materials used for the drainage layer can participate in increasing the water retention capacity of green roof systems. Ngan (Ngan, 2004) demonstrated that the crushed brick, as a lightweight porous material, reduced pressure on the substrate and drainage layers while enhancing the green roof system's ability to retain water. Coma et al. (Coma et al., 2016) showed that using more porous materials, like crushed bricks and pozzolana (porous volcanic gravel), might be a promising strategy to increase the drainage layer's ability to absorb water. Eksi and Rowe (Eksi & Rowe, 2016) used recycled crushed porcelain as a component of green roof substrates. The results revealed that reducing the recycled crushed porcelain particle size could probably lead to increasing the water retention capacity of the substrate layer. Yang et al. (M. Yang et al., 2022) showed that using coarse biochar increased the water retention capacity and reduced the weight of green roof substrate layer.

The green roof layers' heat resistance capability depends on their thickness and material type (Bellazzi et al., 2020; M. Kazemi & Courard, 2021b, 2022). Researchers have praised different kinds of materials' impact on the performance of green roof layers (Sleiman et al., 2011). Concerning this, Parizotto and Lamberts (Parizotto & Lamberts, 2011) constructed a green roof's drainage layer using natural gravel aggregates, which effectively reduced the daily temperature fluctuation and slowed down the heat transfer conduction. Almeida et al. (Almeida et al., 2019) demonstrated that the substrate layer boosted the thermal insulation of green roof systems; however, in a wet state, its insulating capability was not as high as in a dry state. He et al. (He et al., 2016) revealed that increasing the substrate's water content boosted the cooling impact of the green roof. Furthermore, when the green roof was employed for the rooftops, the cooling and heating loads of the structures dropped. Fabiani et al. (Fabiani et al., 2018) found that the water content had a noticeable impact on the thermal characteristics of the green roof layers, where it caused to increase in the substrate's thermal conductivity by three times on rainy days.

Natural mineral and energy resources are heavily utilized to construct building envelope components (such as roofing systems) and provide adequate indoor thermal comfort (Jahandari et al., 2021; M. Kazemi et al., 2019; M. Kazemi & Courard, 2021a; Kilmartin-Lynch et al., 2021, 2022; Mehrabi et al., 2021; Mohammadifar et al., 2022; Nematzadeh et al., 2019, 2021; Shahmansouri et al., 2021, 2022). For instance, consuming an estimated 40% of primary energy for construction sectors has produced a series of insoluble environmental concerns (Abergel et al., 2017; Directive, 2010). Since the rooftop is one of the main sources of energy loss, partially replacing natural components with recycled and artificial coarse materials in green roof layers with adequate thermal resistance can help to address these environmental issues (AzariJafari et al., 2021; Coma et al., 2014, 2016; M. Kazemi & Courard, 2021b; Nematzadeh & Baradaran-Nasiri, 2019). Regarding this, the green roof's drainage layer was constructed by Coma et al. (Coma et al., 2014, 2016) using pozzolana and rubber crumbs and its performance was assessed in the Mediterranean environment. According to the findings, the green roof's poor thermal efficiency was developed in winter with increased drainage and substrate layers' depth. Cascone et al. (Cascone et al., 2018) compared the thermal resistance of three different granular drainage materials: perlite, expanded clay and rubber crumb. The results showed that the highest values of thermal conductivity were obtained for the rubber crumb. Also, Cascone (Cascone, 2019) revealed that, compared to the non-insulated conventional roof, the extensive green roof with recycled rubber had a much lower environmental impact. To analyze the thermal resilience of the same roofing system with pozzolana and rubber crumbs, Kazemi et al. (M. Kazemi & Courard, 2021b, 2022) modeled temperature fluctuations within its layers. The findings showed that the increment of the substrate and drainage layers' thickness improved the roofing system's thermal efficiency, despite the effects of thicker layers being the same. In 2021 and 2022, Kazemi et al. (M. Kazemi et al., 2022; M. Kazemi & Courard, 2021a) assessed how the green roof with a 15cm-substrate of coarse recycled materials and a 5-cm drainage layer of recycled coarse aggregates was able to resist the heat-flow in which the R-value as a heat resistance indicator was measured for green roof layers in accordance to ISO 9869-1 standard (ISO 9869-1, 2014). As per the results, the Rc-value of green roof layers with and without coarse recycled materials was near to each other. Also, Kazemi et al. (M. Kazemi et al., 2021) assessed the thermal resistance of green roofs with a 15cm-substrate of coarse recycled materials and a 5-cm drainage layer of incinerated municipal

solid waste aggregates and compared the results of a dry substrate with a wet substrate. As per the results, the heat transfer decreased through the green roof substrate with air voids in dry state.

In this context, it is clear that some studies have been done on the heat flow measurement of layers, including coarse recycled materials for green roofs, where the Rc-value was assumed as a heat resistance indicator (ISO 9869-1, 2014). However, more research is mandatory to measure the other artificial materials' thermal resistance for the green roof drainage and substrate layers and compare their results to each other. On the other hand, since water permeability and water retention capacity are other critical indicators for green roofs (FLL guidelines, 2008), the coarse recycled and artificial materials' water permeability and water holding capacity need to be measured. Therefore, in this research, a comparative study on thermal resistance of different granular materials as the green roof drainage layer was performed in which the Rc-value of green roof with a dry and wet substrate including coarse recycled materials and the drainage layer of LECA was measured in accordance to ISO 9869-1 standard (ISO 9869-1, 2014). Then, the results were compared with those given by Kazemi et al. (M. Kazemi et al., 2021, 2022; M. Kazemi & Courard, 2021a) for the green roof system with the same substrate but with drainage layers made up of other granular coarse aggregates. The water drainage and water holding capacity of commercial substrate and drainage materials including coarse recycled and artificial aggregates were also measured.

2.2. Materials and Methods

Considering that, in Europe, 90% of recycled aggregates and 67% of artificial aggregates are produced in Northwestern European countries (Belgium, France, Germany, Netherlands and the UK) (UEPG, 2021), this study mainly focused on substrate and drainage layers of green roof systems in which coarse recycled and artificial materials could be used. Therefore, the coarse recycled and artificial materials were considered independent variables in this study and were chosen for the substrate and drainage layers according to some selection criteria. After that, three leading indicators as dependent variables were measured and analyzed for green roof systems: Rc-value as heat resistance indicator, water permeability as water drainage indicator and water retention capacity as water holding indicator.

2.2.1. Selection criteria and screening of tested materials

This study considered some criteria for selecting materials for the green roof layers: lightweight, high porosity, availability in the market, recycling and artificial production, as presented in Table 2.1. Concerning this, the Zinco substrate, including recycled tiles, bricks and organic matter, was considered for the substrate layer in dry and wet states (SP_Dry and SP_Wet), similarly to what was used by Kazemi et al. (M. Kazemi et al., 2021, 2022; M. Kazemi & Courard, 2021a). This lightweight substrate, including coarse recycled materials, was commercially available for extensive green roof systems in Northwestern Europe. The substrate without coarse recycled materials in dry and wet states (SC_Dry and SC_Wet) was used for the control substrate layer.

Different granular coarse aggregates available in the market were suggested for the drainage layer according to the selection criteria: Recycled Coarse Aggregate (RCA), Incinerated Municipal Solid Waste Aggregate (IMSWA) and LECA. The RCA and IMSWA were classified as recycled coarse aggregates. LECA was a coarse artificial aggregate chosen for the drainage layer owing to its lightweight and high porosity (Madandoust et al., 2019; Nematzadeh et al., 2021; Nematzadeh &

Baradaran-Nasiri, 2019; Strzałkowski et al., 2021). Natural Coarse Aggregate (NCA) was considered as a control coarse granular aggregate for the drainage layer. It is noteworthy that the possibility of using other aggregates like coarse crushed brick aggregates for the drainage layer was also assessed in this study. However, the coarse crushed brick aggregates without contamination were not commercially available in Northwestern Europe.

Table 2. 1. Selection criteria for green roof materials.

Selection Criteria				Lightweight	High porosity	Commercial production	Recycled material	Artificial material
Materials	Substrate layer	Control	SC_Wet & SC_Dry	-	-	✓	-	-
		Suggested	SP_Wet & SP_Dry	✓	✓	✓	✓	-
	Drainage layer	Control	NCA	-	-	✓	-	-
		Suggested	RCA	✓	✓	✓	✓	-
			IMSWA	✓	✓	✓	✓	-
			LECA	✓	✓	✓	-	✓

2.2.2. Materials' characteristics

Green roof materials' properties are presented in Table 2.2. LECA's characteristics were measured in this study. The corresponding attributes for other materials were determined by Kazemi et al. (M. Kazemi et al., 2021, 2022; M. Kazemi & Courard, 2021a). Specific heat capacity, water vapor diffusion resistance factor and water absorption coefficient of materials were measured according to standards ASTM D4611-16 (ASTM D4611 - 16, 2018), EN 1015 (EN 1015-19, 1999) and EN 1925 (EN 1925, 1999), respectively, as explained in detail by Kazemi et al. (M. Kazemi et al., 2022; M. Kazemi & Courard, 2021a). Porosity is the volume of void spaces and pores of materials to the total volume (volume of void spaces, materials and their pores) as determined by Kazemi et al. (M. Kazemi et al., 2021; M. Kazemi & Courard, 2021a). The materials' ability to hold water is their free water content. Indeed, with a relative humidity of 100%, this characteristic is determined by the materials' capillary action, trapping the water molecules within their pore structure (M. Kazemi & Courard, 2021a; Künzel, 1995). Reference water content is the sorption moisture corresponding to a relative humidity of 80% (Krus, 1996). More details about the free and reference water content of materials were presented by Kazemi et al. (M. Kazemi et al., 2021; M. Kazemi & Courard, 2021a).

Table 2. 2. Green roof materials' properties (Appendix 1).

Materials	Density (kg/m^3)	Porosity	Specific heat capacity, Dry (J/kg K)	Water vapour diffusion resistance factor	Reference water content (kg/m^3)	Free water content (kg/m^3)	Water absorption coefficient ($kg/m^2.s^{0.5}$)
SC_Wet(M. Kazemi & Courard, 2021a)	1075	0.48	-	-	10.31	380.95	-
SP_Wet(M. Kazemi & Courard, 2021a)	1001	0.486	-	-	7.73	285.71	-
SC_Dry(M. Kazemi et al., 2022)	856	0.48	880	3.62	-	-	0.47
SP_Dry(M. Kazemi et al., 2022)	944	0.47	810	3.35	-	-	0.22
NCA(M. Kazemi & Courard, 2021a)	1437	0.42	770	1	1.16	42.86	0.03
RCA(M. Kazemi & Courard, 2021a)	1165	0.50	730	1	3.32	122.76	0.07
IMSWA(M. Kazemi et al., 2021)	1147	0.47	750	1	2.74	101.2	0.07
LECA	439	0.55	710	1	2.83	141	0.11

2.2.3. Rc-value measurement (heat resistance indicator)

Fig. 2.1 shows the configuration of green roof layers to measure their thermal performances. Rc-value, as the rate of transfer of heat through a building element either a single material or a composite, was used for heat flow measurement and analysis (ISO 9869-1, 2014). This study constructed 15- and 5-cm moulds to measure the thermal resistance of substrate and drainage layers, respectively (Figs. 2.1(a) and 2.2(b)). A 20-cm mould was also made to measure the substrate and drainage layers' thermal resistance simultaneously (Fig. 2.1(c)). The temperatures were applied to each mould's top and bottom using a thermal device. After that, the Rc-value of each specimen was obtained based on the criteria given by ISO 9869-1 standard (ISO 9869-1, 2014). Kazemi et al. (M. Kazemi et al., 2021, 2022; M. Kazemi & Courard, 2021a) presented the detailed criteria for green roof layers' heat flow measurement specified by ISO 9869-1 standard (ISO 9869-1, 2014). They also optimized the substrate and drainage layers' thickness using modelling outputs.

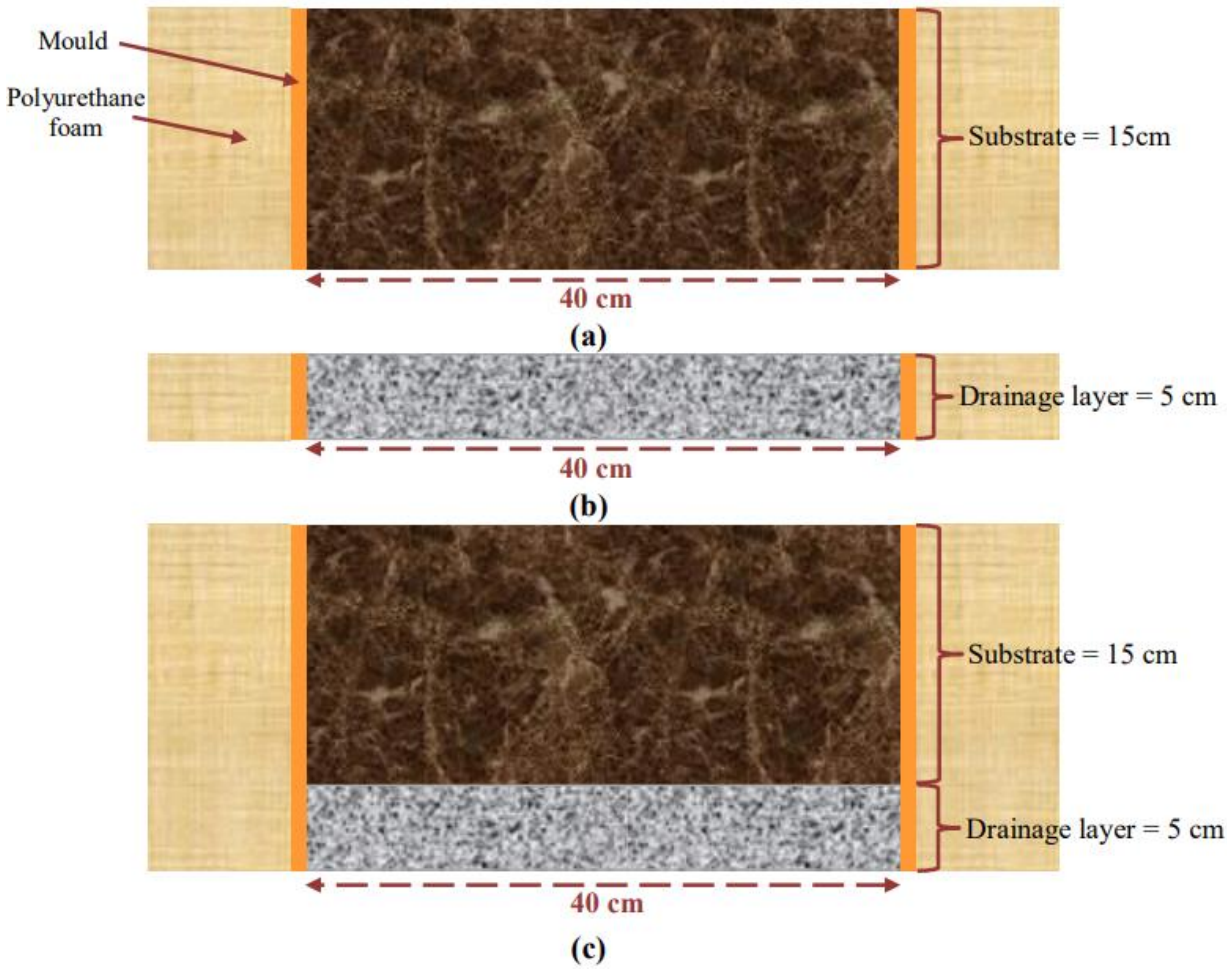

Fig. 2. 1. Schematic representations of 15-cm mould for substrate layer (a); 5-cm mould for drainage layer (a); 20-cm mould for a green roof with substrate and drainage layers (c).

The green roof specimens' component details and thicknesses are presented in Table 2.3. For all coarse granular aggregates as the drainage layer, a size of 7 mm was selected. The Rc-value of the 5-cm drainage layer of LECA (LECA5) was measured in this study. After that, Rc-values of green roofs with a 5-cm drainage layer of LECA and a 15-cm wet and dry substrate layer with coarse recycled materials (LECA5-SP15_Wet and LECA5-SP15_Dry) were determined and the results were compared with those given by Kazemi et al. (M. Kazemi et al., 2021, 2022; M. Kazemi & Courard, 2021a) for the green roof layers made up of other materials. Kazemi et al. (M. Kazemi et al., 2022; M. Kazemi & Courard, 2021a) considered a 5-cm natural coarse aggregate drainage layer and a 15-cm wet and dry substrate layer with no coarse recycled materials (recycled tiles and bricks) as the reference green roofs (NCA5-SC15_Wet and NCA5-SC15_Dry).

Table 2. 3. Details of green roof layers.

Specimens ID	Type of materials			Thickness (cm)		Substrate state
	Drainage layer	Substrate		Drainage layer	Substrate	
		Without coarse recycled materials	With coarse recycled materials			
NCA5(M. Kazemi & Courard, 2021a)	Natural coarse aggregate	-	-	5	-	-
RCA5(M. Kazemi & Courard, 2021a)	Recycled coarse aggregate	-	-	5	-	-
IMSWA5(M. Kazemi et al., 2021)	Incinerated municipal solid waste aggregate	-	-	5	-	-
LECA5	Lightweight expanded clay aggregate	-	-	5	-	-
SC[a]15_Wet(M. Kazemi & Courard, 2021a)	-	✓	-	-	15	Wet
SC15_Dry(M. Kazemi et al., 2022)	-	✓	-	-	15	Dry
SP[b]15_Wet(M. Kazemi & Courard, 2021a)	-	-	✓	-	15	Wet
SP15_Dry(M. Kazemi et al., 2022)	-	-	✓	-	15	Dry
NCA5-SC15_Wet(M. Kazemi & Courard, 2021a)	Natural coarse aggregate	✓	-	5	15	Wet
NCA5-SC15_Dry(M. Kazemi et al., 2022)	Natural coarse aggregate	✓	-	5	15	Dry
RCA5-SP15_Wet(M. Kazemi & Courard, 2021a)	Recycled coarse aggregate	-	✓	5	15	Wet
RCA5-SP15_Dry(M. Kazemi et al., 2022)	Recycled coarse aggregate	-	✓	5	15	Dry
IMSWA5-SP15_Wet(M. Kazemi et al., 2021)	Incinerated municipal solid waste aggregate	-	✓	5	15	Wet
IMSWA5-SP15_Dry(M. Kazemi et al., 2021)	Incinerated municipal solid waste aggregate	-	✓	5	15	Dry
LECA5-SP15_Wet	Lightweight expanded clay aggregate	-	✓	5	15	Wet
LECA5-SP15_Dry	Lightweight expanded clay aggregate	-	✓	5	15	Dry

[a] Substrate with no coarse recycled materials
[b] Substrate with coarse recycled materials

2.2.4. Water permeability (water drainage indicator)

As a key indicator for assessing the water draining ability of green roof materials, the water permeability was measured according to standard ISO 17892-11 (ISO 17892-11, 2019). The materials' water permeability values were obtained and those for substrates were controlled using the German FLL guidelines (FLL guidelines, 2008), providing performance criteria for constructing green roof systems. The materials were immersed for 24h in water until the date of testing as recommended by the German FLL guidelines (FLL guidelines, 2008). Note that the water permeability of the green roof's substrate layer should be in the range of 10^{-5}-1.17×10^{-3} m/s as recommended by FLL guidelines (FLL guidelines, 2008).

Fig. 2.2 shows a cross-sectional view of the permeability test, in which L is the specimen's length in m and Δh is the water head difference between the water level in the reservoir and that out of the specimen in m. The discharge velocity, v, (m/s) can be calculated using Eq. (2.1):

$$v = \frac{Q}{A} \tag{2.1}$$

where Q is the flow rate in m^3/s and A is the cross-sectional area of specimen in m^2.

Eq. (2) was used for calculating the hydraulic gradient (i):

$$i = \frac{\Delta h}{L} \tag{2.2}$$

Considering Eqs. (2.1) and (2.2), in this study, the water permeability (k) was obtained using Eq. (2.3):

$$k = \frac{v}{i} = \frac{Q}{A \times i} = \frac{Q}{A} \times \frac{L}{\Delta h} \tag{2.3}$$

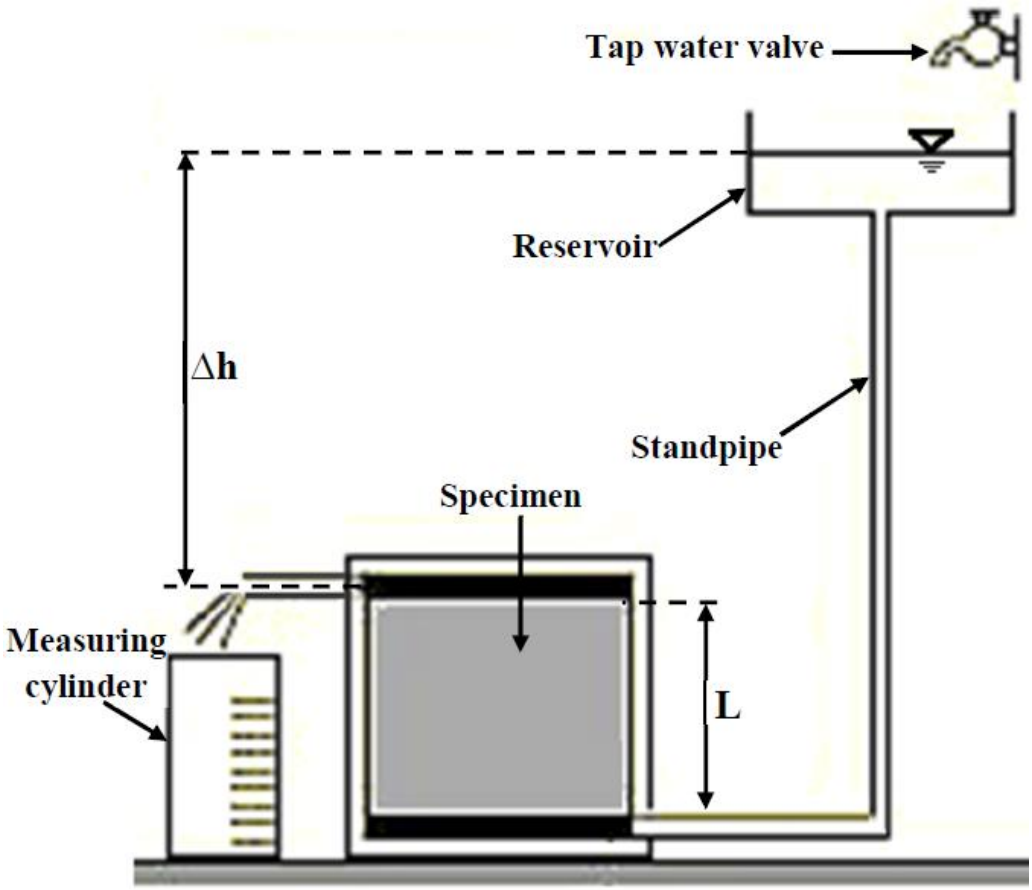

Fig. 2. 2. Schematic representation of water permeability test.

To assess the scatter of the data, the standard deviation (SD) value for each specimen was obtained, where the results were the average of three specimens. For each layer, it was required to assess whether the proposed materials had the same water permeability as the reference material. For the drainage layer, the mean of water permeability for IMSWA, RCA and LECA was compared with that of the coarse control aggregate (NCA). For the substrate layer, the result of the substrate with coarse recycled materials (SP) was compared with the reference substrate without coarse recycled materials (SC). Concerning this, the two-sample t-test method (t_{test}) was used in accordance with ISO 3301 (ISO 3301, 1975), which is suitable for assessing whether two materials' unknown population means are equal or not. Indeed, this method can consider the sample number (n) and SD of two materials to

compare their mean values (Daya, 2003; Gönen et al., 2005). To make a combined estimate of the two materials' standard deviations, the pooled standard deviation (S_p) can be calculated using Eq. (2.4):

$$S_p^2 = \frac{((n_1-1)SD_1^2)+((n_2-1)SD_2^2)}{n_1+n_2-2} \quad (2.4)$$

where n_1 and n_2 are the number of first and second groups of materials whose results were used to obtain their standard deviation (SD_1 and SD_2).

The value of t_{test} can be calculated using Eq. (2.5):

$$t_{test} = \frac{Difference\ of\ two\ materials'averages}{Standard\ error\ of\ difference} = \frac{(\bar{x}_1-\bar{x}_2)}{S_p\sqrt{\frac{1}{n_1}+\frac{1}{n_2}}} \quad (2.5)$$

where $\bar{x}_1$ and $\bar{x}_2$ are the average values for the first and second groups of materials.

To compare the test statistic to the t-test method's result, the degrees of freedom (d_f) were obtained using Eq. (2.6) and the t value was extracted from the t_{test} table given in ISO 3301 (ISO 3301, 1975) with the assumption of 95% confidence ($\alpha = 0.05$).

$$d_f = n_1+n_2-2 \quad (2.6)$$

When the t-test method's result for two materials is less than the t value extracted from the t_{test} table, the mean of the proposed materials and the reference material can be considered the same with 95% confidence. Otherwise, there is a difference between the mean of the former and the latter.

2.2.5. Water retention capacity (water holding indicator)

The water retention measurement of green roof materials was carried out according to FLL guidelines (FLL guidelines, 2008), where this indicator's range for the substrate materials should be within 35% and 65%. Fig. 2.3 shows the apparatus used for the water retention capacity test. The results were the average of three specimens. Therefore, three steel frames with 150 mm diameter and 165 mm height were used for molding each type of material. As recommended by FLL guidelines (FLL guidelines, 2008), the substrate materials were compacted in three layers using the proctor hammer, where a 4.5 kg hammer was dropped 6 times from 450 mm height onto the surface of each layer and molded into steel frames. However, since dropping the hammer caused to break of the coarse granular aggregates of the drainage layer, they were not compacted using the proctor hammer. Instead of it, the coarse aggregates for the drainage layer were shaken and compacted using a shaker table. After the material compaction, the steel frames were immersed in baskets of water and taken out after 24 h. Then, the water hose (Fig. 2.3) was used to drain the water for 2 h as recommended by FLL guidelines (FLL guidelines, 2008). Note that the top and bottom of steel frames were covered using stainless steel wire meshes with a size of 0.6 mm to prevent fine washing particles out. Thereafter, the materials were dried and kept in the oven at 105 °C until achieving a constant weight. To analyze the results of the water retention capacity test, the two-sample t-test method (t_{test}) was used according to ISO 3301 (ISO 3301, 1975), similar to the water permeability test.

Fig. 2. 3. Apparatus used for the water retention capacity test.

2.3. Results

2.3.1. Green roof materials' physical properties

Green roof materials' properties are presented in Table 2.2. As per the results, the density of the SC was about 10% more than that of the SP, either in the wet state or in dry state. The density of coarse granular aggregates, including NCA, IMSWA, RCA and LECA was 1437, 1147, 1165 and 439 kg/m^3, respectively. Therefore, the drainage layer with LECA had the lowest weight in comparison to other coarse granular aggregates layers used for green roof systems.

The soil porosity is dependent on the arrangement and texture of solid soil (Bahmani et al., 2019; Fatehi et al., 2018; Hao et al., 2008; Miller, 2003; Miraki et al., 2022; Stovin et al., 2015). For example, the typical range of porosity of soil for sandy surface soils is between 35% and 50%, while the corresponding value for finer textured soil is between 40% and 60% (Hao et al., 2008). In this study, the porosities of SC and SP were obtained at 48.2% and 48.63%, respectively, which were within the ranges of porosity given for the sandy surface soils (35%-50%) and finer textured soil (40%-60%) (Hao et al., 2008). Furthermore, comparing the porosity of SC and SP showed that no significant difference was observed between substrate porosity without coarse recycled materials (48.2%) and coarse recycled materials (48.63%). Concerning the coarse granular aggregates' porosity, the values of 41.67%, 47.26%, 49.56% and 55.08% were obtained for NCA, IMSWA, RCA and LECA, respectively, demonstrating that LECA was the most porous aggregates for the drainage layer.

The water absorption coefficient of the SC (0.47 kg/m^2.s$^{0.5}$) was about twice more than that of the SP (0.22 kg/m^2.s$^{0.5}$). The free water content of the former (380.95 kg/m^3) was about 33% more than that of the latter (285.71 kg/m^3). The water absorption coefficients for coarse granular aggregates of NCA, IMSWA, RCA and LECA were 0.03, 0.07, 0.07 and 0.11 kg/m^2.s$^{0.5}$, respectively. Therefore, the highest value was obtained for LECA as the drainage layer's granular aggregate. This was also observed for the free water content results, where the values of 42.86, 101.2, 122.76 and 141 kg/m^3 were obtained for NCA, IMSWA, RCA and LECA, respectively. So, LECA had the greatest water holding capacity compared to other coarse granular aggregates.

2.3.2. Rc-value

The green roof layers' heat flow measurement results are presented in Table 2.4. To ensure that the data was valid and reliable, the Rc-values needed to be assessed during the convergence time, which should be considered at least 72 h as recommended by ISO 9869-1 (ISO 9869-1, 2014). According to Rc-values in convergence time, less than a 3.9% difference was detected between the first and final 67% of data. The discrepancy between data collected 24 hours before the end of the heat flow measurement and data collected at the end of the test was no more than 2.4%. Based on the criteria given by standard ISO 9869-1 (ISO 9869-1, 2014), the differences above should not be more than 5%.

According to the heat flow measurement results, Rc-values were obtained at about 0.44 m^2 K/W for all 5-cm drainage layers (NCA5, RCA5 and IMSWA5), except for LECA5 (0.726 m^2 K/W). The Rc-value of 15-cm dry substrate layers (SC15_Dry and SP15_Dry) was about twice more than that of 15-cm wet substrate layers (SC15_Wet and SP15_Wet). The slight discrepancies of 4.3% (wet state) and 6.4% (dry state) were observed between Rc-values of 15-cm substrate layers with and without coarse recycled materials.

In the dry state, the Rc-value for 20-cm green roof specimens of NCA5-SC15_Dry, RCA5-SP15_ Dry, IMSWA5-SP15_Dry and LECA5-SP15_Dry were obtained 1.38, 1.31, 1.26 and 1.36 m^2 K/W, respectively. The corresponding values in the wet state for NCA5-SC15_Wet, RCA5-SP15_Wet, IMSWA5-SP15_Wet and LECA5-SP15_Wet were 0.75, 0.72, 0.735 and 1.04 m^2 K/W, respectively. Considering the same order of the above specimens, the Rc-values of the green roof specimens in dry state was 84%, 82%, 71.4% and 30.1% greater than those in wet state. Comparing the proposed green roof specimens with the reference green roof in a dry state, the Rc-value of 20-cm green roof specimens with drainage layers of RCA, IMSWA and LECA (RCA5-SP15_Dry, IMSWA5-SP15_Dry and LECA5-SP15_Dry) was respectively 0.95, 0.92 and 0.99 times that of the reference green roof (NCA5-SC15_Dry). In the wet state, the corresponding difference was 0.96, 0.98 and 1.39 times, respectively.

Table 2. 4. Green roof layers' heat flow measurement results.

Specimens ID	Test duration (h)	Convergence duration (h)	Thermal conductivity (W/m·K)	Rc-value (m^2 K/W)				
				24 h before the end of data set	End of data set	The first 67% of data during the convergence period	The last 67% of data during the convergence period	Average value during the convergence period
NCA5(M. Kazemi & Courard, 2021a)	101	76	0.114	0.443	0.443	0.441	0.44	0.44
RCA5(M. Kazemi & Courard, 2021a)	101	76	0.11	0.44	0.446	0.449	0.446	0.446
IMSWA5(M. Kazemi et al., 2021)	101	76	0.115	0.432	0.43	0.43	0.43	0.43
LECA5	101	76	0.067	0.733	0.732	0.725	0.727	0.726
SC15_Wet(M. Kazemi & Courard, 2021a)	122	73	0.31	0.481	0.48	0.481	0.48	0.48
SC15_Dry(M. Kazemi et al., 2022)	140	116	0.15	1.038	1.04	1.036	1.043	1
SP15_Wet(M. Kazemi & Courard, 2021a)	122	73	0.32	0.462	0.463	0.461	0.462	0.46
SP15_Dry(M. Kazemi et al., 2022)	165	75	0.16	0.94	0.93	0.93	0.94	0.94
NCA5-SC15_Wet(M. Kazemi & Courard, 2021a)	166	118	0.27	0.743	0.75	0.748	0.746	0.75
NCA5-SC15_Dry(M. Kazemi et al., 2022)	165	120	0.142	1.42	1.4	1.4	1.4	1.38
RCA5-SP15_Wet(M. Kazemi & Courard, 2021a)	166	118	0.28	0.713	0.72	0.715	0.724	0.72
RCA5-SP15_ Dry(M. Kazemi et al., 2022)	166	120	0.151	1.27	1.3	1.27	1.32	1.31
IMSWA5-SP15 _Wet(M. Kazemi et al., 2021)	168	120	0.27	0.732	0.735	0.728	0.726	0.735
IMSWA5-SP15 _Dry(M. Kazemi et al., 2021)	168	120	0.16	1.25	1.26	1.26	1.25	1.26
LECA5-SP15 _Wet	168	120	0.192	1.044	1.047	1.04	1.042	1.04
LECA5-SP15 _Dry	168	120	0.147	1.358	1.364	1.362	1.357	1.36

2.3.3. Water permeability

The green roof materials' water permeability values are shown in Fig. 2.4. According to the results, the water permeability values of granular aggregates, including NCA, IMSWA, RCA, LECA, SC and SP, were about 3.8×10^{-3}, 4.3×10^{-3}, 4.1×10^{-3}, 2.5×10^{-3}, 2.6×10^{-5} and 1.7×10^{-5} m/s, respectively. Their SD values were 3.42×10^{-4}, 4.86×10^{-4}, 1.15×10^{-4}, 6.2×10^{-6}, 8.7×10^{-7} and 3.6×10^{-7}, respectively.

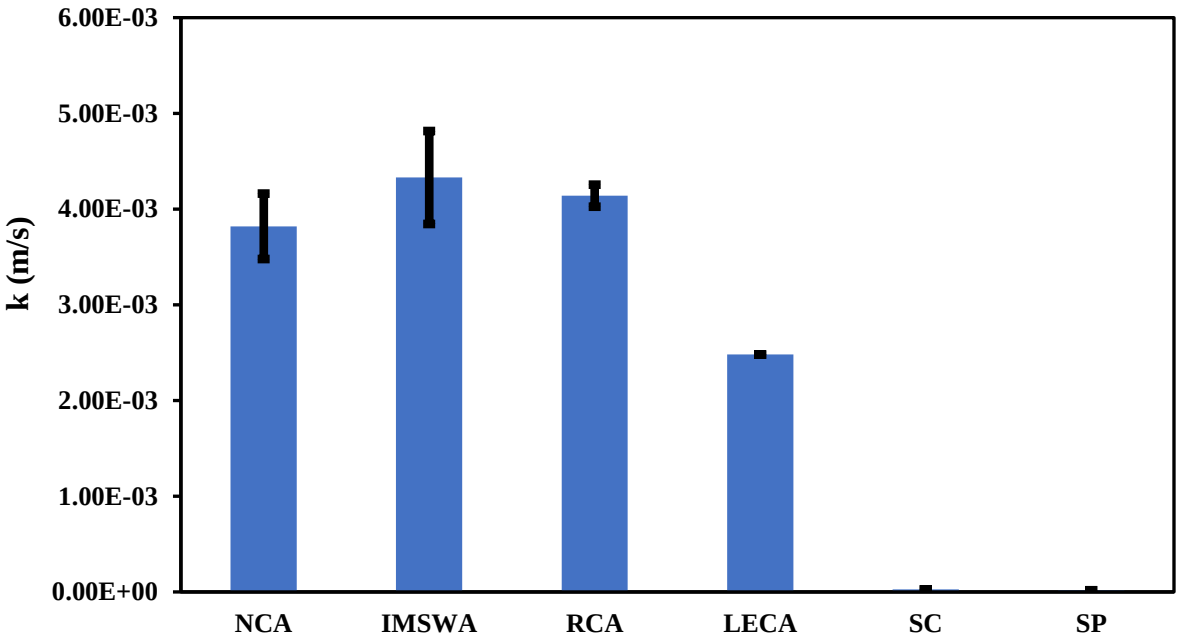

Fig. 2. 4. Results of water permeability test.

Table 2.5 presents the two-sample t-test method's results for the water permeability test, which were calculated using Eq. (2.5). For each layer, the mean of water permeability for the proposed materials was compared with that for the reference materials. As per the results, the t_{test} value of IMSWA, RCA and LECA compared to that of NCA was obtained at 1.487, 1.536 and 6.785, respectively. The corresponding value for SP was attained at 15.855 in comparison to SC.

Considering that the results were the average of three specimens, the sum of n_1 and n_2 was 6, d_f was equal to 4 using Eq. (2.6). Therefore, the t value was extracted from the t_{test} table and obtained 2.132 with 95% confidence ($\alpha = 0.05$) and 4 degrees of freedom (d_f). As presented in Table 2.5, the t_{test} results for IMSWA and RCA (1.487 and 1.536) were obtained at less than 2.132, demonstrating that the water permeability performance of the IMSWA and RCA was nearly the same as that of NCA. However, the t_{test} value between LECA and NCA was obtained at 6.785, which was more than 2.132. Therefore, there was a difference between the mean of the LECA and NCA. The t_{test} value for SP (15.855) was greater than 2.132, indicating that the mean water permeability for SC was more than that for SP.

Table 2. 5. The two-sample t_{test} method's results for the water permeability test.

Materials ID	t_{test}
NCA	-
IMSWA	1.487
RCA	1.536
LECA	6.785
SC	-
SP	15.855

2.3.4. Water retention capacity

Fig. 2.5 shows the water retention values of green roof materials. As per the results, the values of 9%, 18.1%, 13.77%, 18.5%, 46.73% and 38.27% were obtained for NCA, IMSWA, RCA, LECA, SC and SP, respectively. Their SD values were 0.71, 1.65, 0.51, 0.48, 0.68 and 0.22, respectively.

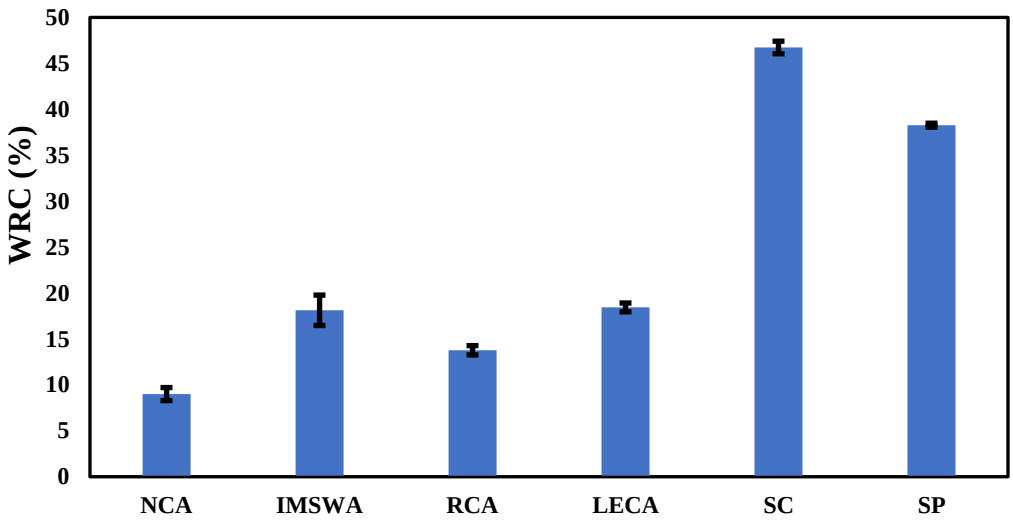

Fig. 2. 5. Results of water retention capacity test.

The two-sample t-test method's results for the water retention capacity test are presented in Table 2.6. According to the coarse granular drainage materials results, the t_{test} value of IMSWA, RCA and LECA was obtained 8.79, 9.45 and 10.2 compared to NCA. For the substrate layer, the value of 20.49 was obtained for SP in comparison to SC.

The results were the average of three specimens. Hence, the *t* value, extracted from the t_{test} table, was obtained 2.132 with 95% confidence. According to Table 2.6, the t_{test} results for IMSWA, RCA and LECA (8.79, 9.45 and 9.06) were more than 2.132. So, there was a difference between the mean water retention capacity for the proposed coarse granular drainage aggregates and NCA. The t_{test} value for SP (20.49) was also obtained at more than 2.132, demonstrating that the mean water retention capacity for SP and SC cannot be considered the same.

Table 2. 6. The two-sample t_{test} method's results for the water retention capacity test.

Materials ID	t_{test}
NCA	-
IMSWA	8.79
RCA	9.45
LECA	19.06
SC	-
SP	20.49

2.4. Discussion

2.4.1. Rc-value measurement (heat resistance indicator)

The air-voids among coarse aggregates were more impacted by air-voids than coarse aggregate types, resulting in similar heat resistance of NCA5, RCA5 and IMSWA5 (0.44 m^2 K/W) (M. Kazemi & Courard, 2021a). However, the higher porosity of LECA than other granular aggregates led to a higher Rc-value for LECA5 (0.726 m^2 K/W). Considering the Rc-value of 15-cm dry substrate layers was twice more than that of 15-cm wet substrate layers, it can be stated that the confined air provided a higher heat resistance than the water content for the substrate layer, as mentioned by Kazemi et al. (M. Kazemi et al., 2021). Partially replacing the organic matter with coarse recycled materials caused

a narrow difference between Rc-values of 15-cm substrate layers with and without coarse recycled materials (4.3% in wet state and 6.4% in dry state). This slight difference showed that the porous coarse recycled materials' ability to withstand heat flow was somewhat lower than that of dry soil particles, even though it was negligible.

The expansion of air spaces among dry, coarse recycled materials and dry soil particles led to a better performance than the water content in soil particles to achieve a greater thermal resistance for green roof systems (M. Kazemi et al., 2021; M. Kazemi & Courard, 2021b, 2022). The highest difference between the Rc-value of dry and wet green roof systems was observed for 20-cm green roofs with a 5-cm drainage layer of NCA or RCA (NCA5-SC15_Dry, RCA5-SP15_ Dry, NCA5-SC15_Wet and RCA5-SP15_Wet). The lowest difference (30.1%) was obtained for 20-cm green roofs with a 5-cm drainage layer of LECA (LECA5-SP15_Dry and LECA5-SP15_Wet) owing to the higher porosity of LECA than other granular aggregates. This in turn caused the drainage layer of LECA participated more in providing thermal resistance for green roof systems than the substrate layer, leading to decreasing the difference between the thermal resistance of green roofs with wet and dry substrate materials.

A comparison between the Rc-value of the proposed green roof specimens with the reference green roof in a dry state demonstrated that although there was no substantial difference between the Rc-value of proposed green roofs and the reference green roof, the LECA5-SP15_Dry specimen had the closest thermal resistance to NCA5-SC15_Dry specimen (0.99). Similar results were observed in wet state where the thermal resistance of the LECA5-SP15_Wet specimen was 1.39 more than that of NCA5-SC15_Wet specimen.

Based on the above, the lowest difference between wet and dry conditions was obtained for 20-cm green roofs with a 5-cm drainage layer of LECA (30.1%) and the highest thermal resistance was also attained for the same specimens. Since researchers have advocated for adopting lightweight roofing solutions with sufficient heat resistance for rooftops (M. Kazemi & Courard, 2022; Sun et al., 2014; Tabares-Velasco et al., 2012), the LECA5-SP15_Wet and LECA5-SP15_Dry specimens can be considered the best configuration and materials for roofing systems due to their lowest weight and highest heat resistance.

2.4.2. Water permeability (water drainage indicator)

According to the t_{test} method's results, the means of water permeability for IMSWA and RCA was nearly identical to that of the coarse control aggregates (NCA). Therefore, although the type of the aggregates above differed, all of them were crushed and their size was the same (7mm). Therefore, the voids among aggregates controlled their water permeability performance rather than the coarse aggregates. However, the t_{test} method's result between NCA and LECA (6.785) specified a difference between the water permeability of the former and the latter. Comparing the water permeability of the NCA (3.8×10^{-3} m/s) and LECA (2.5×10^{-3} m/s) showed that the water permeability of the former was about 1.5 times more than that of the latter. The LECA was composed of rounded expanded clay aggregates, while NCA was crushed coarse materials.

Moreover, the porosity of LECA (55%) was higher than that of NCA (41.67%). In addition, LECA had the highest water absorption coefficient (0.11 $kg/m^2.s^{0.5}$) and free water content (141 kg/m^3) compared to other coarse granular aggregates, leading to increasing its water holding capacity and

subsequently decreasing its water permeability value. Therefore, the rounded shape and physical properties of LECA caused its water permeability performance to be less than that of NCA.

Among coarse aggregates, the highest and lowest SD values were obtained for IMSWA (4.86×10^{-4}) and LECA (6.2×10^{-6}), respectively. It can be stated that since IMSWAs included different crushed and recycled materials, their results were more scattered than other aggregates, while the shape and type of LECAs were the same, leading to lower dispersion of data and lower SD value.

The water permeability of the green roof's substrate layer should be in the range of 10^{-5}- 1.17×10^{-3} m/s, according to the recommendations given by the FLL guidelines (FLL guidelines, 2008). This parameter for SC and SP was obtained 2.6×10^{-5} and 1.7×10^{-5} m/s, which were within the range given by FLL guidelines (FLL guidelines, 2008). Therefore, the soil materials (SC and SP) provided an adequate water passing ability for the green roofs' substrate layer. The t_{test} results showed that the mean of water permeability for SC was more than that for SP. This value for the SC and SP was 2.6×10^{-5} and 1.7×10^{-5} m/s, respectively. The water permeability of the former was about 1.5 times more than that of the latter. Although the substrate materials' water permeability depends on their porosity and shape (Karczmarczyk et al., 2017; Olszewski & Young, 2011) and using high porous materials can lead to increasing the green roof systems' water permeability (Wong & Jim, 2014), there was no significant difference between the porosity of SC (48.2%) and SP (48.63%). The difference between the water permeability of SC and SP can be a consequence of coarse recycled materials in the latter, leading to generating tortuous paths for passing water through the substrate layer and subsequently decreasing the water permeability of green roof systems, similar to what was revealed by Miller (Miller, 2003). Therefore, the water could easily pass through the soil's fine particles in SC. However, the partial replacement of these fine particles with coarse recycled materials in SP prevented effortlessly passing water through the substrate layer. Consequently, the ability of SC was better than that of SP.

2.4.3. Water retention capacity (water holding indicator)

According to the t_{test} method's results, there was a difference between the means of water retention capacity values of the proposed coarse drainage aggregates and NCA. Also, comparing the results showed that the water retention capacity value of LECA (18.5%) and IMSWA (18.1%) was obtained about 2 times more than that of NCA (9%). Moreover, the result of RCA (13.77%) was about 1.5 times more than that of NCA (9%). Therefore, higher porosity of recycled and artificial coarse aggregates (IMSWA, RCA and LECA) than NCA led to a greater water retention capacity for the drainage layer. Moreover, the water retention capacity value of LECA and IMSWA was obtained more than that of RCA. LECA is an artificial aggregate with a high water absorption coefficient (0.11 $kg/m^2.s^{0.5}$). IMSWA included crushed brick, inert waste, crushed aggregate, crushed ceramic and crushed glass (M. Kazemi et al., 2021), while RCA was more composed of recycled concrete coarse aggregates. Therefore, since LECA was an aggregate with high water absorption and IMSWA included different types of recycled materials such as crushed brick, inert waste and crushed aggregate, they were proved to outperform RCA to hold more water for the drainage layer of green roof systems. It is noteworthy that due to different types of materials in IMSWA, its water retention capacity values (SD = 1.65) were more dispersed than other aggregates, while the results of LECAs were less scattered (SD = 0.48) because of their single type and regular ball-shaped form.

On the other hand, it has been suggested to choose lightweight materials for the green roof layers to apply less load to the top of structures (Teemusk & Mander, 2009). The density of IMSWA (1147 kg/m^3) was 2.6 times more than LECA (439 kg/m^3). Therefore, LECA is recommended for the drainage layer to provide the highest water retention capacity and impose the lowest load on buildings compared to other coarse granular aggregates.

There was a difference between the mean of water retention capacity of SC and SP for the substrate materials according to the t_{test} method's results (Table 2.6). As shown in Fig. 2.5, the water retention capacity of the former (46.73%) was about 1.2 times more than the latter (38.27%). It can be stated that fine particles of soil materials in SC absorbed slightly more water than recycled coarse materials in SP. However, the results of SC and SP were within the range (35%-65%) recommended by the FLL guidelines (FLL guidelines, 2008), demonstrating that both SC and SP provide an adequate water retention capacity for growing plants and species, and they don't overload rooftops.

2.5. Conclusions

This research work assessed the water permeability, water retention capacity and thermal resistance of green roof layers made with different recycled and artificial aggregates. The following conclusions for roofing systems can be drawn based on experimental outputs:

- The presence of air voids among dry soil particles resulted in superior thermal resistance for green roof systems than the water content in soil particles. Comparing wet and dry green roof systems' results, the highest difference was obtained between the Rc-value of 20-cm green roofs with a 5-cm drainage layer of natural coarse aggregate or recycled coarse aggregate (about 80%). The lowest difference was obtained for 20-cm green roofs with a 5-cm drainage layer of lightweight expanded clay aggregate (30.1%).
- Of all proposed green roof systems, 20-cm green roofs with a 15-cm substrate layer and 5-cm drainage layer of lightweight expanded clay aggregate had the lowest weight and the highest thermal resistance. Hence, they were introduced as the best configuration for rooftops.
- The water permeability performance of incinerated municipal solid waste aggregate and recycled coarse aggregate was nearly the same as the coarse control aggregate. Therefore, the voids among aggregates dictated their water permeability performance rather than the coarse aggregates.
- Among coarse granular aggregates used for the drainage layer, the highest porosity (55%), water absorption coefficient (0.11 kg/m^2.s$^{0.5}$) and free water content (141 kg/m^3) were obtained for lightweight expanded clay aggregate. Indeed, its physical properties and rounded shape caused the water permeability of natural coarse aggregate was obtained 1.5 times more than that of lightweight expanded clay aggregate, while the water retention capacity of the latter was obtained two times more than that of the former. Therefore, the use of lightweight expanded clay aggregate for the drainage layer provided the highest water for growing the plants and species and applied the lowest load to buildings due to its high water retention capacity and low weight, even though its water permeability was not as much as other coarse granular aggregates.
- The water permeability of the substrate without coarse recycled materials was about 1.5 times more than that of the substrate with coarse recycled materials. Considering this, the former outperformed the latter in passing the water through the substrate layer. However, the substrate

either with or without coarse recycled materials provided the required water permeability for green roof systems.

- Although the water retention capacity of the substrate without coarse recycled materials was obtained slightly more than that of substrate with coarse recycled materials (1.2 times), the results of both were within the required range given for the water holding capacity of green roof substrate materials. Therefore, substrate with coarse recycled materials offered sufficient water holding capacity for growing plants, and it also didn't overload green roof systems.

Water passing and holding capacity and thermal resistance of substrate and drainage layers were measured in this study to assess the possibility of using recycled and artificial materials for green roof systems. Analysis methods have now to be employed to assess the sensitivity to physical characteristics of artificial and recycled materials used for drainage and substrate layers of green roof systems.

Chapter 3: Rainfall detention performance of green roof layers including coarse recycled materials

3.1. Introduction

Urbanization substitutes relatively impermeable roof systems with permeable ones to increase the stormwater runoff's mass and temporal responses. Urban runoff might put the drainage systems under a lot of stress after heavy rains, causing combined sewer overflow and floods (Wong & Jim, 2014). Regarding this, the use of green roofs can be considered as a sustainable stormwater management solution for rooftops by reducing the sources of runoff. The green roof is a multi-layered system including substrate and drainage layers, buffering and absorbing rainfall effectively (Oberndorfer et al., 2007). Due to green roof layers' water retention capacity, they have a positive impact on the regulation of surface runoff (Zölch et al., 2017). However, the detention of green roof systems may be more crucial than retention under prolonged periods of heavy rain (Wong & Jim, 2014). Therefore, the substrate of green roof systems should have adequate water permeability to enable infiltration in order to lessen surface runoff and minimize floods on rooftops (FLL guidelines, 2008).

The effect of green roofs on the rainfall-runoff response of rooftops has been assessed by researchers. Row et al. (Rowe et al., 2003) showed that, for the runoff reduction, the green roof substrate layer (and its depth) was more important than the type of plant. Peak flow rates of runoff from green roof systems have been found to be 60–80% lower than those from conventional roof systems (Bliss et al., 2009; Carter & Jackson, 2007; Palla et al., 2012). Miller (Miller, 2003) found that green roof systems' water permeability and detention times increased as the number of tortuous paths for water through the substrate layer increased. In a study by Soulis et al. (Soulis et al., 2017), higher runoff reductions were seen in the deeper substrates if the initial moisture content of the substrate or the depth of the rainfall was low. Stovin et al. (Stovin et al., 2015) showed that the substrates with the lowest levels of retention and detention are the most porous/permeable ones. Pettersson et al. (Pettersson et al., 2020) revealed that the required green roof's detention time can be achieved by adjusting the particle size and thickness of green roof substrate layer. A study by Hamouz et al. (Hamouz et al., 2020) showed that the detention performance under extreme precipitation in the current and future climate circumstances was significantly improved by adding a layer of expanded clay under the green roof substrate layer. Another study by Liu et al. (Liu et al., 2021) demonstrated that increased rainfall duration and delayed peak intensity both improved runoff detention. Recently, Rivière (Rivière, 2023) examined experimentally the impact of plant functional traits on the runoff of green roof including recycled materials under different levels of precipitation in Gembloux Agro-Bio-Tech, Belgium. The simulated rains with return periods of two years (7.4 mm and 8.5 mm) and 20 years (15 mm and 17.1 mm) were applied during 160 and 300 seconds. According to the results, the vegetated green roof retained 90% of the precipitation quantity for shorter precipitation events (a two years return period) and 30-40% for higher precipitation events (a 20 years return period). Also, the root type, aerial biomass and vegetation height were identified as vegetation traits influencing water runoff quantity only for more intense precipitation events with higher runoff. In addition to this, at low precipitation regimes, the variation of vegetation traits has only a minor impact on water runoff. Conversely, the vegetation traits influenced the runoff in higher precipitation regimes. Furthermore, to regulate the water runoff under severe rain patterns, the type of substrate materials should be taken into account.

It is evident in this context that a set of research has been done on the rainfall-runoff response of green roof systems. However, the response of green roof systems including coarse recycled materials

has received less attention. On the other hand, the detention of green roof systems can be more important than their retention under long periods of severe rain (Wong & Jim, 2014). Considering this, the main objective of this study is to evaluate the rainfall detention performance of green roof layers including coarse recycled materials under high and low rainfall intensities. Also, the research aims to answer the following question:

What is the influence of using coarse recycled materials on the rainfall detention of green roof layers under high and low rainfall intensities?

Therefore, this study artificially simulated two rainfall patterns (high and low rainfall intensities) on a lab-scale. The rainfall patterns were applied to the green roof layers including coarse recycled materials to assess their ability for the rainfall detention. The results were compared to those of green roof layers without coarse recycled materials.

It is worth mentioning that after evaluating the rainfall detention performance of green roof layers in this chapter, the hygrothermal behaviour of green roof layers is modeled and validated in the next chapter (chapter 4).

3.2. Materials and method

The substrate and drainage layers of green roof systems, where coarse recycled materials could be used, were the main focus of this study. Two different intensities of rainfall were simulated on a lab-scale: low rainfall intensity (50 mm/h) for a 100-year return period based on the intensity–duration–frequency curves of rainfall from Liège (IRM, 2012) and high rainfall intensity (100 mm/h) based on some frequencies reported for some areas (Nagase & Dunnett, 2012). The two rainfall patterns were applied to the green roof systems including substrate with coarse recycled materials (SP) and drainage layer of recycled coarse aggregate (RCA). Their results were compared with those of the control green roof systems including substrate without coarse recycled materials (SC) and drainage layer of natural coarse aggregate (NCA).

3.2.1. Green roof specimens

Table 3.1 shows the details of green roof specimens under low and high rainfall intensities. To assess the effect of substrate depth on the results, two thicknesses of 15 cm and 10 cm were considered for the substrate layer, because a 15-cm substrate depth of the green roof can offer an acceptable depth for a variety of plant growth (Ladani et al., 2019). Also, the substrate with a minimum depth of 10 cm was able to keep water for a longer period of time after the cessation of watering (Lu et al., 2015). A depth of 5 cm was considered for the drainage layer as suggested by Kazemi and Courard (M. Kazemi & Courard, 2021a) when RCA is used.

Table 3. 1. Details of green roof layers.

Specimens ID	Type of materials			Thickness (cm)		Rainfall intensity
	Drainage layer	Substrate layer		Drainage layer	Substrate layer	
		Without coarse recycled materials	With coarse recycled materials			
SC[a]10-NCA[b]5-L[c]	Natural coarse aggregate	✓	-	5	10	Low
SP[d]10-RCA[e]5-L[f]	Recycled coarse aggregate	-	✓	5	10	Low

SC10-NCA5-H[f]	Natural coarse aggregate	✓	-	5	10	High
SP10-RCA5-H	Recycled coarse aggregate	-	✓	5	10	High
SC15-NCA5-L	Natural coarse aggregate	✓	-	5	15	Low
SP15-RCA5-L	Recycled coarse aggregate	-	✓	5	15	Low
SC15-NCA5-H	Natural coarse aggregate	✓	-	5	15	High
SP15-RCA5-H	Recycled coarse aggregate	-	✓	5	15	High

[a] Substrate without coarse recycled materials
[b] Natural coarse aggregate
[c] Low rainfall intensity
[d] Substrate with coarse recycled materials
[e] Recycled coarse aggregate
[f] High rainfall intensity

3.2.2. Experimental setup

Fig. 3.1 shows the schematic representation and the experimental setup to apply high and low rainfall intensities to green roof layers. A rainfall box was used to artificially apply the rainfall patterns to green roof mould. Then, the water leakage from green roof mould was collected using a collecting water tank. To prevent rainfall detention results from being affected by water absorption ability of green roof layers, substrate and drainage materials were used nearly in saturated conditions.

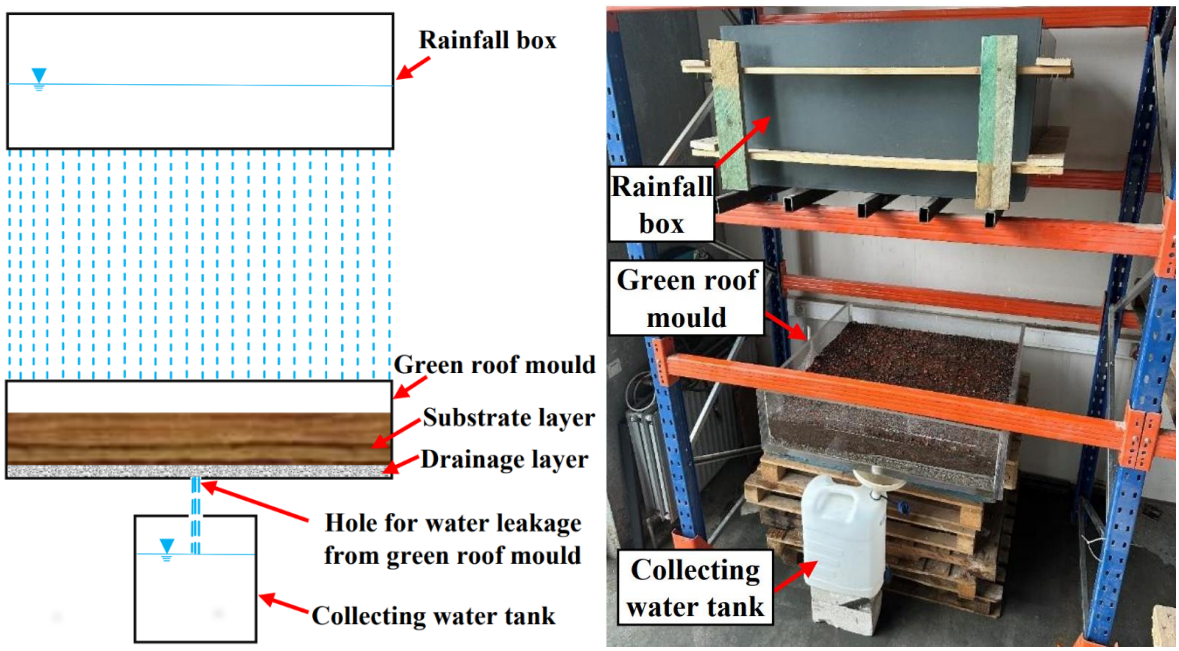

(a) (b)

Fig. 3. 1. Schematic representation (a) and experimental setup (b) for green roof test.

The rainfall box had dimensions of 100 × 100 × 50 cm (Fig. 3.2). The base of the rainfall box was drilled with a grid of holes of 2 mm diameter at 48 mm intervals as suggested by Dunnett et al. (Dunnett et al., 2008). The sewing pearl needle was put in each hole to produce drops similar to real rainfall. To simulate high rainfall intensity, the rainfall box was filled up to 21.5 cm and the water allowed to run out until the depth was 10.5 cm. For low rainfall intensity, the rainfall box was filled up to 10 cm and the water allowed to run out until the depth was 5 cm. High and low rainfall intensities lasted 55 min and 52 min, respectively.

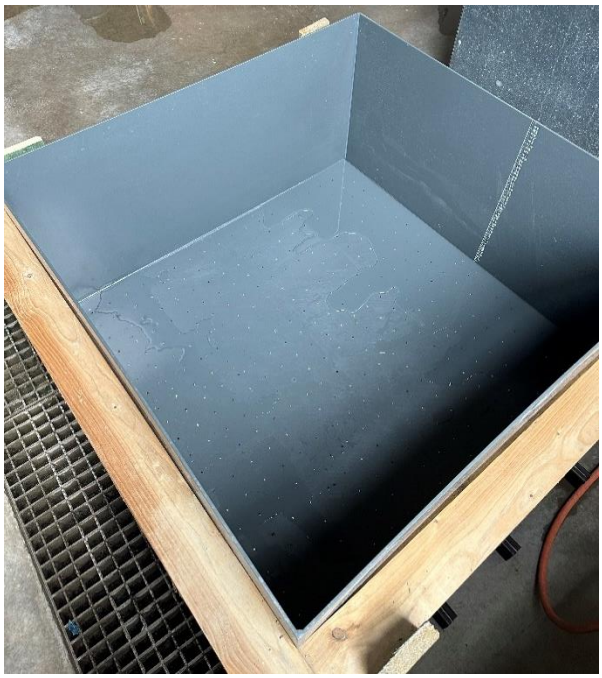

Fig. 3. 2. Rainfall box.

The detail of mini-experimental green roof mould with a base of 100 × 100 cm is shown in Fig. 3.3. A 5-cm hole for the leakage of water was generated at the bottom of the green roof mould. The slope of green roof mould's base was 2% as suggested for flat green roofs (Ampim et al., 2010; Nawaz et al., 2015).

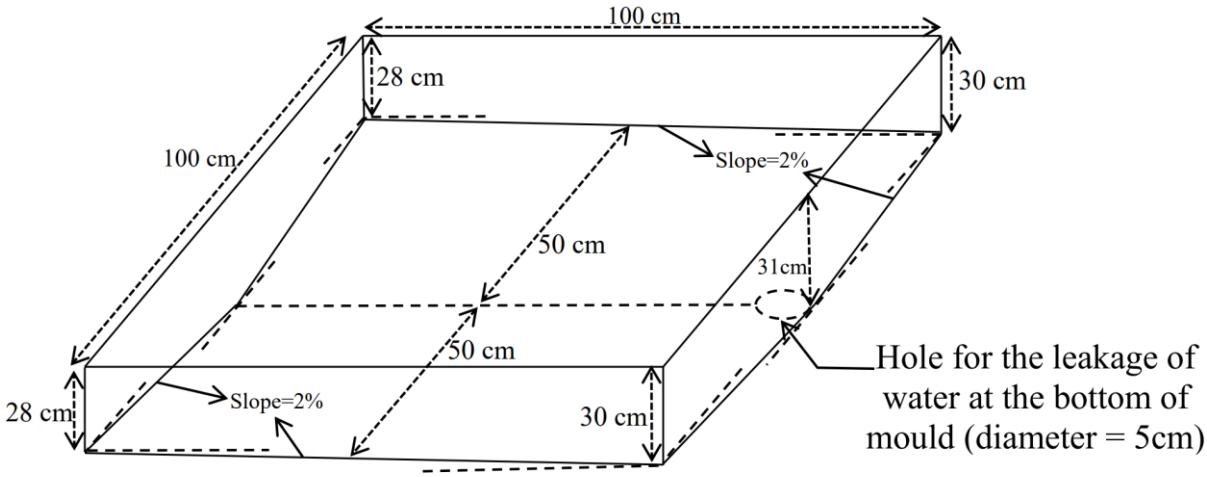

Fig. 3. 3. Detail of mini-experimental green roof mould.

3.3. Results

Fig. 3.4 shows all amounts of drained water for all specimens when the leakage of water from green roof mould stopped (4 hours after rainfall). As all materials were saturated before starting the test, the final drained water for all specimens under low rainfall intensity was near to 49 L, respectively. The respective value for specimens under high rainfall intensity 97 L.

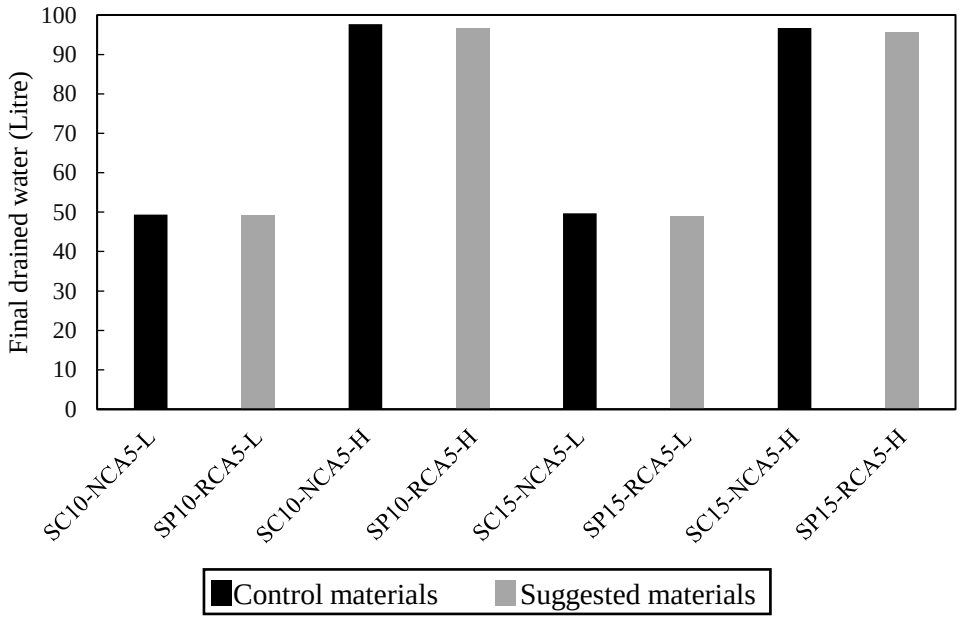

Fig. 3. 4. Final drained water.

The drained water amounts in the collecting water tank until the end of rainfall are indicated in Fig. 3.5. According to the results of low rainfall intensity, 45.7 L and 42.1 L were passed through green roofs with a 10-cm substrate layer of SC and SP, respectively. The respective values for green roofs with a 15-cm substrate layer of SC and SP were 43.5 L and 39.6 L, respectively. Therefore, the rainfall detention of green roofs with 10-cm and 15-cm substrate layer of SC was 8.6% and 10% more than those of SP.

Regarding the results at the end of high rainfall intensity (Fig. 3.5), the detained water of green roofs with a 10-cm substrate layer of SC and SP was obtained 81.8 L and 77.7 L, respectively. The corresponding values for green roofs with a 15-cm substrate layer of SC and SP were 78.6 L and 75 L, respectively. Considering this, the results of green roofs with 10-cm and 15-cm substrate layer of SC were 5.3% and 4.8% more than those of SP. In general, the detained water of green roof layers without coarse recycled materials was slightly obtained more than those of green roof layers with coarse recycled materials, similarly what was observed for water permeability results given by Kazemi et al. (M. Kazemi et al., 2023).

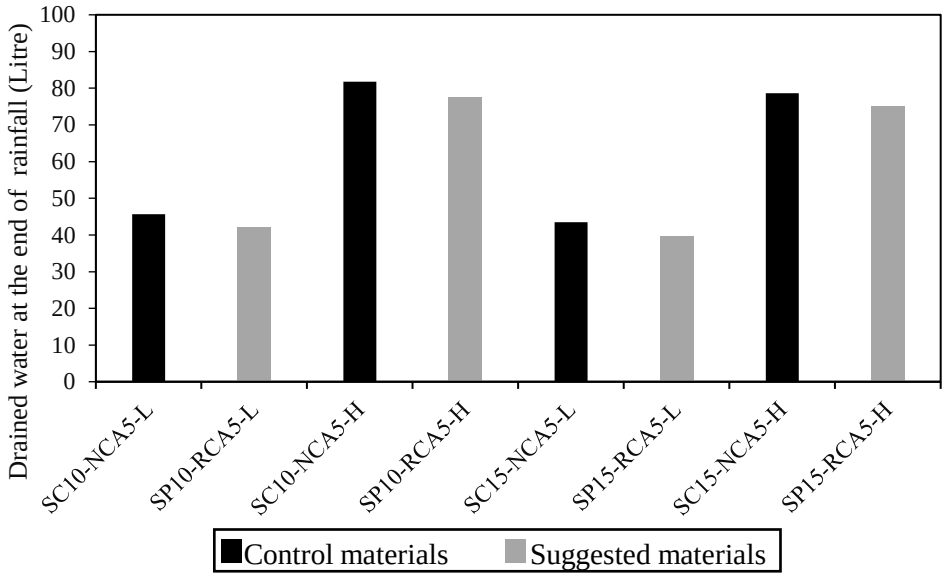

Fig. 3. 5. Drained water at the end of rainfall.

3.4. Discussion

According to Fig. 3.4, all specimens were well-saturated as the final drained water (49 L and 97 L) was near to the amount of low and high rainfall intensities (50 L and 100L). In such a condition, the narrow and complex paths among materials can play a key role in the rainfall detention of green roof layers as already reported for green roof substrate materials (Miller, 2003).

The rainfall detention of green roofs without coarse recycled materials was slightly higher than that of green roofs with coarse recycled materials under low (8.6% and 10%) and high (5.3% and 4.8%) rainfall intensities as shown in Fig. 3.5. It seems that the use of coarse recycled materials with high porosity led to generation of more tortuous paths through substrate layer, similar to what was found by other researchers (Miller, 2003; Stovin et al., 2015).

According to Fig. 3.5, for low rainfall intensity, increasing the substrate layer's thickness from 10 cm to 15 cm led to decreasing the rainfall detention of the green roof without coarse recycled materials by 4.8%. The corresponding decrease for the green roof with coarse recycled materials was 6%. Also, the respective reductions for green roofs under high rainfall intensity were less than 5%. Therefore, increasing the thickness of substrate layer from 10 cm to 15 cm marginally affected the rainfall detention performance of green roof systems either with or without coarse recycled materials, similarly to what was revealed by Pettersson et al. (Pettersson et al., 2020).

3.5. Conclusions

This study evaluated the rainfall detention performance of green roof layers including coarse recycled materials under high and low rainfall intensities. According to the results, when compared to green roofs with coarse recycled materials, the rainwater detention of green roofs without coarse recycled materials was marginally higher under low (8.6% and 10%) and high (5.3% and 4.8%) rainfall intensities. Moreover, the water detention of green roof systems was only slightly decreased (about 5%) by increasing the substrate layer's thickness from 10 cm to 15 cm either with or without coarse recycled materials.

Chapter 4: Modelling hygrothermal conditions of unsaturated substrate and drainage layers for the thermal resistance assessment of green roof: effect of coarse recycled materials

Introduction

The heat and moisture transfer within green roof layers can be affected by the type of substrate and drainage materials. Considering this, the main contribution of this chapter (paper based) is to assess whether recycled and artificial materials are able to provide nearly the same hygrothermal conditions for the green roof models as conventional materials. Therefore, the main objective of this chapter (paper based) is to model the hygrothermal behaviour of green roof materials and optimize the thickness of substrate and drainage layers. In order to shed some light on heat and moisture transfer within green roof layers including recycled materials, the hygrothermal performance is modeled using WUFI software. The measured temperatures within green roof layers' depth are used to validate the modeling outputs with experimental results. Also, a parametric study based on temperature variations is proposed to obtain the optimum thickness for green roof layers.

Further modeling research on the hygrothermal performance of green roof models under the temperate climate of Liège city is presented in the next chapter (chapter 5). In addition to this, the heat flux sensitivity to the thickness and physical characteristics of green roofs with artificial and recycled materials is assessed in chapter 5.

Abstract

Alternative materials exist for green roof layers: secondary resources like coarse or fine recycled aggregates may be used as a substitute to natural materials. For using these new types of materials, it is needed to assess their heat resistance which is performed according to ISO 9869-1 standard. Moreover, the initial hygrothermal conditions of unsaturated substrate and drainage layers have also to be modelled and assessed for optimizing the layers' thickness. In this study, the green roofs with unsaturated substrate and drainage layers incorporating coarse recycled materials were tested and assessed. The hygrothermal conditions of unsaturated substrate and drainage layers were simulated using WUFI software. A small difference (4.2%) was observed between the Rc-value of the green roofs with and without coarse recycled materials, confirming that these materials provided a sufficient thermal resistance, similar to soil particles for the substrate layer. Considering a constant thickness for the substrate layer (15 cm), a 6-cm drainage layer with coarse aggregates was considered as the optimum design for green roof systems. Besides, 18-cm unsaturated substrate layer was the optimum design when the drainage layer' thickness was considered constant (5 cm). The 6-cm drainage layer and 18-cm unsaturated substrate layer were definitely the best design for the roofing systems with the simultaneous change in the substrate and drainage layers' thickness.

Keywords: Thermal transfer modelling; parametric study; substrate; drainage layer; coarse recycled materials.

Article: Kazemi, M., & Courard, L. (2021). Modelling hygrothermal conditions of unsaturated substrate and drainage layers for the thermal resistance assessment of green roof: Effect of coarse recycled materials. Energy and Buildings, 250, 111315.
https://doi.org/10.1016/j.enbuild.2021.111315

4.1. Introduction

The rapid urbanization growth in the developing world has raised a series of intractable challenges over the environment with the overuse of natural resources to provide the internal thermal comfort in buildings, accounting for nearly 40% of the worldwide energy consumption (Abergel et al., 2017; Ascione et al., 2016; Directive, 2010; Nematzadeh et al., 2020). The energy demand of dwelling houses in urban regions is highly dependent on the building envelope components such as exterior walls and roofs (Ascione et al., 2016; Coma et al., 2016; Fan & Xia, 2017; Mirrahimi et al., 2016; Sadineni et al., 2011; Sleiman et al., 2011). Specially for poorly insulated rooftops, replacing the conventional flat roofs with the extensive green roof has drawn the attention of researchers (Coma et al., 2016; Ebadati & Ehyaei, 2020; M. Kazemi et al., 2020; Oberndorfer et al., 2007; Raji et al., 2015). As a nature-based solution, the extensive green roof has lower weight and shallower depth compared to the intensive green roof and the former is able to play a fundamental role in improving the energy efficiency of houses and rooftops (Perini & Rosasco, 2016; Sadineni et al., 2011; Van Renterghem et al., 2013).

From the top of the green roof to its bottom, its layers are composed of vegetation, substrate, filter, drainage and insulation layers (Cascone et al., 2018; Tabares-Velasco et al., 2012). Since the green roof's thermal resistance was found to be dependent on the materials' physical characteristics used for its layers including the substrate and drainage layers (M. Kazemi & Courard, 2021b), the influence of different types of materials over the green roof layers' performance has been highly regarded by researchers (M. Kazemi & Courard, 2021b, 2022; Sleiman et al., 2014). For instance, the

polyethylene modular panel and natural gravel have been used for the drainage layer (Chenani et al., 2015; Jim, 2014; Mickovski et al., 2013; Papafotiou et al., 2013; Vesuviano & Stovin, 2013). The influence of the aforementioned materials over the green roof systems' performance was compared to each other by Wanielista and Hardin (Wanielista et al., 2008). As a result, the water flowed away from the bottom of green roof system had nearly the same quality either with the natural gravel aggregate or with the polyethylene modular panel as the drainage layer. A study by Parizotto and Lamberts (Parizotto & Lamberts, 2011) demonstrated that the diffusion characteristics of substrate and the drainage layer of pebble and gravel aggregates improved the heat retention capacity of green roof systems by generating the thermal mass at the rooftops, contributing to increasing the heat transfer resistance of green roof layers and subsequently decreasing the diurnal temperature change.

Due to the dependence of the heat flux on the water content of substrate and drainage layers, the hygrothermal performance of green roof layers has already been investigated by researchers (M. Kazemi & Courard, 2021b; Ouldboukhitine et al., 2011; Qin et al., 2011; Sumner & Jacobs, 2005; Zirkelbach, 2017). Yang and Wang (J. Yang & Wang, 2014) showed that the thermal performance of green roof systems was highly dependent on the hygrothermal properties of the substrate layer. Ouldboukhitine et al. (Ouldboukhitine et al., 2011) showed that the thermal properties of the soil effectively influenced the energy balance at the substrate surface. Besides, the internal thermal comfort was improved by replacing the classical roof (concrete slab) with the green roof due to lower temperature of soil medium and better reflection of solar radiation from the substrate surface. A study by Sun et al. (Sun et al., 2013) showed that the thermal performance of the green roof was noticeably influenced by the substrate layers' moisture and the incoming solar radiation, while the effect of the relative humidity on the thermal resistance of green roof layers was not so much. He et al. (He et al., 2016) showed that the soil water content remarkably affected the evapotranspiration phenomenon and the green roof's thermal performance was improved by increasing the soil moisture level owing to increasing the evaporated water during the summer period. Vertaľ et al. (Vertal' et al., 2018) simulated the initial hygrothermal conditions of green roof layers using WUFI software and then they assessed their heat and moisture performance. According to the results, the roof membrane's temperature was affected by the substrate's water content. Moreover, the roof structure's life cycle increased owing to the participation of the substrate's water content for decreasing the membrane temperature as well as the heat flux across the roof. This process prevented overheating in buildings during the summer season. Fabisni et al. (Fabiani et al., 2018) demonstrated the thermal properties of substrate and drainage layers were influenced by their water content. As a result, the raining processes increased the substrate's thermal conductivity up to triple. According to a study by He et al. (He et al., 2020), the green roof decreased the heating and cooling loads of buildings by 6.2% and 3.6%, respectively. More importantly, increasing the substrate's water content increased the green roof's cooling effect.

The effect of the substrate and drainage layers' thickness on the green roof's thermal performance has gained much attention in recent years. Sun et al. (Sun et al., 2014) demonstrated that the water content stored on the thin substrate layer evaporated faster, leading to reducing the evapotranspiration phenomena at the rooftops and subsequently decreasing the green roof' thermal performance. On the other hand, the use of a thicker substrate layer caused to absorb more moisture by its bottom section, preventing the soil water content from participating the evapotranspiration phenomenon at the rooftop. This process resulted in decreasing the green roof's thermal resistance. In general, the

insulation performance of the green roof with a thick substrate layer was better than that of the green roof with a thin substrate layer, even though it was recommended to find the substrate layer's optimum thickness somewhere in the middle. According to a study by He et al. (He et al., 2017), the substrate layer's thickness had a remarkable effect on the heat flux through the green roof system either in winter or in summer. This effect was more in the latter. Besides, increasing the substrate's thickness positively influenced the delay time of heat flux wave and subsequently improved the insulation performance of the green roof; however, the positive effect of the substrate gradually decreased by increasing its thickness, demonstrating the fact that there was a demand to determine an optimum thickness for the substrate layer. The use of rubber crumbs and pozzolana as the drainage layer for green roof systems was tested and assessed by Coma et al. (Coma et al., 2014, 2016) in the Mediterranean climate. They showed that increasing the substrate and drainage layers' thickness might compensate low thermal performance of green roof, mainly in the winter season. Subsequently, Kazemi et al. (M. Kazemi & Courard, 2021b, 2022) simulated the green roof layers including the substrate and the drainage layer of rubber crumbs and pozzolana to assess the layers' thickness effect on the roofing system's thermal performance during the cold and warm periods. Since the WUFI software has been known as one of the best modelling tools to simultaneously stimulate the thermal and moisture transfer processes through green roof layers (Schafaczek & Zirkelbach, 2013; Vertal' et al., 2018; Zirkelbach et al., 2017), it was used by Kazemi et al. (M. Kazemi & Courard, 2021b, 2022) for modelling the heat and moisture distribution through substrate and drainage layers. Note that the materials' thermal insulation performance has been referred to some indicators, depending on the temperature (Cascone, 2019; M. Kazemi & Courard, 2022; Ling et al., 2016). Considering this, Kazemi et al. (M. Kazemi & Courard, 2021b, 2022) assessed the temperature fluctuation within green roof layers to evaluate the roofing systems' thermal resistance. The results demonstrated that increasing the substrate and drainage layers' thickness improved the thermal performance of the roofing system either for winter or for summer period, even though there were no differences between the results of thicker layers. Thus, after the optimization of green roof layers' thickness, the model with 8-cm drainage layer of pozzolana and 10-cm substrate was found to provide a sufficient thermal performance for the roofing systems.

In general, there is a demand for optimizing the green roofs' layers owing to the thermal performance sensitivity of roofing systems to the substrate and drainage layers' thickness (Coma et al., 2014, 2016; M. Kazemi & Courard, 2021b, 2022), because no information was reported by European standards about the optimum thickness of green roof layers, mainly made with different types of materials (Bellazzi et al., 2020; Saadatian et al., 2013). Additionally, it is questionable whether the use of coarse recycled materials was able to provide a sufficient thermal resistance for the green roof layers, because these materials might affect the hygrothermal conditions of substrate and drainage layers due to their great porosity porosity (Akbarzadeh Bengar et al., 2020; M. Kazemi et al., 2019, 2021; Mehrabi et al., 2021; Nematzadeh et al., 2018; Nematzadeh & Baradaran-Nasiri, 2019; Toghroli et al., 2020; Z. Zhao et al., 2020). In light of the foregoing background, in this study, green roofs with the unsaturated substrate incorporating coarse recycled materials and the drainage layer of recycled coarse aggregate were tested and assessed following ISO 9869-1 (ISO 9869-1, 2014). Later on, the hygrothermal conditions of unsaturated substrate and drainage layers were translated into the WUFI software and the modelling outputs were compared with green roof specimens' results. Considering the fact that the thermal insulation performance was related to the

temperature distribution through the depth of materials (Cascone, 2019; M. Kazemi & Courard, 2022; Ling et al., 2016; Simões et al., 2020), the temperature variation within green roof layers was evaluated, where the substrate and drainage layers' thickness was changed to achieve an optimum design of green roof systems with an adequate thermal performance.

4.2. Methodology

The reference green roof specimen was composed of the unsaturated substrate without coarse recycled materials and the drainage layer of natural coarse aggregate (Figs. 4.1(a) and 4.1(b)): the substrate will act as a support for growing plants and the drainage layer will play an important role beneath the substrate for evacuating water. Besides, the alternative green roof specimen considered unsaturated substrate with recycled tiles and bricks and the drainage layer of recycled coarse aggregate (Figs. 4.1(c) and 4.1(d)).

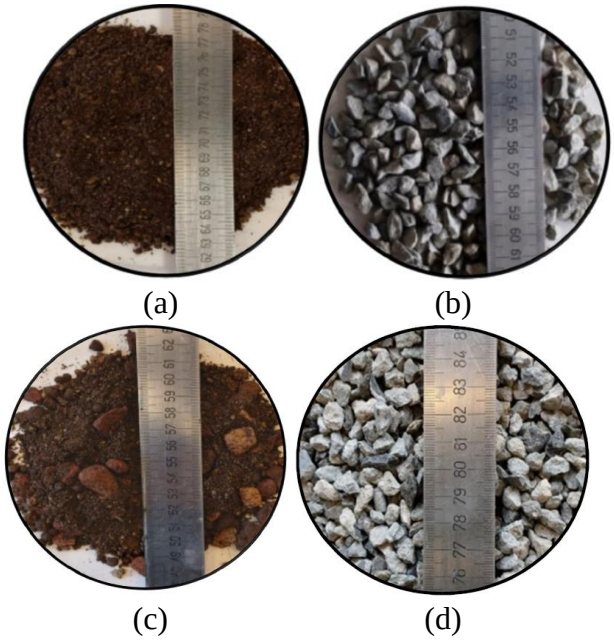

Fig. 4. 1. The unsaturated substrate without coarse recycled materials (a); the natural coarse aggregate for the drainage layer (b); the unsaturated substrate containing recycled tiles and bricks (c); the recycled concrete coarse for drainage layer (d).

The minimum coarse aggregate size is 5 mm according to EN 12620 (EN 12620, 2013). On the other hand, the use of aggregates with very big size is not suitable for the thin depth of the drainage layer (5 cm). Therefore, since the water flux should easily pass through the drainage layer (Vesuviano & Stovin, 2013; Wanielista et al., 2008), the size of 7 mm was considered for the natural and recycled coarse aggregates.

The total thickness of green roof specimens was 20 cm, where the substrate and drainage layers' thicknesses were considered to be 15 cm and 5 cm, respectively (Fig. 4.2(a)). A thin filter layer was used to separate the substrate and drainage layer from each other as shown in Fig. 4.2(a). The green roof including substrate and drainage layers was put in a 40 × 40 × 20 cm experimental mould and then, they were placed in the centre of thermal transfer measurement device between the cold and hot plates ((Fig. 4.2(b)), where the surrounding area of the mould was insulated using the polyurethane foam. After that, the mould mentioned above was compressed between the hot and cold plates and

their bottom and top were exposed to the temperatures. The thermal conductivity value was automatically measured using the device by means of a sensor installed in the hot plate.

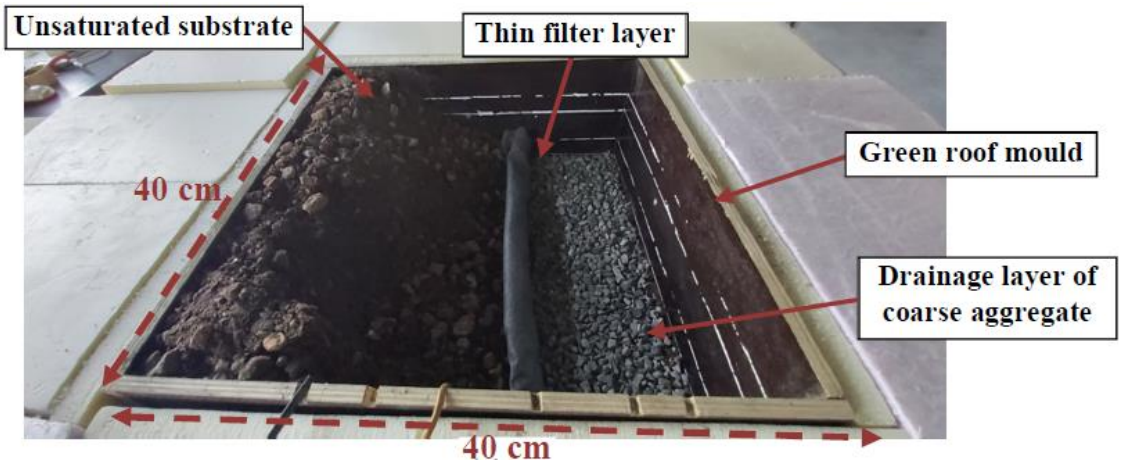

(a)

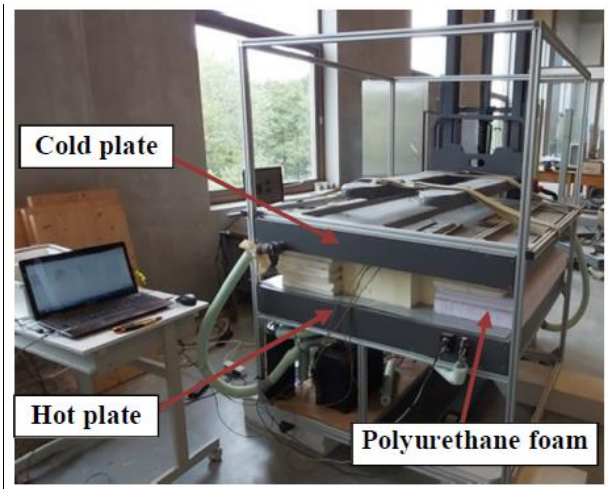

(b)

Fig. 4. 2. Thermal transfer measurement device (a); green roof mould (b).

Fig. 4.3(a) shows a sketch of the control and the proposed green roofs with substrate and drainage layers (NCA5-SC15 and RCA5-SP15). The NCA and RCA were referred to the natural (N) and recycled (R) coarse (C) aggregates (A). Moreover, the substrate layers without and with coarse recycled materials were the control (SC) and the proposed (SP) substrate layers. A cross-sectional view for the 15-cm unsaturated substrate without and with coarse recycled materials (SC15 and SP15) is shown in Fig. 4.3(b). The unsaturated substrate layers were put in a 40 × 40 × 15 cm experimental mould and they were separately placed in the centre of the thermal transfer measurement device to obtain their thermal resistance. Fig. 4.3(c) presents the 5-cm natural and recycled coarse aggregates as the drainage layers (NCA5 and RCA5). These layers were separately put in a 40 × 40 × 5 cm experimental mould. After that, they were placed in the centre of the thermal transfer measurement device to assess their thermal performance as the drainage layer. In brief, after the heat resistance measurement of green roof layers following ISO 9869-1 (ISO 9869-1, 2014), their thermal resistance was compared to each other.

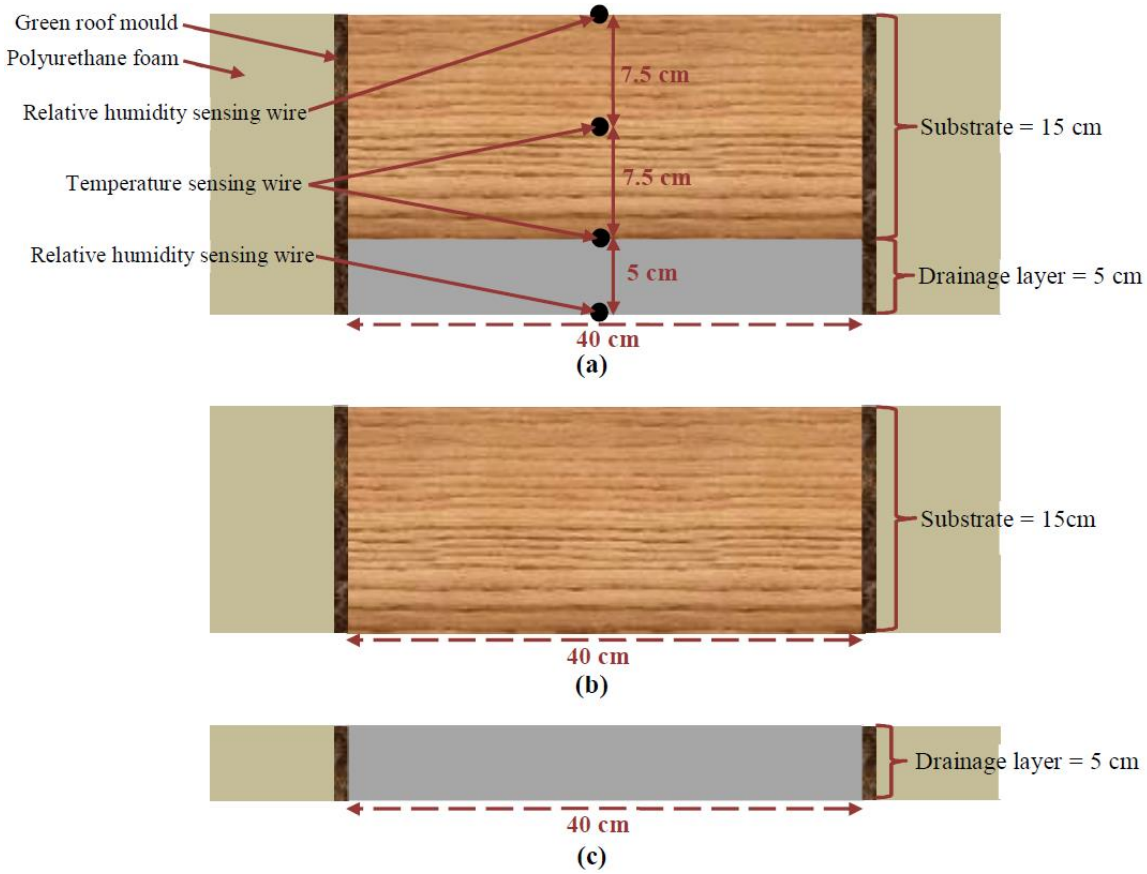

Fig. 4.3. Sketches of green roof layers including the substrate and drainage layers (a); the substrate layer (b); drainage layer (c).

In the next step, the hydrothermal conditions (heat and moisture properties) of the unsaturated substrate layers and coarse aggregates were measured and they were introduced to the WUFI software for modelling the control and the proposed green roof specimens (NCA5-SC15 and RCA5-SP15). Note that the temperatures of the cold and hot plates were applied to the top and the bottom of green roof models. Apart from these temperatures, the air relative humidity at the top and the bottom of the roofing specimens was introduced to the top and bottom of green roof models as well. The air relative humidity was measured using two relative humidity sensing wires installed at the top and the bottom of green roof specimens as shown in Fig. 4.3(a). Moreover, the temperatures in the middle of substrate and between the substrate and the drainage layer were recorded using two temperature sensing wires (Fig. 4.3(a)). These two measured temperatures through green roof layers' depth were used to validate the modelling outputs with experimental results.

After the validation of green roof models, since the materials' thermal insulation performance has been related to some indicators depending on the temperature (Cascone, 2019; M. Kazemi & Courard, 2022; Ling et al., 2016), the temperature distribution within green roof models was evaluated for the optimization of green roof layers. Indeed, by increasing the thickness of the substrate and drainage layers, the optimum design of green roof layers could be determined when no change in the temperature through green roof's depth was observed.

4.3. Materials properties and characteristics

4.3.1. Thermal heat transfer (ISO 9869-1)

The thermal conductivity value (λ) was automatically measured by the thermal transfer measurement device (Fig. 4.2(b)). The lower value of thermal conductivity indicates the higher ability of materials to resist the heat flow (Berardi, 2019). Eq. (4.1) presents the difference between the top and bottom surfaces of specimen (ΔT):

$$\Delta T = T_h - T_c \quad (4.1)$$

Where T_h and T_c are the temperatures in the thermal device's heating and cooling sides, respectively (K).

According to Fourier's law, the density of heat flow rate (q) with the unit of W/m^2 was calculated using Eq. (4.2):

$$q = \lambda.\frac{\Delta T}{l} \quad (4.2)$$

Where *l* is the thickness of green roof layers (m).

Eq. 4.3 was used to evaluate the convergence of R_c-value (m^2K/W) using the Average Method given by ISO 9869-1 (ISO 9869-1, 2014). The higher amount of R-value demonstrates the more thermal resistance and better insulation performance of materials (ISO 9869-1, 2014; Peng & Wu, 2008).

$$R_c = \frac{\sum_{t=0}^{m} \Delta T^t}{\sum_{t=0}^{m} q^t} \quad (4.3)$$

Where *t* is the time interval and *m* is the minimum required measurement period (h).

To report an acceptable R_c-value based to the Average Method, three main criteria to fulfill and stop the measurement have to be considered as mentioned in the following:

- The measurement period should take at least 72 h.
- The value calculated at the end of the data set should not deviate more than ±5% from the respective value obtained 24 h before.
- The resulting value when applying the method to the first 67% of data should not deviate by more than ±5 % from the respective value when analyzing the last 67% of the data.

To converge R_c-value using the Average Method given by ISO 9869-1 (ISO 9869-1, 2014), it has been recommended that the difference between exterior and interior surface temperature should be at least 5-10 °C when using the Average Method (Desogus et al., 2011; ISO 9869-1, 2014; Rodler et al., 2019). Therefore, the top and bottom of green roof specimens were subjected to 16.5 °C and 23.5 °C, respectively, resulting in the surface temperature difference of 7 °C.

4.3.2. Green roof layers' properties

Table 4.1 presents the properties of the substrate and coarse aggregates. To model the green roof layers using WUFI software, it was required to obtain the specific capacity of materials in the dry condition. To dry the substrate and coarse aggregates, they were kept in the 40°C oven for 7 and 2 days, respectively. After that, their specific heat capacity was measured using the Calorimetric method based on ASTM D4611-16 (ASTM D4611 - 16, 2018). This parameter for the dry substrate without and with coarse recycled materials was 880 J/kg K and 810 J/kg K, respectively. The specific heat capacity for recycled and natural coarse aggregates was obtained 730 J/kg K and 770 J/kg K,

respectively. The aforementioned values were nearly within the specific heat capacity ranges given for the dry soil and dried aggregate (Engineering ToolBox, 2003; IES VE, 2018). To consider the moisture content effect of green roof layers on their thermal conductivity values, it was required to measure this parameter for the substrate and coarse aggregate layers in both dry and unsaturated conditions according to ISO 9869-1 (ISO 9869-1, 2014) using the thermal transfer measurement device. Therefore, the relationship between water content of materials and their conductivity could be automatically generated as described in the section 4.3.2.5.

Table 4. 1. Green roof layers' properties.

Materials	Substrate without coarse recycled materials	Substrate with coarse recycled materials	Natural coarse aggregate	Recycled coarse aggregate
Bulk density, ρ_s (kg/m^3)	1075.23	1000.95	1436.56	1164.47
Porosity	0.482	0.4863	0.4167	0.4956
Specific heat capacity, Dry (J/kg K)	880	810	770	730
Thermal conductivity, Dry, λ (W/m·K)	0.15	0.17	0.114	0.11
Water vapour diffusion resistance factor, μ	3.62	3.35	1	1
Reference water content, W_{80} (kg/m^3)	10.31	7.73	1.159	3.321
Free water content (kg/m^3)	380.95	285.71	42.86	122.76
Water absorption coefficient, A_1 (kg/m^2.s$^{0.5}$)	0.47	0.22	0.0256	0.072
Typical Built-in moisture (kg/m^3)	125.46	87.35	4.21	14.34

The moisture properties, porosity, water vapour diffusion resistance factor and water absorption coefficient of substrate and coarse aggregates were measured in the laboratory as described in the following sections:

4.3.2.1 Water content

The unsaturated substrate and coarse aggregates' water contents were measured using the gravimetric analysis following NF ISO 16586 (ISO 16586, 2003) in which they were put and kept inside of the oven at 105°C for 48 h to become completely dried out.

The free water content (W_f) is the ability of materials for holding the water content. Indeed, this parameter is dependent on the capillary action of materials, trapping the water molecules within their pore structure at a relative humidity of 100%. However, due to the trapped air in the porous structure, the value of free water content is lower than the maximum water content (W_{max}). In fact, the latter can be measured by the materials' porosity (Künzel, 1995). Therefore, a method for measuring the free water content of soil and coarse aggregates was used as suggested by other researchers (Awulachew et al., 2009; Brouwer et al., 1985). In this method, a specific volume of the dry soil was put inside of the funnel in which a cotton wool in its neck was used to prevent washing soil particles away as shown in Fig. 4.4. After that, the specific amount of water was added to the dry soil using the measuring beaker to assess its water-holding capacity. By subtracting the collected water in the measuring cylinder from the water added using the measuring beaker, the trapped water by the dry soil was measured. Therefore, the free water content (W_f) for a specific volume of soil medium was obtained. As presented in Table 4.1, the W_f value for the substrate without coarse recycled materials was obtained 380.95 kg/m^3 ,which was close to the value for the conventional soil as obtained by other researchers (Vertal' et al., 2018).

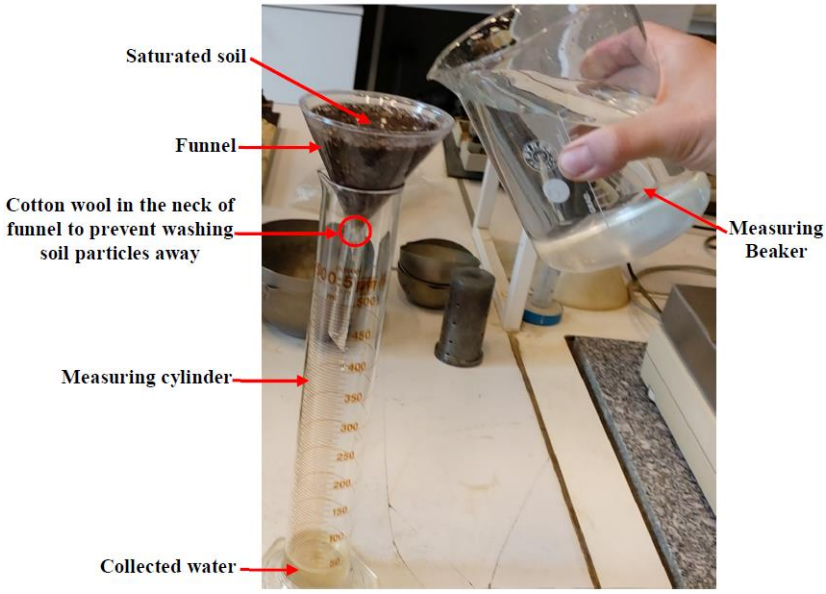

Fig. 4. 4. Determining water-holding capacity of soil.

4.3.2.2 Porosity

To obtain the porosity of the drainage layer, the aggregate was first added to the beaker with a volume 900 cm^3 as shown in Fig. 4.5. Then, the water was added to the same beaker to fill all voids among aggregates. Obviously, some water could be absorbed by pores of aggregates. The water absorption for recycled coarse aggregates was more than that for natural coarse aggregates as expected. To ensure that the aggregates' pores were fully filled with water, the beaker was closed and kept for 24 h after adding the water. Later on, the surface of water in the beaker with natural coarse aggregates remained constant. After 24 h, the water surface slightly decreased in the beaker with recycled coarse aggregates due to their high porosity. Therefore, a few amount of water was added to the beaker with recycled coarse aggregates to return its surface to 900 cm^3. According to the results, to fill all void spaces and pores of recycled coarse aggregates in beaker with the volume of 900 cm^3, it was required to add 446 cm^3. The corresponding value for natural coarse aggregate was 375 cm^3. Considering the density of water of 1 g/cm^3, the porosity of drainage layer of aggregates was calculated using Eq. 4.4. This value for recycled and natural coarse aggregates was obtained 49.56 % and 41.67%, respectively. It is noteworthy that the aforementioned method was also used by other researchers (Madandoust et al., 2019) in which the aggregates can be submerged in the water for 24 h (the saturated surface-dry condition) to make them fully saturated.

$$\text{Porosity of drainage layer} = \frac{\text{Volume of void spaces and pores of aggregates filled with water content}}{\text{Total volume (including volume of void spaces,aggregates and their pores)}} \times 100 \qquad (4.4)$$

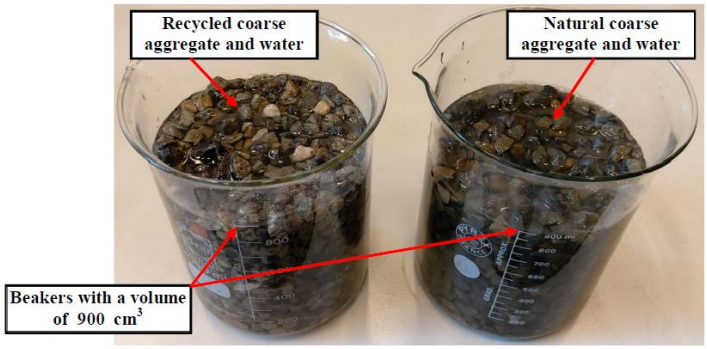

Fig. 4. 5. Beakers filled with aggregates and water.

By measuring the volume of void spaces among soil particles, the porosity of substrate was calculated using Eq. 4.5. For this purpose, the volume of dry substrate was determined. Considering the density of water of 1 g/cm^3, the dry substrate with the same volume was fully saturated by water to fill all void spaces among soil particles. Thereafter, the saturated soil was kept in an oven at 105 °C for 48 h to measure the water content in the sample using the gravimetric method in accordance with the NF ISO 16586 (ISO 16586, 2003). As per the results, the porosity of the substrate with coarse recycled materials was obtained 48.63%. The corresponding value for the substrate without coarse recycled materials was 48.2%.

$$\text{Porosity of substrate} = \frac{\text{Volume of void spaces among soil particles}}{\text{Total volume (including volume of void spaces and soil particles)}} \times 100 \quad (4.5)$$

4.3.2.3 Water vapour diffusion resistance

The μ-value is the water vapour diffusion resistance factor, representing the ratio of the diffusion coefficients of water vapour in air (D_{w0}) and in the building materials (D_w) as shown in Eq. 4.6. Due to very low diffusion resistance of porous materials like coarse aggregate layers, the μ-value was assumed to be close to 1, while higher amounts of this parameter should be measured and calculated for the materials with more diffusion resistance (Krus, 1996).

$$\mu = \frac{D_{w0}}{Dw} \quad (4.6)$$

According to DIN 52 615 (DIN 52 615, 1973), in the physics of building materials, the vapour diffusion coefficient in air was calculated using an empirical equation given by Schirmer (Schirmer, 1938) as presented in Eq. 4.7:

$$D_{w0} = 2.3\times10^{-5}\times \frac{P_0}{P_L} \times \left(\frac{T}{273.15}\right)^{1.81} \quad (4.7)$$

Where P_0 was the standard pressure in Pa (101325 Pa), P_L was ambient atmospheric pressure in Pa (for Liège city = 102300 Pa) and T was absolute temperature in K (295.15 K). Considering these values, the vapour diffusion coefficient in air, D_{w0}, was obtained $2.62 \times 10^{-5}\ \frac{m^2}{s}$.

As mentioned by Togkalidou et al. (Togkalidou et al., 2013), assuming the isothermal conditions and the ideal gas behavior of water vapour, the water vapour diffusivity (D_w) can be attributed to the water vapour permeability (D_v) as shown in Eq. 4.8:

$$D_w = \frac{D_v.R.T}{M} \quad (4.8)$$

Where D_w is the water vapour diffusivity in $\frac{m^2}{s}$, D_v is water vapour permeability in $\frac{m^2}{s}$, R is molar gas constant in m^2 kg s^{-2} K^{-1} mol^{-1} (8.3144598 m^2 kg s^{-2} K^{-1} mol^{-1}), T is temperature in K and M is the water vapour molecular weight in $\frac{kg}{mol}$ (0.01801528 $\frac{kg}{mol}$).

According to ISO 12572 (ISO 12572, 2001) and EN 1015-19 (EN 1015-19, 1999), the cup test method can be used for obtaining the water vapour permeability (D_v). In this method, the testing samples should be sealed on the open mouth of cups in which the water vapour pressure is kept constant at appropriate levels by means of saturated salt solutions. The cups are placed in a temperature controlled environment with a constant water vapour pressure different from that inside the cups. The rate of moisture transfer is determined from the change in weight of cups under steady state conditions. As per EN 1015-19 (EN 1015-19, 1999), the water vapour permeability (D_v) can be obtained by multiplying the water vapour permeance (Λ) by the thickness of specimen (ℓ) as presented in Eq. 4.9:

$$D_v = \Lambda.\ell \tag{4.9}$$

Where the units of water vapour permeance (Λ) and thickness of specimen (ℓ) are $\frac{kg}{m^2.s.Pa}$ and m, respectively.

Eq. 4.10 can be used for obtaining the water vapour permeance (Λ):

$$\Lambda = \frac{1}{A.\frac{\Delta P}{(\frac{\Delta G}{\Delta t})} - R_A} \tag{4.10}$$

Where A is the area of the open mouth of the test cup in m^2 (0.02 m^2) based on EN 1015-19 (EN 1015-19, 1999), R_A is the water vapour resistance of the air gap between the specimen and the salt solution (0.048×10^9 $\frac{Pa.m^2.s}{kg}$ per 10 mm air gap), $\frac{\Delta G}{\Delta t}$ is the water vapour flux in $\frac{kg}{s}$, which can be obtained using the cup test method and ΔP is the difference in water vapour pressure between the ambient air and the salt solution. Eq. 4.11 is proposed by BS 5250 (BS 5250, 2011) for the calculation of the pressure, P (hPa =100Pa).

$$P = \varphi \times 610.5 \times e^{\frac{17.269 \times \theta}{237.3+\theta}} \tag{4.11}$$

Where φ is the relative humidity and θ is the temperature in ^oC.

Based on the above equations, cup test method was used for measuring the water vapour transmission rate (EN 1015-19) (EN 1015-19, 1999). To calculate the water vapour permeance (Λ) using Eq. 4.10, it was required to obtain some parameters including A, R_A, ΔP and $\frac{\Delta G}{\Delta t}$. Concerning this, cubic specimens with a thickness of 4 cm were prepared (Fig. 4.6(a)). The area of the open mouth of the test container (A in Eq. 4.10) was 0.02 m^2 (0.14×0.14 m). The thickness of air layer (Fig. 4.6(a)) was equal to 10 mm used for determining R_A in Eq. 4.10. To obtain the ΔP, the pressures inside and outside of the container (P_{in} and P_{out}) were calculated using Eq. 4.11. The container was placed in a conditioning chamber with a Heating Ventilation and Air Conditioning (HVAC) system (Fig. 4.6(b)), where according to the EN 1015-19 (EN 1015-19, 1999), the relative humidity and

temperature were required to be 50 ± 5% and 20 ± 2 ºC, respectively. The outside relative humidity (φ) and temperature (θ) in the conditioning chamber were equal to 0.51 and 22 ºC, respectively. Considering these values in Eq. 4.11, P_{out} was obtained 134762.8 Pa. Inside of the container (22°C), a saturated solution of potassium nitrate KNO_3 guaranteed a relative humidity of 93.2% as proposed by EN 1015-19 standard (EN 1015-19, 1999). So, the inside relative humidity (φ) and temperature (θ) in Eq. 4.11 were equal to 0.932 and 22 ˚C, respectively. Based on these values, P_{in} was obtained 246272.5 Pa. Hence, ΔP value was equal to 111509.635 Pa. Another parameter in Eq. 4.10 was $\frac{\Delta G}{\Delta t}$, representing the water vapour permeability rate. This parameter could be defined as a function of the amount of water vapour, passing through the soil specimen's surfaces. As shown in Fig. 4.7, $\frac{\Delta G}{\Delta t}$ values were determined from the graphs of substrate specimens, regardless of lines' negative slope. It is noteworthy that the lateral faces of plastic container were water proofed with epoxy resin to prevent passing the moisture transfer from its edges as shown in Fig. 4.6(b); moreover, a stainless steel woven mesh at the bottom of the container of specimen was holding the sample in place. After obtaining all parameters in Eq. 4.10, the water vapour permeance (Λ) was calculated. Later on, the water vapour permeability (D_v) was calculated using Eq. 4.9. After that, the water vapour diffusivity of specimen (D_w) was obtained using Eq. 4.8. Finally, the water vapour diffusion resistance Factor (μ) was calculated using Eq. 4.6. Therefore, the μ-value of the substrate with and without coarse recycled materials was obtained 3.35 and 3.62, respectively. These values were nearly within the ranges given for soil materials (Cagnon et al., 2014; Giada et al., 2019; Vertal' et al., 2018).

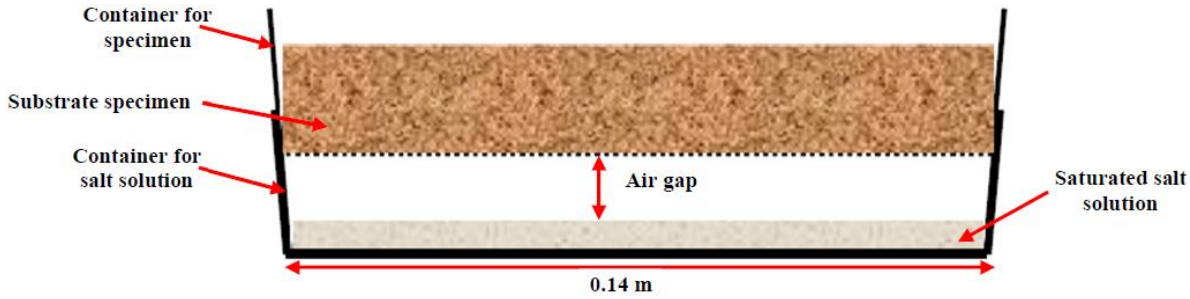

(a)

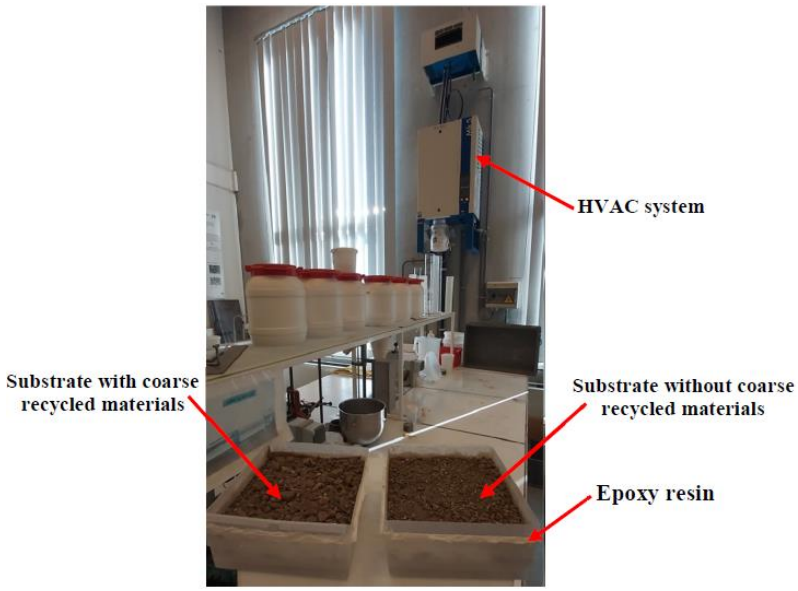

(b)

Fig. 4. 6. A cross-sectional view of cup test method (a); Substrate specimens in the conditioning chamber (b).

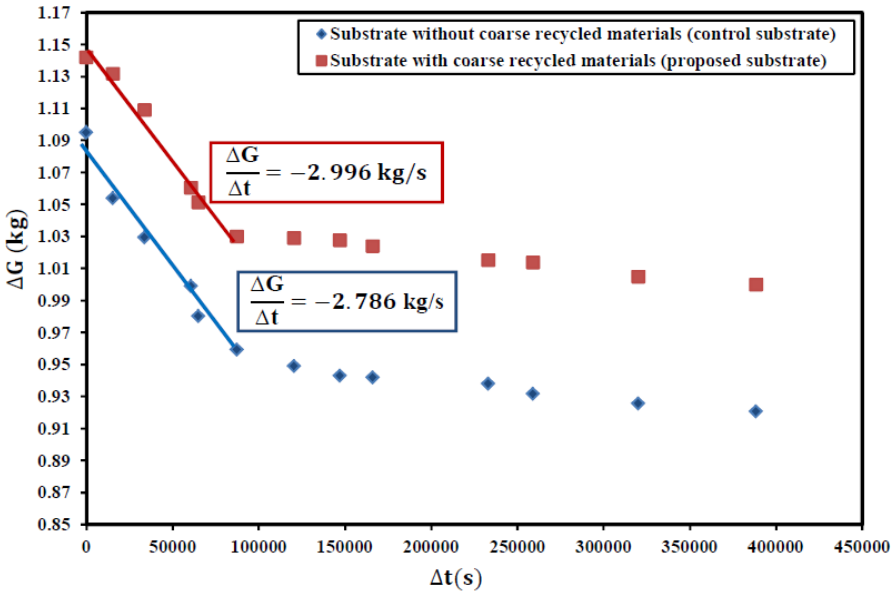

Fig. 4. 7. The water vapour flux for the substrate with and without coarse recycled materials.

4.3.2.4 Water absorption coefficient

A cross-sectional view of capillary test is shown in Fig. 4.8(a). According to EN 1925 (EN 1925, 1999), the soil specimens were put in the right circular cylinder with a diameter of 50 ± 5 mm and then, they were immersed in 3 ± 1 mm of water on one of their sides. As indicated in Fig. 4.8(b), the specimens were hung from the bottom of the weighing scale to record their weight over time by sucking the water from their bottom side. The water absorption coefficients for the substrate and coarse aggregates are shown in Fig. 4.9. Depending on the type of materials, this coefficient varies remarkably. For instance, the water absorption coefficients of the substrate with and without coarse

recycled materials were obtained 0.22 kg/m^2.s$^{0.5}$ and 0.47 kg/m^2.s$^{0.5}$, respectively, which were within the ranges given by Soudani et al. (Soudani et al., 2018) for soil materials.

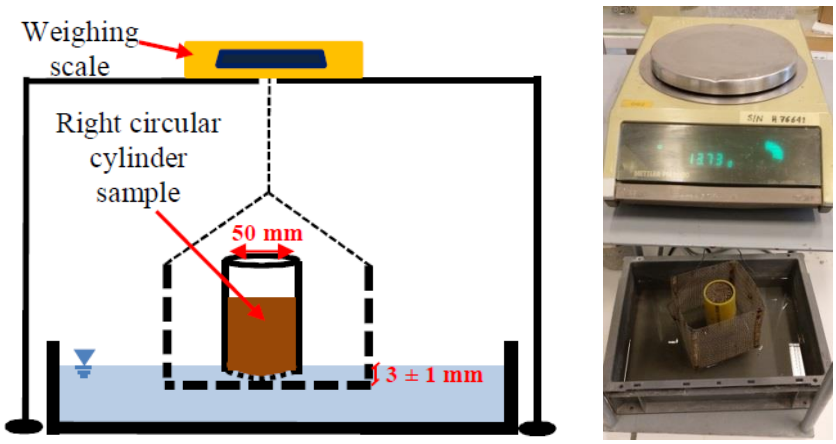

(a) (b)

Fig. 4. 8. A cross-sectional view of capillary test (a); testing setup in lab (b).

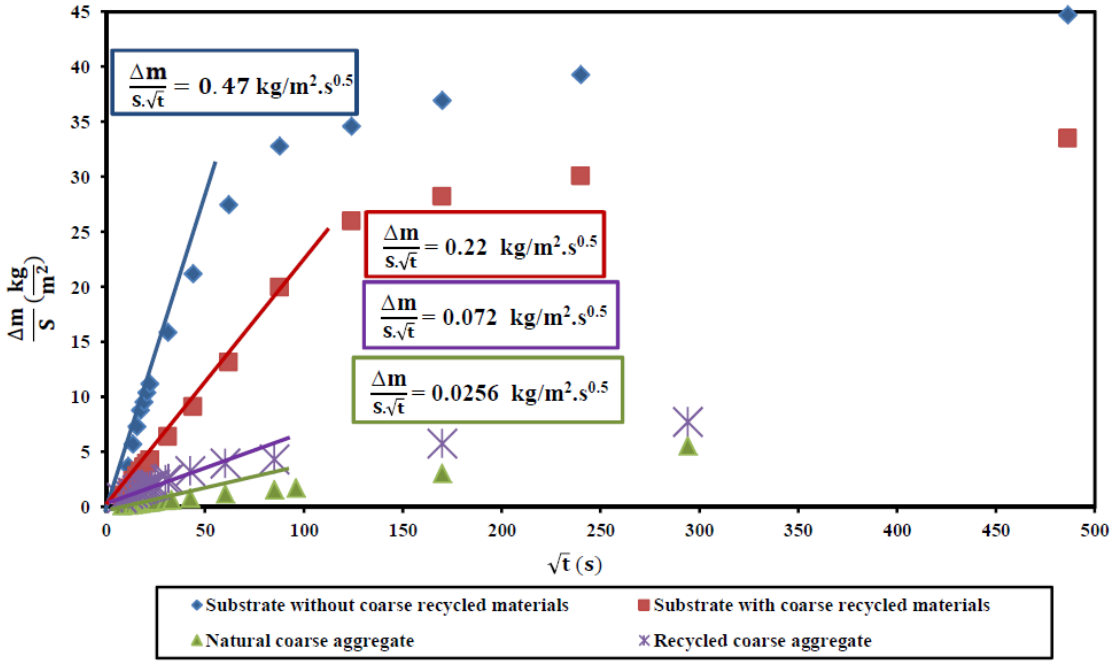

Fig. 4. 9. Water absorption coefficients for the materials used for the green roof layers.

4.3.2.5 Modelling green roof layers parameters

In this study, the WUFI simulation software was implemented for modelling and optimizing the green roof layers' thickness. To reliably validate the numerical models with the roofing systems' results, the green roof layers were automatically meshed using the fine grids available in the WUFI software. After introducing the free water content (W_f) to the software, the moisture storage function (Eq. 4.12) could be automatically used by WUFI (Holm et al., 1996; Krus, 1996) to obtain the moisture storage graphs of substrate and coarse aggregates as shown in Fig. 4.10(a).

$$W = W_f \times \frac{(b-1).\varphi}{b-\varphi} \quad (4.12)$$

Where W is the moisture content corresponding to relative humidity ($\frac{kg}{m^3}$) and b is the approximation factor that can be empirically specified by recognizing the moisture content of substrate and coarse aggregates in equilibrium at a relative humidity of 0.8 (Pérez-Bella et al., 2015). This factor ranges from 0 to 1 and it is close to 1 for free water saturation (Ochs et al., 2008). Note that the typical built-in moisture was the moisture corresponding to the materials' relative humidity of 0.8 (Holm et al., 1996; Krus, 1996). This parameter for the substrate and coarse aggregates was calculated using Eq. 4.12 as presented in Table 4.1. Moreover, to obtain the moisture storage graphs of materials in WUFI software, the reference water content, W_{80}, was calculated using Eq. 4.12 when the relative humidity of materials should be assumed 0.8 (Holm et al., 1996; Krus, 1996).

Another parameter was the moisture-induced heat conductivity supplement (b_1), which could be defined as the percentage increment in thermal conductivity per the percentage increment in moisture content. To calculate b_1, the values of bulk density, thermal conductivity of materials with a specific amount of water content were substituted into Eq. 4.13 (Allinson & Hall, 2010).

$$b_1 = \frac{(\frac{\lambda(w)}{\lambda_0} - 1) \times \rho_s}{W} \tag{4.13}$$

Where the $\lambda(w)$ and λ_0 are the thermal conductivity of materials in moist and dry conditions, respectively (W/m·K). After introducing b_1 values to the WUFI software, a linear relationship between the thermal conductivity and the normalized water content could be automatically generated using Eq. 4.13 as shown in Fig. 4.10(b) (Allinson & Hall, 2010; Veas, 2006; Vertal' et al., 2018). The normalized water content was the ratio of the water content (kg/m^3) to the maximum water content (kg/m^3).

The capillary uptake of water for the fully saturated materials can be defined as a parameter in WUFI software, namely the liquid transport coefficient for suction (D_{ws}). The liquid transport coefficient for redistribution (D_{ww}) represents the spread of the imbibed water when the fully saturated condition is finished. This process is associated with the beginning of the water redistribution through the material's depth without uptaking the water (Krus, 1996; Künzel, 1995) . The D_{ws} parameter could be related to the normalized water content using Eq. 4.14 after introducing the materials' water absorption coefficient to the WUFI software as shown in Fig. 4.10(c) (Krus, 1996; Krus & Künzel, 1995; Torres & de Freitas, 2001).

$$D_{ws}(w) = 3.8\ (\frac{A_1}{w_f})^2 \times 1000^{(\frac{w}{w_f})^{-1}} \tag{4.14}$$

Where A_1 is the water absorption coefficient. As shown in Fig. 4.10(d), the D_{ww} parameter was automatically identical to the D_{ws} parameter using the WUFI software for simplicity (Kordziel et al., 2020; Krus, 1996; Vertal' et al., 2018).

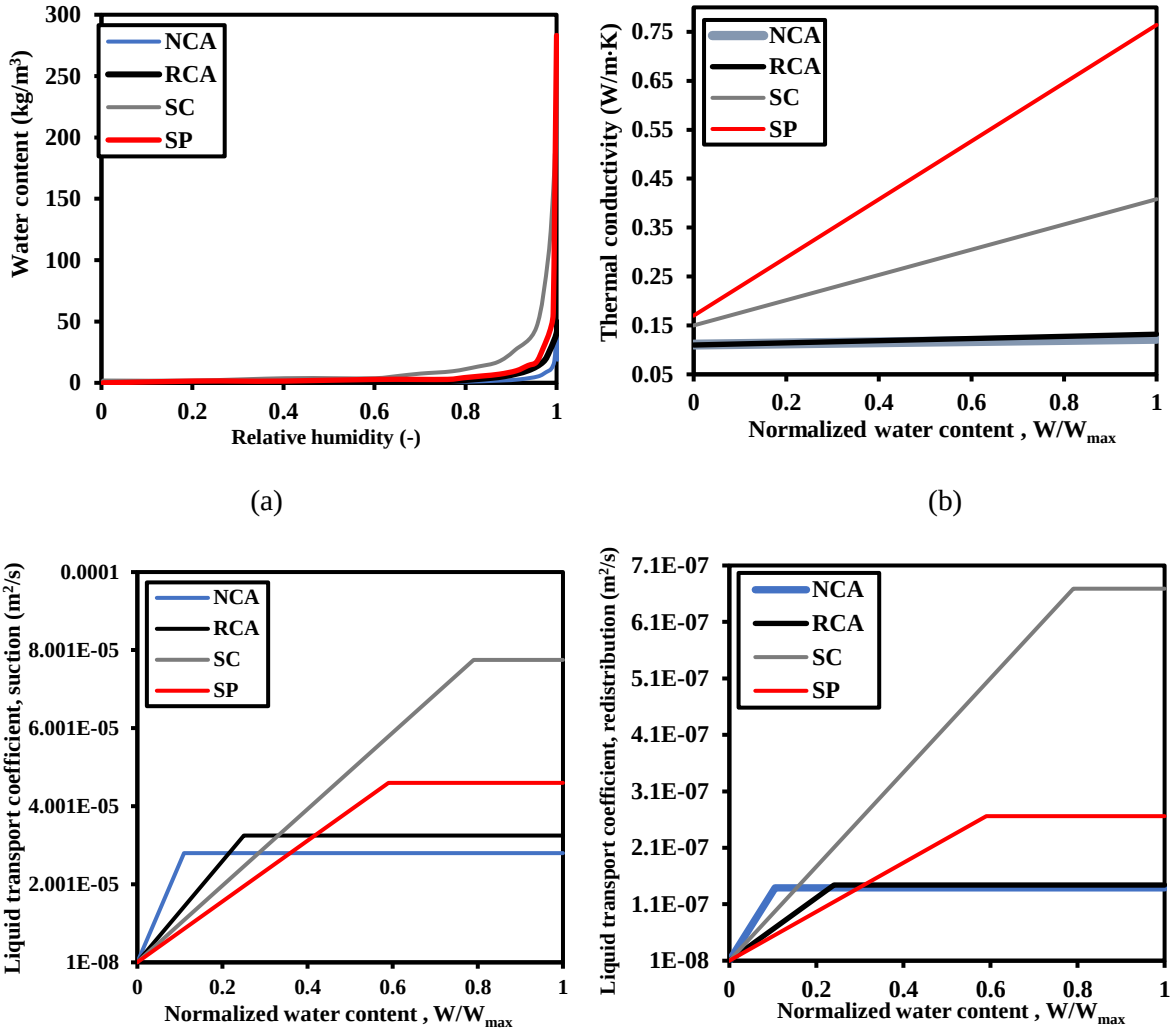

Fig. 4. 10. Moisture storage graph (a); thermal conductivity versus materials' water content (b) ; liquid transport coefficient for the capillary suction (Dws) (c); liquid transport coefficient, for the capillary redistribution (Dww) (d).

4.3.2.6 Green roofs' geometrical characteristics

Table 4.2 presents the green roof layers' geometrical characteristics. After validation of the control and the proposed green roof models with 15-cm substrate and 5-cm coarse aggregate layers (NCA5-SC15 and RCA5-SP15), their thicknesses were numerically changed using the WUFI software to achieve an optimum design of roofing systems. First, the drainage layer's thickness was changed from 5 cm to 4, 6, 7 and 8 cm when the substrate layer's thickness was kept 15 cm for both the control and the proposed green roof models. Later on, the substrate's thickness was changed from 15 cm to 12, 18, 21 cm when the drainage layer's thickness was kept 5cm for both the control and the proposed green roof models. After that, as presented in Table 4.1, the substrate and drainage layers' thickness was simultaneously changed by keeping the ratio of substrate to drainage layer constant (3).

Table 4. 2. Green roofs' geometrical configurations.

No.	Specimens ID	Thickness (cm)	
		Drainage layer	Substrate
1	NCA[a]4-SC[b]15	4	15
2	NCA5-SC15	5	15
3	NCA6-SC15	6	15
4	NCA7-SC15	7	15
5	NCA8-SC15	8	15
6	NCA5-SC12	5	12
7	NCA5-SC18	5	18
8	NCA5-SC21	5	21
9	NCA4-SC12	4	12
10	NCA6-SC18	6	18
11	NCA7-SC21	7	21
12	RCA[c]4-SP[d]15	4	15
13	RCA5-SP15	5	15
14	RCA6-SP15	6	15
15	RCA7-SP15	7	15
16	RCA8-SP15	8	15
17	RCA5-SP12	5	12
18	RCA5-SP18	5	18
19	RCA5-SP21	5	21
20	RCA4-SP12	4	12
21	RCA6-SP18	6	18
22	RCA7-SP21	7	21

[a] Natural coarse aggregate
[b] Substrate without coarse recycled materials (control substrate)
[c] Recycled coarse aggregate
[d] Substrate with coarse recycled materials (proposed substrate)

4.4. Results

4.4.1. Heat transfer measurement using the ISO-conversion method

The thermal conductivity and R_c-values of green roof layers are presented in Figs. 4.11 and 4.12, respectively. The heat flux measurements were based on the Average Method's criteria given by ISO 9869-1 (ISO 9869-1, 2014).

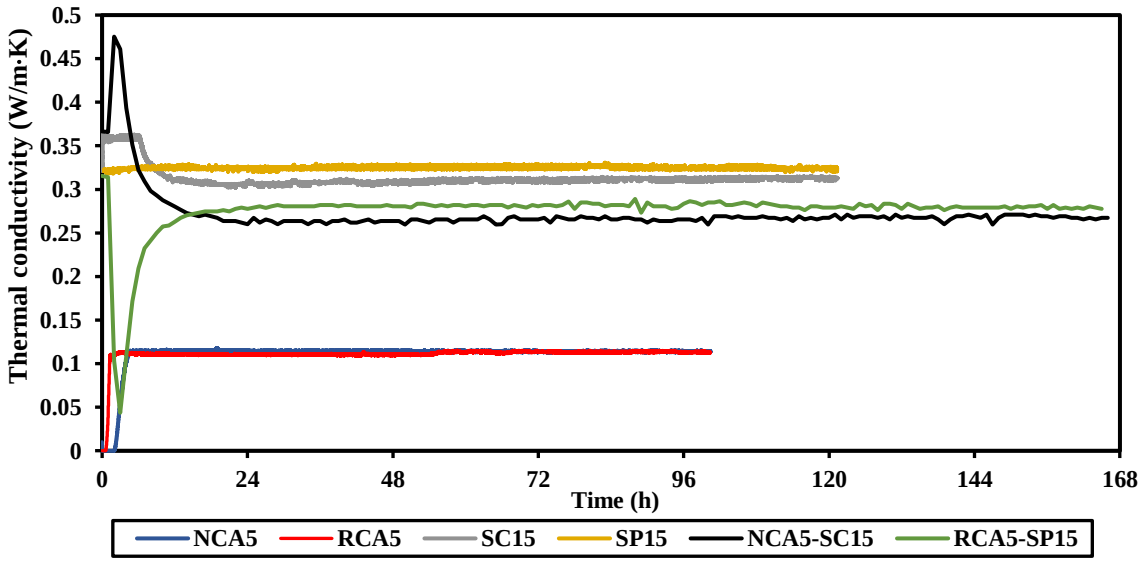

Fig. 4. 11. Green roof layers' thermal conductivity.

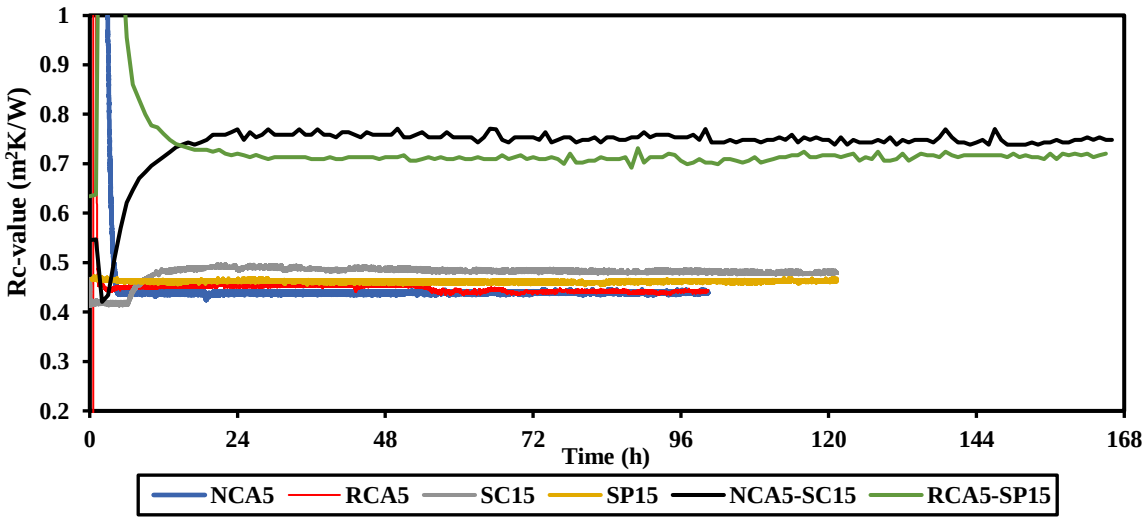

Fig. 4. 12. Green roof layers' Rc-value curves.

According to the first requirement given by the ISO-conversion method, the measurement period should take at least 72 h. Table 4.3 presents all specimens' test durations. For the control and the proposed green roof specimens (NCA5-SC15 and RCA5-SP15), the last 118 h of the test duration was considered for assessing their R_c-value convergence. The last 76 h of the test duration for the natural and recycled coarse aggregate layers (NCA5 and RCA5) was supposed to assess their R_c-value convergence. The last 73 h of the test duration for the unsaturated substrate without and with coarse recycled materials (SC15 and SP15) was considered as their convergence duration.

Table 4. 3. Green roof layers' thermal properties.

Specimens ID	NCA5	RCA5	SC15	SP15	NCA5-SC15	RCA5-SP15
Test duration (h)	101	101	122	122	166	166
Convergence duration (h)	76	76	73	73	118	118
Thermal conductivity unsaturated, (W/m·K)	0.114	0.11	0.31	0.32	0.27	0.28
Rc-value (m^2K/W)	0.44	0.446	0.48	0.46	0.75	0.72

As per the second requirement given by ISO 9869-1 (ISO 9869-1, 2014), the value calculated at the end of the data set should not deviate more than ±5% from the respective value obtained 24 h before. Concerning this, 24 h before the end of the data set, the Rc-values for NCA5-SC15, RCA5-SP15, SC15, SP15, NCA5 and RCA5 were 0.743, 0.713, 0.481, 0.462, 0.443 and 0.44 m^2K/W, respectively. The resulting values at the end of the data set were 0.75, 0.72, 0.48, 0.463, 0.443 and 0.446 m^2K/W, respectively. Therefore, the difference between the Rc-values at the end and 24 h before the end of the data set was not more than 1.4%, satisfying the second requirement given by ISO 9869-1 (ISO 9869-1, 2014).

Based on another requirement of the ISO-conversion method, the resulting value when applying the method to the first 67% of data should not deviate by more than ±5 % from the respective value when analyzing the last 67% of the data. The results showed that the average R_c-values for the first 67% of the convergence duration for NCA5-SC15, RCA5-SP15, SC15, SP15, NCA5 and RCA5 were 0.748, 0.715, 0.481, 0.461, 0.441 and 0.449 m^2K/W, respectively. The corresponding values for the last 67% convergence duration were 0.746, 0.724, 0.48, 0.462, 0.44 and 0.446 m^2K/W, respectively. According to the results, the

difference between the obtained Rc-values for the first and the last 67% of the convergence duration was not more than 1.3%. In general, the results of heat transfer measurements met the ISO-conversion method's requirements.

4.4.2. Validation of the models with the roofing systems

The air relative humidity variations at the top and bottom of the control and proposed green roofs as well as temperature fluctuations through their depths are shown in Figs. 4.13(a) and 4.13(b). For the validation of the models, the temperature fluctuations through their depths were compared with those of roofing systems (NCA5-SC15 and RCA5-SP15).

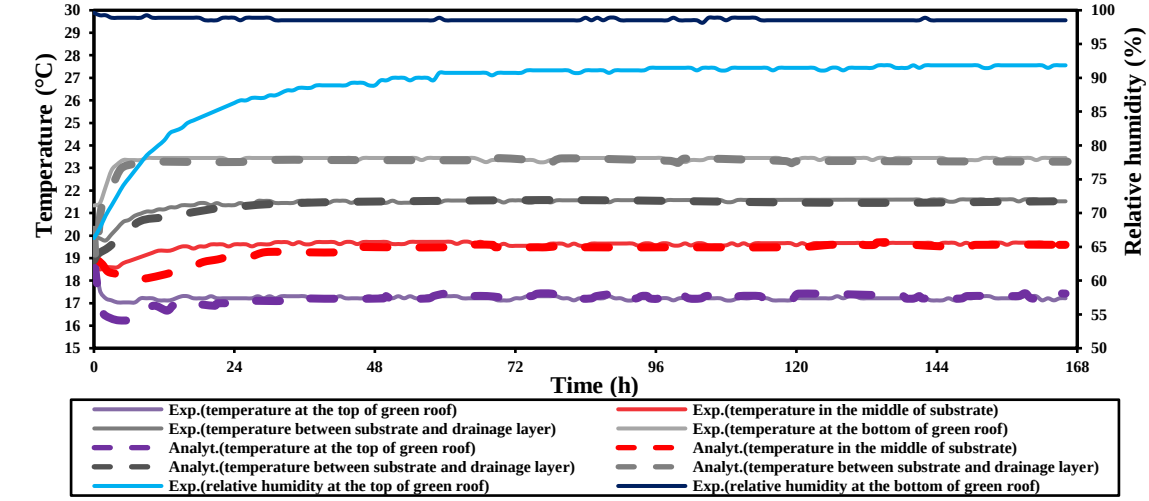

(a)

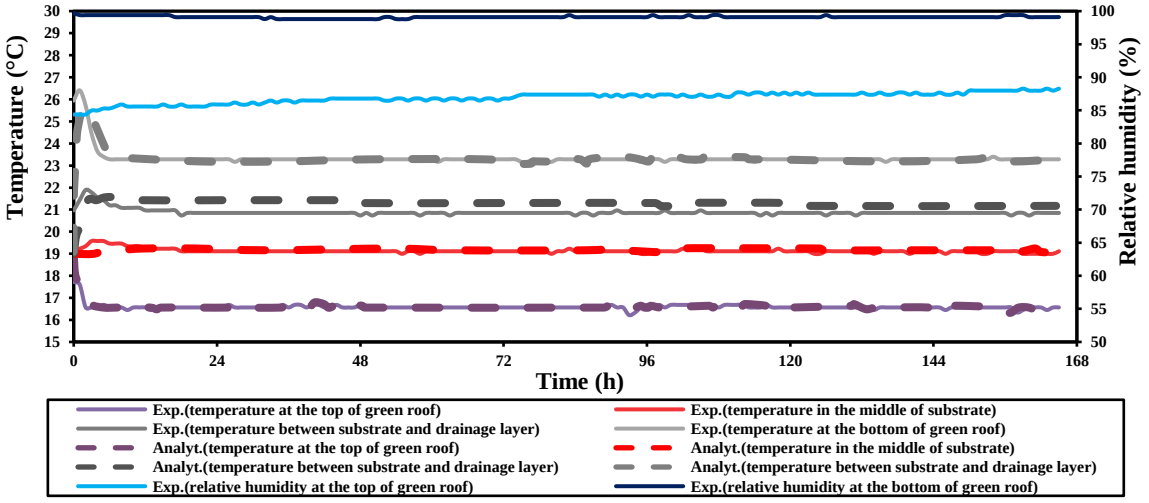

(b)

Fig. 4. 13. Experimental results and modeling outputs for the control green roof specimen, NCA5-SC15, (a) and the proposed green roof specimen, RCA5-SP15, (b).

As expected, the temperature distribution at the top and the bottom of green roof models had the same trend as observed for the roofing systems. Based on the results of the control green roof specimen during the convergence period, the average temperatures of 19.64 °C and 21.56 °C were attained in the middle of the substrate and between the substrate and drainage layer, respectively. The corresponding temperatures for the control model were 19.6 °C and 21.5 °C, respectively. According to the proposed green roof specimen' results during the

convergence period, the average temperatures of 19.1 °C and 20.84 °C were attained in the middle of the substrate and between the substrate and drainage layers, respectively. The corresponding temperatures were equal to 19.05 °C and 21.19 °C for the proposed model. Consequently, the general trend of the temperature distribution through the models' depth was nearly the same as observed for the roofing specimens. Moreover, the difference between the modelling and experimental specimens' temperatures through the layers' depth was no more than 1.7%.

4.4.3. Effect of layers' thickness

4.4.3.1. Thickness of drainage layer

By changing drainage layer's thickness, the average temperature values within green roof layers' depth were obtained during the convergence duration of Rc-value (the last 118 h of the test duration) as presented in Fig. 4.14.

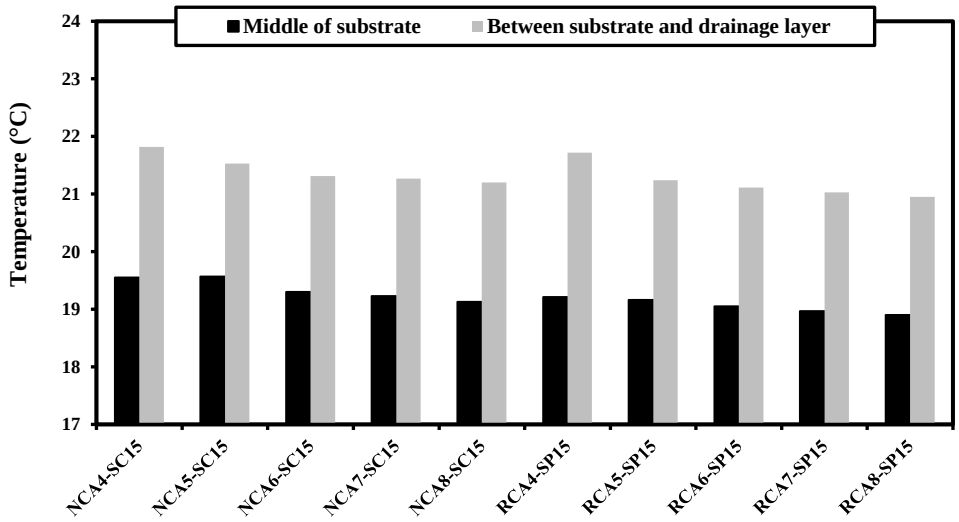

Fig. 4. 14. Effect of drainage layer's thickness on the average temperature value in the models' depth.

By increasing the drainage layer's thickness, its optimum design could be determined when no change in the temperature through green roof's depth was observed. The temperature between substrate and drainage layer for the control models with different thicknesses of drainage layer was ranging from 21.2 °C to 21.82 °C. It can be stated that there was a mild decrease in temperature when the thickness of drainage layer of natural coarse aggregate increased. However, the average temperature value for 6-cm drainage layer was found to be nearly the same as 7- and 8-cm drainage layer (21.2 °C). The same result was observed in the middle of substrate layer, where the temperature for the models with 6-, 7- and 8-cm drainage layer was near to 19.2 °C. On the other hand, the temperature of 21 °C was observed between substrate and drainage layer for the proposed models with 6-, 7- and 8-cm drainage layer. Moreover, the temperature in the middle of substrate layer for the proposed models was about 18.9 °C.

4.4.3.2. Thickness of the substrate layer

The average temperature values within green roof layers' depth were obtained during the convergence duration of Rc-value (Fig. 4.15) when the unsaturated substrate layer's thickness was changed.

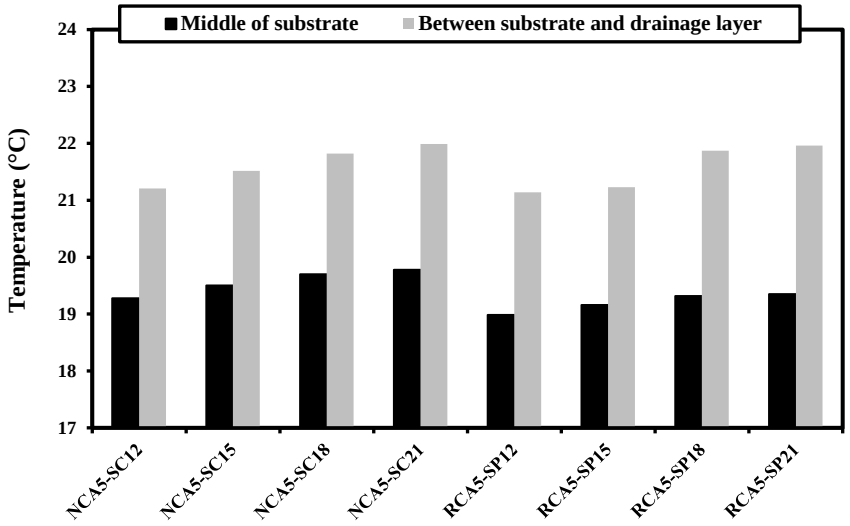

Fig. 4. 15. Effect of substrate layer's thickness on the average temperature value in the models' depth.

The optimum design of substrate layer was ascertained by increasing its thickness when no change in the temperature was observed through green roof's depth. For the control models, the middle of the substrate's temperature for green roofs with 12- and 15-cm substrate layer was 19.28 °C and 19.5 °C, respectively. Besides, the average temperature value for 18-cm substrate layer was nearly the same as 21-cm substrate layer (19.7 °C). The same result was obtained between the substrate and drainage layer, where the temperature for the control models with 18-, 21-cm substrate layer was near to 21.9 °C. On the other hand, the temperature value of 19.32 °C was obtained in the middle of substrate for the proposed model with 18- and 21-cm substrate containing coarse recycled materials. Similar to this, the temperature between the substrate and drainage layer for the proposed model with 18-cm substrate was obtained near to the same as the propose model with 21-cm substrate (21.9 °C).

4.4.3.3. Thickness with constant ratio of substrate to drainage layer

By simultaneously changing the substrate and drainage layers' thickness, the average temperature values within green roof layers were attained as shown in Fig. 4.16.

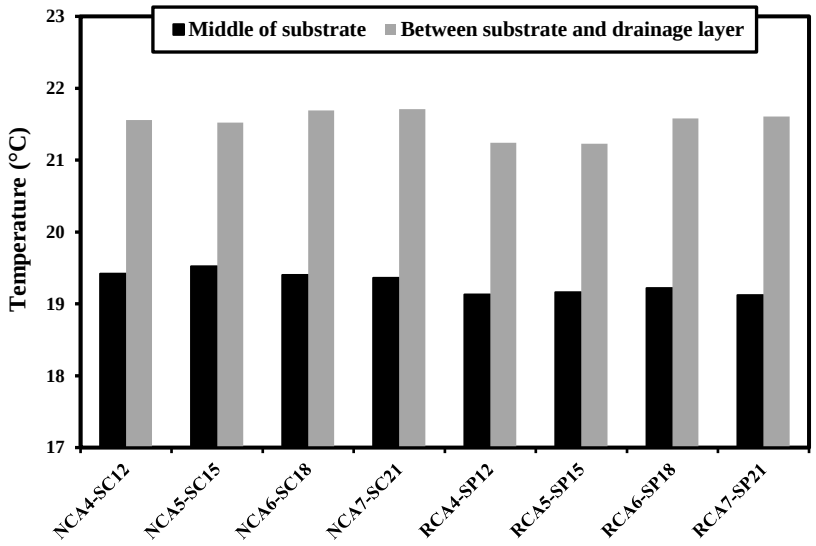

Fig. 4. 16. Effect of substrate and drainage layers' thickness on the average temperature value in the models' depth.

As per the modelling outputs, no remarkable difference was observed in the middle of the substrate's temperature when the substrate and drainage layers' thicknesses were simultaneously changed. As an example, the aforementioned temperature for the control models ranged from 19.4℃ to 19.5 ℃. The range of 19.1-19.2 ℃ was obtained for the proposed models. On the other hand, a moderate temperature increment between the substrate and drainage layer was observed for both control and proposed models by increasing green roof layers' thickness. However, this temperature for the model with 18-cm substrate was obtained near to the same as the model with 21-cm substrate. For instance, this temperature for the proposed models with 18- and 21-cm substrate (RCA6-SP18 and RCA7-SP21) was about 19.2 ℃. The control models' corresponding temperature for the same designs of substrate layer was about 19.4 ℃.

4.5. Discussion

4.5.1. Green roof layers' thermal performance

Table 4.3 presents the thermal conductivity and Rc-value of roofing systems' layers following the ISO-conversion method. The aforementioned parameters can be used for the materials' thermal transmission and resistance (M. Kazemi & Courard, 2021b, 2022; Pianella et al., 2016; Sailor & Hagos, 2011). The thermal conductivity of 0.11 W/m·K and Rc-value of 0.44 m^2K/W were obtained for both the natural and recycled coarse aggregate layers (NCA5 and RCA5) as presented in Table 4.3. Although natural coarse aggregates' properties were different to that of the recycled coarse aggregates, the thermal performance of the layer including either the natural coarse aggregates (NCA5) or recycled coarse aggregates (RCA5) were found to be similar to each other. It is noteworthy that the building materials' heat resistance can be improved by trapping the air-voids among their particles (Hu et al., 2019; M. Kazemi & Courard, 2021b, 2022; Suleiman et al., 1999; Zhou et al., 2010). Therefore, similar thermal performance of NCA5 and RCA5 could be attributed to the air-voids among coarse

aggregates and indeed, their Rc-values were more affected by air-voids than coarse aggregate types.

The materials used for the soil medium play a key role for improving the heat resistance of green roof systems. Therefore, the thermal sensitivity of substrate with different types of materials should be assessed(He et al., 2020; M. Kazemi & Courard, 2021b; Vertal' et al., 2018). As per the modelling outputs, no significant difference was observed between the thermal conductivity of unsaturated substrate layer without coarse recycled materials, SC15 (0.31 W/m·K) and the unsaturated substrate layer with coarse recycled materials, SC15, (0.32 W/m·K). Following this, the Rc-value of the former, 0.48 m^2K/W, was close to that of the latter, 0.46 m^2K/W, demonstrating less than 4.3 % difference between their thermal resistances. It can be stated that the substrate layer's thermal performance was not changed so much with the presence of coarse recycled materials. Therefore, they created a sufficient thermal resistance and water retention capacity like soil particles for the substrate layer. In brief, both the control and the proposed substrate layers (SC15 and SP15) provided a sufficient thermal mass for the roofing systems, similar to the conventional substrate layers used by other researchers for green roofs (Parizotto & Lamberts, 2011; Y. Yang et al., 2021).

The difference between the control and the proposed green roof systems (NCA5-SC15 and RCA5-SP15) showed a narrow difference between their thermal conductivity values (3.7%). The same result was observed for their Rc-values (4.2%). This small difference was due to the effect of coarse recycled materials on the substrate layer, even though it was negligible. The recycled coarse aggregate for the drainage layer and coarse recycled materials for the substrate layer of green roof systems was able to provide a sufficient thermal resistance. Note that the thickness of substrate layer was three times more than that of coarse aggregates as the drainage layer, while the Rc-value of the former was 9% more than that of the latter at the most. It is worth bearing in mind that the coarse aggregate layer's thermal resistance could be better than that of the unsaturated substrate layer by considering an equal thickness for both of them owing to air-voids among aggregates, generating high heat resistance for the drainage layer.

4.5.2. Parametric study

Assuming a constant thickness for the substrate layer (15 cm), no change was observed among the green roof models with 6-, 7- and 8-cm coarse aggregate layers. This result was observed for both the control and the proposed green roof models, due to the fact that their thermal performance was dominated more by the air-voids among aggregates than the coarse aggregate types. That's why the Rc-value of green roofs either with the natural coarse aggregates or with the recycled coarse aggregates as the drainage layer was obtained nearly the same as presented in Table 4.3. Based on the above, the presence of air-void among coarse aggregates with 6-cm drainage layer sufficiently provided the thermal performance for green roofs. Therefore, the NCA6-SC15 and RCA6-SP15 models were the optimum designs of the roofing systems, while a constant thickness of 15 cm was assumed for the substrate layer.

Increasing the unsaturated substrate layer's thickness contributed to improving the thermal resistance of the models, similarly to what Sun et al. (Sun et al., 2014) concluded. However, considering a constant thickness for the drainage layer (5 cm), no difference was seen between

the green roof models with 18- and 21-cm substrate layer. It can be said that the positive influence of the unsaturated substrate layer gradually decreased by increasing its thickness as observed by other researchers (He et al., 2017). This may be due to the fact that more moisture could be absorbed by one side of the thicker substrate (21 cm), leading to decreasing the participation of the soil's water content for reducing the heat flux through the substrate layer as revealed by Sun et al. (Sun et al., 2014). So, it was required to determine the unsaturated substrate layer's optimum thickness somewhere in the middle (18 cm) (M. Kazemi & Courard, 2021b). As a result, the NCA5-SC18 and RCA5-SP18 models were introduced as the optimum designs of the roofing systems, while a constant thickness of 5 cm was assumed for the drainage layer.

By simultaneously changing the substrate and drainage layers' thickness and keeping constant their thickness ratio, the models with 6-cm drainage layer and 18-cm unsaturated substrate layer (NCA6-SC18 and RCA6-SP18) were introduced as optimum designs of the roofing systems. Note that the use of lightweight roofing systems for the rooftops has been suggested by researchers (M. Kazemi & Courard, 2021b, 2022). Therefore, the proposed green roof (RCA6-SP18) was suggested to be employed in this regard owing to its lower weight than the control green roof (NCA6-SC18).

In general, for the control models, a separate increase in the substrate and drainage layers' thickness resulted in the introduction of NCA5-SC18 and NCA6-SC15 as the optimum designs of the roofing systems, while NCA6-SC18 was assumed as the optimum design by simultaneously changing the substrate and drainage layers' thickness. Therefore, a simultaneous increment in the unsaturated substrate and drainage layers' thickness contributed to creating better thermal performance for the green roofs. Of all optimum designs for the control models, the lowest weight was obtained for NCA6-SC15 (247.48 kg/m^2) by considering the materials' density values in Table 4.1. Among all optimum designs for the proposed models, RCA6-SP15 had the lowest weight (220.01 kg/m^2). In brief, it is recommended to use the coarse recycled materials for the roofing systems' layers owing to their low weight and sufficient thermal performance.

4.6. Conclusions

This study experimentally assessed the thermal resistance of green roof layers with coarse recycled materials following ISO 9869-1 standard. The initial moisture and thermal properties of the layers were simultaneously simulated and their thickness was optimized. Based on the experimental and modelling outputs for the roofing systems, the following conclusions can be considered:

- On the basis of ISO 9869-1 standard, the Rc-value of the drainage layer either with the natural coarse aggregates or with recycled coarse aggregates was the same (0.44 m^{2}K/W). It means that drainage layer' thermal resistance was mainly influenced by the air-voids among coarse aggregates and not by the porosity of recycled aggregates.
- A small difference (4.3 %) appeared between the Rc-value of the control substrate layer (SC15) and the proposed substrate layer (SP15). Therefore, considering the

fact that the substrate layer' thermal performance was dependent on soil moisture content, the coarse recycled materials provided an adequate thermal resistance, similar to soil particles for the substrate layer.

- A small difference (4.2%) was observed between the Rc-value of the control and the proposed green roof systems (NCA5-SC15 and RCA5-SP15), owing to the presence of coarse recycled materials in the substrate layer of the latter. However, this negligible difference demonstrated a sufficient thermal performance of the proposed green roof with coarse recycled materials.
- The substrate layer's thickness was three times higher than that of coarse aggregates for the drainage layer, while its Rc-value was mostly 9% higher. Considering an equal thickness for the aforementioned layers, the coarse aggregate layer's thermal resistance could be better than that of the unsaturated substrate layer.
- After translating green roof layers' initial hygrothermal properties into WUFI software, the thermal performance of the models with and without coarse recycled materials was reliably validated with that of roofing systems. Besides, a stable distribution of temperature through green roof models' depth was observed, similarly to what occurred for the lab-scale green roof specimens, where the difference between the modelling and experimental specimens' temperatures through the layers' depth was no more than 1.7%.
- Considering a constant thickness for the substrate layer (15 cm), 6-cm drainage layer either with natural coarse aggregates or with recycled coarse aggregates represents the optimum design for the roofing system. The 18-cm unsaturated substrate layer with and without coarse recycled materials was considered as an optimum design for the rooftops, while a constant thickness of 5 cm was considered for the drainage layer.
- A simultaneous change in the substrate and drainage layers' thickness showed that 6-cm drainage layer and 18-cm unsaturated substrate layer (NCA6-SC18 and RCA6-SP18) were the best design to provide a sufficient thermal resistance for the roofing systems.

Finally, the proposed green roof models with optimized thicknesses can be recommended to be used for the green roof systems, owing to the importance of choosing lighter materials with an adequate thermal performance for the rooftops.

Chapter 5: Sensitivity analysis and weather condition effects on hygrothermal performance of green roof models characterized by recycled and artificial materials' properties

Introduction

The hygrothermal performance of green roof materials can be impacted by climate conditions, but this significant issue has rarely been assessed for drainage and substrate layers composed of recycled and artificial materials. Moreover, the sensitivity of heat flux to the thickness and physical properties of green roofs made of artificial and recycled materials has scarcely been assessed. Considering this, the main contribution of this chapter is to evaluate what the influence of using artificial and recycled materials is on green roof performance under the temperate climate of Liège city. In addition to this, it is required to assess to what extent green roofs' thermal resistance is sensitive to drainage and substrate layer characteristics, including artificial and recycled materials. Therefore, the first objective of this chapter (paper based) is to assess the influence of using artificial and recycled materials on green roof performance under the temperate climate of Liège city till the end of the 21st century. Regarding this, three temperate weather scenarios of Liège city are applied to green roof models with artificial and recycled materials: the climatic conditions for the beginning, the middle and the end of the 21st century, as well as perspectives for future use are compared. Another objective of this chapter is to evaluate the heat flux sensitivity to the thickness and physical characteristics of green roofs with artificial and recycled materials. In light of this, the sensitivity of heat flux value to green roof layers' thickness and materials properties is assessed using analytical methods.

Abstract

This study conducted a sensitivity analysis and assessed the effects of long-term weather conditions on green roof models, including recycled and artificial materials. Climate conditions can affect the hygrothermal performance of green roof materials, but this important issue has hardly been evaluated for drainage and substrate layers made of recycled and artificial materials. Climate change makes it unclear how well green roofs will perform hygrothermally. Moreover, the heat flux sensitivity to the thickness and physical characteristics of green roofs with artificial and recycled materials has received less attention. This study applied three weather scenarios on green roof models with artificial and recycled materials: the beginning, middle and end of the 21st century. As per the results, at the beginning and middle of the 21st century, substrate layers' water content was roughly nine times more than the drainage layers'. At the end of the 21st century, the comparable difference was 6.5 times larger. During the summer and the beginning of autumn, the green roofs' thermal performance with recycled and artificial materials was improved until the end of the 21st century. The entire parameter change demonstrated the scatter of thermal conductivity, density and thickness effectively influenced the dispersion of heat flux for the green roof layers. Also, the scatter of density was more effective in heat flux dispersion for substrate layer than drainage layer.

Keywords: weather condition; local and global methods; heat flux; coarse granular aggregates; green roof layers.

Article: Kazemi, M., Rahif, R., Courard, L., & Attia, S. (2023). Sensitivity analysis and weather condition effects on hygrothermal performance of green roof models characterized by recycled and artificial materials' properties. Building and Environment, 237, 110327. https://doi.org/10.1016/j.buildenv.2023.110327

Abbreviations:

SC	Substrate without coarse recycled materials (Control Substrate)
SP	Substrate with coarse recycled materials (Proposed Substrate)
RH	Relative Humidity
COV	Coefficient Of Variation
TMY	Typical Meteorological Year
RCA	Recycled Coarse Aggregate
LECA	Lightweight Expanded Clay Aggregate
NCA	Natural Coarse Aggregate
IMSWA	Incinerated Municipal Solid Waste Aggregate

5.1. Introduction

Green roofs' ability to provide thermal protection may help buildings to use less energy and experience less thermal load (Cirrincione et al., 2021; Peri et al., 2022; Tariku & Hagos, 2022; M. Zhao & Srebric, 2012). Also, the configuration (thickness) of drainage and substrate layers and their materials' thermal and physical properties can affect the insulation performance and water-holding capacity of green roof systems (M. Kazemi et al., 2023; M. Kazemi & Courard, 2022; Tams et al., 2022). On the other hand, since green roofs with different materials'

characteristics can be highly affected by climate conditions (Coma et al., 2016; M. Kazemi & Courard, 2021b; Klein & Coffman, 2015; Pérez, Vila, et al., 2012; K. Zhang et al., 2022), their thermal performance and workability have been assessed under different weather conditions. Regarding this, Getter et al. (Getter et al., 2011) compared the performance of green roofs with traditional gravel roofs in a Midwestern U.S. climate with hot, humid summers and cold, snowy winters. The heat flux from the building was lower for the green roof than the gravel roof, even under chilly and wet conditions. The gravel roof consistently experienced more extreme maximum and minimum average monthly temperatures and heat fluxes than the green roof over a year. Green roofs' effects on heat fluxes and surface temperatures during the winter were assessed by Stella and Personne (Stella & Personne, 2021) in a temperate climate. The results showed green roofs decreased heat flux fluctuations at the building surface. Also, the building surface's temperature and heat flux variations were lessened by deeper substrates.

The thermal, hydrodynamic and physical characteristics and thickness of green roof materials and layers play a fundamental role in hygrothermal performance of roofing systems (M. Kazemi & Courard, 2022; Sandoval et al., 2017). Scharf and Zluwa (Scharf & Zluwa, 2017) investigated different green roof systems' building physical properties. They concluded that the thicker the green roof construction was, the better the building's physical properties were. However, it was unreliable to estimate the average U-value of green roofs based only on construction thickness. When paired with a drainage layer with a high pore volume, substrate materials with a high-water storage capacity improved the building's physical characteristics. Zhang et al. (Y. Zhang et al., 2019) carried out a sensitivity analysis on green roof systems. The results showed that the rate at which the green roof reduced cooling load rose as insulation effectiveness declined owing to an increase in the inward heat flux. Mechelen et al. (Van Mechelen et al., 2015) revealed that small amounts of irrigation were needed for green roofs in temperate climate to have a more sustainable future for urban life. A study was done by Chan and Chow (Chan & Chow, 2013) on green roof performance under future climate conditions. According to the results, in comparison to the base case, the building case with soil thickness of 0.4 m and plant height of 0.05 m kept the energy consumption no more or less than the current level, ranging from −2.4% to −10%.

The recycled materials have been found to work well for commercial green roofs (Nagase, 2020). Regarding this, Eksi et al. (Eksi et al., 2020) showed that the particle dispersion of zeolite prevented it from supporting plant growth, despite performing well in terms of nutrient and water retention. Concrete as the coarse and heavy material performed well as a substrate for the plant growth. Cascone (Cascone, 2019) revealed that rubber crumbs had the greatest density and thermal conductivity measurements of all the drainage materials analyzed. Mickovski et al. (Mickovski et al., 2013) found that the green roof substrate made from recycled inert construction waste material was effective in providing good drainage, promoting plant development, and being resistant to slippage and erosion. Substrates made from a combination of recycled red brick and clay pellets were very promising for maximizing plant diversity of green roof systems as reported by Molineux et al. (Molineux et al., 2015). A study by Bates et al. (Bates et al., 2015) demonstrated for green roof plant diversity, the crushed brick or recycled aggregates with a high proportion of crushed brick were ideal for substrate materials. Also, recycled bricks and cork were introduced by Tams et al. (Tams et al., 2022) as

promising green roof materials. Rincón et al. (Rincón et al., 2014) revealed that, compared to pozzolana as a drainage material for green roof systems, recycled rubber showed a lower environmental impact. Shafique et al. (Shafique et al., 2020) reported that recycled materials in green roof layers might decrease the environmental impacts. However, the use of by-products and recycled materials for green roof layers should be studied more deeply as recommended by Scolaro and Ghisi (Scolaro & Ghisi, 2022).

Long-term experimental and modeling efforts have been conducted by Kazemi et al. (M. Kazemi et al., 2021, 2022, 2023; M. Kazemi & Courard, 2021b, 2022) to evaluate the hygrothermal, physical and configuration of the drainage layer and substrate of green roofs made of artificial and recycled components. Kazemi et al. (M. Kazemi et al., 2023) suggested three commercial drainage materials as artificial and recycled production: Lightweight Expanded Clay Aggregate (LECA), Incinerated Municipal Solid Waste Aggregate (IMSWA) and Recycled Coarse Aggregate (RCA). Their results were compared with Natural Coarse Aggregate (NCA) as a control coarse granular aggregate. For the substrate layer, the results of a commercial substrate material, including coarse recycled materials (SP), were compared with those of the control substrate without coarse recycled materials (SC). Based on heat flow measurement results and hygrothermal modeling outputs, Kazemi and Courard (M. Kazemi & Courard, 2021b) demonstrated that a 15-cm SP and a 15-cm SC in a wet state differed marginally from one another (4.3%). The respective difference in the dry state was slightly more (6.4%) (M. Kazemi et al., 2022). Also, 5-cm RCA and 5-cm NCA both had the same Rc-value (M. Kazemi & Courard, 2021a). In a wet state, considering the substrate and drainage layers together, there was a slight variation between the RC values of the green roof with 15-cm SP and 5-cm RCA and the green roof with 15-cm SC and 5-cm NCA (4.2%) (M. Kazemi & Courard, 2021a). The corresponding difference in the dry state was 5.3%, as presented by Kazemi et al. (M. Kazemi et al., 2022). Following that, measurements and presentations of three key indicators, including Rc-value, water permeability and water retention capacity, were made by Kazemi et al. (M. Kazemi et al., 2023) for different substrate and drainage materials and their outputs were compared with each other. The results showed that in comparison to SP, the water retention capacity of SC was nearly 1.2 times. The corresponding difference for water permeability test was 1.5 times. However, the values of water retention capacity and water permeability for both SC and SP were in the required ranges given by FLL guidelines (FLL guidelines, 2008). For drainage materials, when compared to NCA, LECA and IMSWA's water retention capacity values were roughly two times higher. Also, the respective value for RCA was around 1.5 times higher. 5-cm LECA obtained the highest Rc-value among coarse granular drainage materials.

Based on the above, it is evident that certain research on the measurement of water retention capacity, water permeability and heat flow, across green roof layers, including coarse artificial and recycled materials, has been conducted. Although the hygrothermal performance of green roof materials can be influenced by climate conditions (Coma et al., 2016; Klein & Coffman, 2015; Pérez, Vila, et al., 2012), this critical issue has scarcely been assessed for drainage and substrate layers including artificial and recycled components. Thus, there is a lack of understanding of the hygrothermal performance of green roof layers including artificial and recycled materials in the future till end of 21st century when the weather conditions will change.

On the other hand, green roof layers' thermal resistance is more sensitive to some parameters that must be taken into account (Y. Zhang et al., 2019). This issue has received less attention for green roof layers, including artificial and recycled materials.

Therefore, in this study, different weather data scenarios for the 21st century were supposed and applied to the validated green roof models. The research aims to answer the following two questions:

1-What is the influence of using artificial and recycled materials on green roof performance under the temperate climate of Liege city till the end of the 21st century?

2-To what extent is green roofs' thermal resistance sensitive to parameters of drainage and substrate layers, including artificial and recycled components?

To answer those questions, the hygrothermal performance of drainage and substrate layers, including different coarse artificial and recycled components, was assessed. Moreover, analytical methods were used to evaluate green roofs' thermal resistance sensitivity to the configuration (thickness) and physical characteristics of drainage and substrate layers made with artificial and recycled components.

This study supposed three weather data scenarios: beginning, middle and end of the 21st century. Considering this, the novelty of this research lies in considering different climate scenarios for the 21st century to apply to green roof models characterized by recycled and artificial materials' properties. The effect of weather data scenarios on heat flux values and water content of green roof layers was assessed and compared to each other. Also, conducting a sensitivity analysis on green roof layers based on the properties of artificial and recycled materials is another novelty of this study.

5.2. Materials and Methods

In this study, three weather data scenarios: beginning, middle and end of the 21st century, were supposed and applied to the validated green roof models, including coarse artificial and recycled. Then, the heat flux and water content variations for different layers and materials were compared to each other through the end of the 21st century. After that, the sensitivity of heat flux value to green roof layers' thickness and materials properties was assessed using analytical methods.

5.2.1. Configuration and characteristics of green roof layers

This study mainly focused on green roof models with substrate and drainage layers, as coarse artificial and recycled aggregates could be used only for these two layers of green roof systems. As Kazemi et al. (Kazemi et al., 2023) suggested, three commercial drainage materials: RCA, IMSWA and LECA were considered where NCA was supposed to control coarse granular aggregate. IMSWA included the crushed brick, crushed glass, crushed aggregate, inert waste and crushed ceramic. For the substrate layer, the results of SP were compared with SC. SP was composed of recycled tiles and bricks and organic matter, while no recycled materials were used for SC. As per Fig. 5.1, the substrate and drainage layers' thicknesses were intended to be 15 cm and 5 cm, respectively, as considered by Kazemi et al.

(M. Kazemi et al., 2021, 2022; M. Kazemi & Courard, 2021a). Green roof materials' properties, introduced to the WUFI software for the validation of green roof models, are presented in Table 5.1. Note that, to separate substrate and drainage layers from each other, a thin filter layer was used in green roof specimens (M. Kazemi et al., 2022; M. Kazemi & Courard, 2021a). This thin filter layer was not modeled in the simulation as it was not needed to be considered for substrate and drainage layers separation and it didn't affect the hygrothermal performance of green roof models.

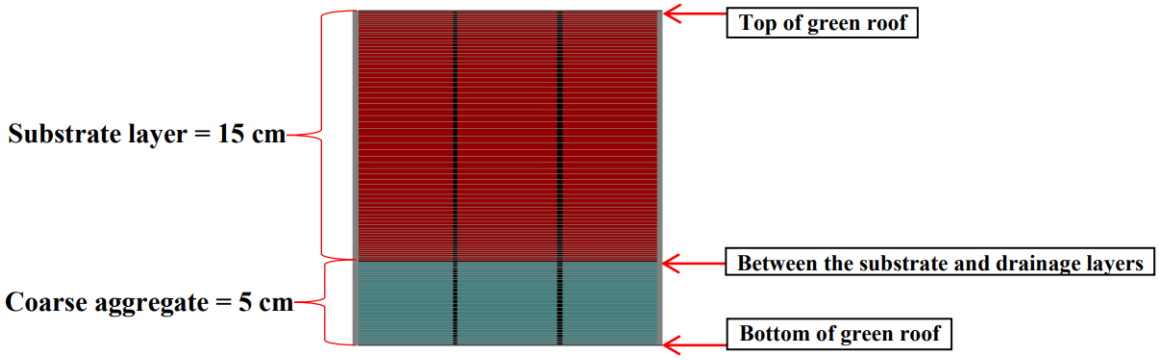

Fig. 5. 1. Two-dimensional green roof model built using WUFI software.

Table 5. 1. Green roof materials' properties.

Green roof layers	Materials	Density (kg/m^3)	Porosity	Specific heat capacity, dry (J/kg K)	Thermal conductivity, dry (W/m·K)	Water vapour diffusion resistance factor	Reference water content (kg/m^3)	Free water content (kg/m^3)	Water absorption coefficient (kg/m^2.s$^{0.5}$)
Substrate layer	SC (M. Kazemi & Courard, 2021a)	1075	0.48	880	0.15	3.62	10.31	380.95	0.47
	SP (M. Kazemi & Courard, 2021a)	1001	0.486	810	0.16	3.35	7.73	285.71	0.22
Drainage layer	NCA (M. Kazemi & Courard, 2021a)	1437	0.42	770	0.114	1	1.16	42.86	0.03
	RCA (M. Kazemi & Courard, 2021a)	1165	0.50	730	0.11	1	3.32	122.76	0.07
	IMSWA (M. Kazemi et al., 2021)	1147	0.47	750	0.115	1	2.74	101.2	0.07
	LECA (M. Kazemi et al., 2023)	439	0.55	710	0.067	1	2.83	141	0.11

For validation, the depth-based temperature changes within green roof models with the IMSWA and LECA drainage layers were compared with experimental outputs measured by Kazemi et al. (M. Kazemi et al., 2021, 2023). The outputs of green roof models with the drainage layer of RCA and NCA have already been validated by Kazemi and Courard (M. Kazemi & Courard, 2021a) in which nearly the same as what was shown for the green roof

specimens, the general trend of the temperature distribution through the green roof models' depth was seen.

5.2.2. Boundary conditions and weather data

According to the Regional Climate Model (MAR) "Modèle Atmosphérique Régional" (Doutreloup et al., 2022), the Typical Meteorological Year (TMY) data file was used to apply weather condition of Liège to green roof models. Liège is a city in Belgium, located at 50°38′23″ N 05°34′14″ E. Considering that TMYs as data sets of hourly values are fairly accurate and practical in projecting long-term building energy and thermal performance (Barnaby & CRAWLEY, 2012), they are frequently employed by those who design and model buildings (Wilcox & Marion, 2008). In this study, different weather parameters were incorporated in the TMYs data files, including solar radiation, air temperature, RH, rain, etc. The weather data were applied to the top of green roof models using WUFI software. For the interior surface, the initial conditions were considered based on EN 15026 (EN 15026, 2007) as provided by WUFI software. According to EN 15026 (EN 15026, 2007), the daily mean of the external air temperature was automatically entered into the graph in Fig. 5.2 to produce the inside air conditions. This simplified approach was suggested only for dwellings and offices to determine the internal temperature and RH for heated buildings. Also, since Liège city has a temperate climate, a high moisture load of RH was supposed for the interior surface.

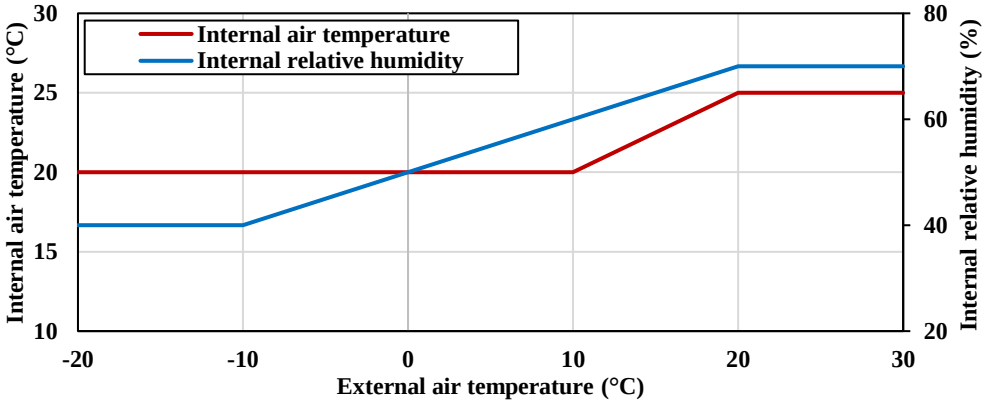

Fig. 5. 2. Dwellings and office buildings' daily mean internal air temperature and RH depending on daily mean external air temperature.

As presented in Table 5.2, three weather scenarios were considered in this study to apply to green roof models. Scenario 1 was based on historical observations between 2001 and 2020. Scenarios 2 and 3 were the predicted weather data for the middle (2040-2060) and end (2080-2100) of the 21st century. In Appendix 2, an average of one year was taken from 20 years for each scenario to apply to green roof models. To present the trends of weather data curves in Appendix 2, solid lines with an average value of 200 points were generated. The solar radiation and air temperature had a similar trend, where their lowest amounts were observed from November (end of autumn) until March (beginning of spring) for all scenarios. The highest RH for scenario 1 was in March, while scenarios 2 and 3 experienced the highest RH in December. For all scenarios, the lowest amount of RH occurred between Jun and September, when solar radiation and air temperature were high. The highest rainfall averagely occurred at the end of autumn, during winter and at the beginning of spring. Also, the lowest rainfall was

observed during summer and at the beginning of autumn. The average value of RH for all scenarios was the same (76%). The average value of rainfall for scenarios 1 and 2 (0.022 Ltr/m^2) was more than that for scenario 3 (0.015 Ltr/m^2). The temperatures for scenarios 1, 2 and 3 averagely were 10.7, 11.6 and 12.2 °C, respectively. The average solar radiation values for the same scenarios were 23.7, 25.7 and 21 W/m^2.

Table 5. 2. Weather data files' scenarios.

No.	Scenarios	Type	Years
1	Beginning of the 21st century	Historical observation	2001-2020
2	Middle of the 21st century	Predicted	2040-2060
3	End of the 21st century	Predicted	2080-2100

5.2.3. Sensitivity analysis (local and global methods)

Since the hygrothermal behavior of green roof systems is highly dependent on the characteristics and thickness of substrate and drainage materials (M. Kazemi & Courard, 2021a; Sandoval et al., 2017), analytical methods were used to evaluate green roofs' heat flux sensitivity. The approach of sensitivity analysis in this study was similar to the work done by Mahar et al. (Mahar et al., 2020). This study considered some parameters (independent variables), including thermal conductivity in a dry state (λ_0), water content (W), density (ρ) and thickness of substrate and drainage layers (L), and then, their effects were evaluated on the heat flux, q (dependent variable). Both local and global sensitivity analyses were taken into account in this study. In the local method, a single independent variable was changed, and others were assumed to be constant. The global method examined the sensitivity regarding the entire parameters change.

As presented in Table 5.3, the maximum and minimum of λ_0 value for drainage and substrate layers was determined based on a variation of green roof materials' thermal properties given by Kazemi et al. (M. Kazemi et al., 2023). Considering that coarse granular aggregates were used for the drainage layer by Kazemi et al. (M. Kazemi et al., 2022; M. Kazemi & Courard, 2021a), its minimum thickness shouldn't be supposed less than 4 cm to easily dewater green roof systems (Coma et al., 2014, 2016). Also, its maximum thickness was assumed 6 cm to prevent applying more load to rooftops as recommended (M. Kazemi et al., 2022; Teemusk & Mander, 2009). On the other hand, since the substrate depth of the green roof, at 15 cm, can offer an acceptable depth for a variety of plant growth (Ladani et al., 2019), and in some cases, a 9-cm substrate can adequately provide plant growth depth, 15 cm and 9 cm were supposed as the maximum and minimum thicknesses of the substrate layer, respectively. According to the water retention capacity of green roof materials given by Kazemi et al. (M. Kazemi et al., 2023), the maximum water content of drainage and substrate materials was determined. As per the weight of green roof materials (M. Kazemi et al., 2023), the maximum and minimum density of drainage and substrate components was chosen.

Table 5.3. Values of independent variables for drainage and substrate layers.

Green roof layer	Independent variables	Max	Min	Mean (μ_1)	Standard deviation (σ)
Drainage layer	λ_0	0.15	0.05	0.1	0.0167
	L	0.06	0.04	0.05	0.0033
	W	200	0	100	33.333
	ρ	1500	400	950	183.333
Substrate layer	λ_0	0.3	0.1	0.2	0.033
	L	0.15	0.09	0.12	0.01
	W	500	0	250	83.33
	ρ	1400	800	1100	100

After determining the maximum, minimum, mean value and standard deviation for materials' properties, it was required to generate the random values belonging to the distribution of each independent variable. To increase the accuracy of distribution, 5000 random values were generated for each independent variable. To achieve this goal, the normal distribution function (f (x, μ_1,σ)) was used, as shown in Eq. (5.1). The value of this function was between 0 and 1.

$$f(x, \mu_1, \sigma) = \frac{1}{\sqrt{2\pi}\,.\,\sigma}\, e^{\frac{-(x-\mu_1)^2}{2\sigma^2}} \quad (5.1)$$

where x is the independent variable for which the function was evaluated, μ_1 is the mean of the distribution, σ is the standard deviation.

To generate random values for each independent variable, f (x, μ_1, σ) was reformulated to obtain the inverse of the normal distribution function (g (f (x, μ_1, σ), μ_1, σ)) as presented in Eq. (5.2):

$$g(f(x, \mu_1, \sigma), \mu_1, \sigma) = \sqrt{2}\,\sigma\,(\mathrm{Ln}\,(\sqrt{2\pi}\,.\,\sigma\,.f(x, \mu_1, \sigma))^2 + \mu_1 \quad (5.2)$$

Fourier's law (Eq. (5.3)) was used to obtain the relationship between independent and dependent variables:

$$q = \lambda\,\frac{\Delta T}{L} \quad (5.3)$$

where q is the heat flux in W/m^2, λ is the thermal conductivity value, L is the thickness in m and ΔT is the difference between the top and bottom surfaces of the specimen in K. ΔT was supposed to be equal to 283.15 K as suggested by other literature (Desogus et al., 2011; ISO 9869-1, 2014; M. Kazemi et al., 2022; La Roche & Berardi, 2014) so that the exterior temperature was more than the interior one.

To generate a linear relationship between the water content and thermal conductivity (λ), Eq. (5.4) is proposed (Allinson & Hall, 2010; Veas, 2006; Vertal' et al., 2018).

$$\lambda = \lambda_0\,(1 + \frac{4W}{\rho})^1 \quad (5.4)$$

[1] Number 4 in equation has been missed in the paper.

where λ_0 is thermal conductivity value in dry condition (W/m^2), W is water content in kg/m^3 and ρ is density kg/m^3.

Eq. (5.4) was used to rearrange Eq. (5.3) as presented in Eq. (5.5):

$$q = \lambda_0 \left(1 + \frac{4W}{\rho}\right) \frac{\Delta T}{L} \quad [1] \tag{5.5}$$

Therefore, Eq. (5.5) was used during the sensitivity analysis process to introduce the relationship between dependent and independent variables.

The coefficient of variation (COV) of independent and dependent variables was calculated using Eq. (5.6):

$$COV = \frac{\sigma}{\mu_1} \tag{5.6}$$

To assess the sensitivity of the dependent variable (q) to the independent variables (λ_0, W, ρ and L), it was required to obtain the ratio of COV of q to COV of each independent variable. Increasing this ratio by more than one demonstrates that independent scattering variables lead to the dispersion of q more. While decreasing the ratio above to less than one shows that q is less dispersed and affected once independent variables are scattered.

It is noteworthy that it was essential to control whether the q values based on the specified values in Table 5.3 were valid or not. Regarding this, after obtaining 5000 random values for each independent variable using Eq. (5.2), it was controlled whether the calculated q was in its expected range (maximum and minimum values) or not. Less than 1% of q values were out of the expected range. Therefore, q values, obtained based on the specified values for independent variables in Table 5.3, were valid with more than 99% confidence.

5.3. Results

5.3.1. Validation of green roof models

For green roofs with the drainage layer of IMSWA and LECA, the modeling and experimental results were compared in Figs. 5.3(a) and 5.3(b).

As expected, the temperature distribution on green roof models' top and bottom followed the same trend as in roofing systems. For the green roof specimen with the drainage layer of IMSWA, between the substrate and drainage layers and in the middle of the substrate layer, respectively, average temperatures of 22.02 °C and 18.87 °C were reached during the convergence period. For the green roof model, the respective values were 22.39 °C and 19.34 °C. For the green roof specimen with the drainage layer of LECA, during the convergence phase, average temperatures of 22.99 °C and 20.39 °C were attained, respectively, between the substrate and drainage layers and in the middle of the substrate layer. The corresponding temperatures for the green roof model were 23.41 °C and 20.25 °C. The general trend of the temperature distribution through the depth of the green roof models can be said to be almost equivalent to what was seen for the green roof specimens. In addition, comparing the average

[1] Number 4 in equation has been missed in the paper.

temperature through the depth of green roof models and specimens showed no greater than a 2.5% difference.

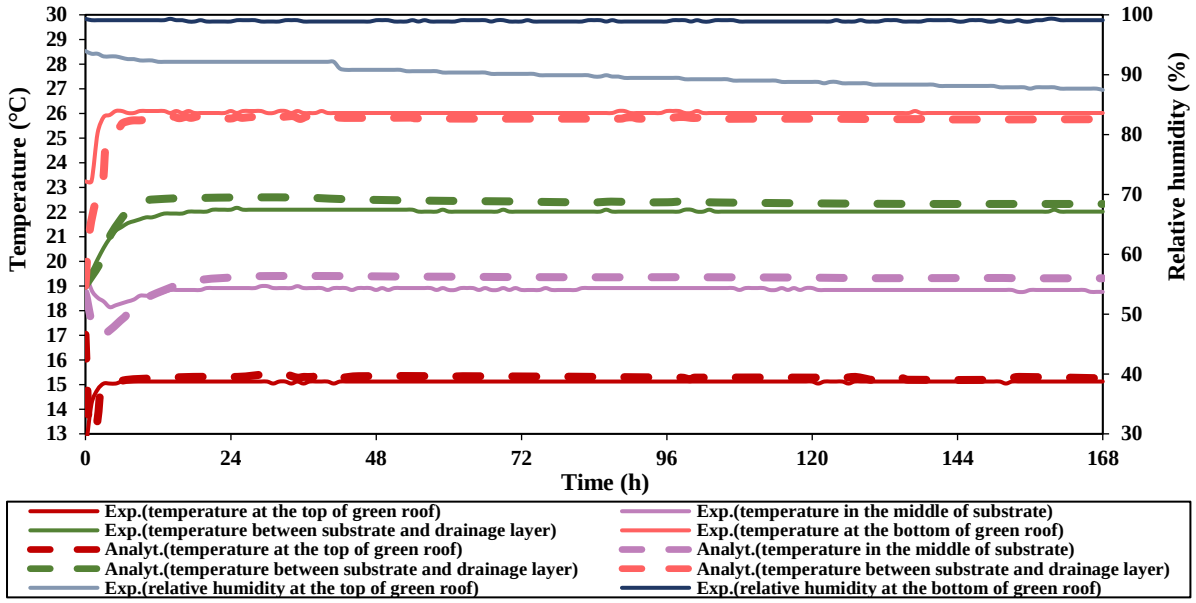

(a)

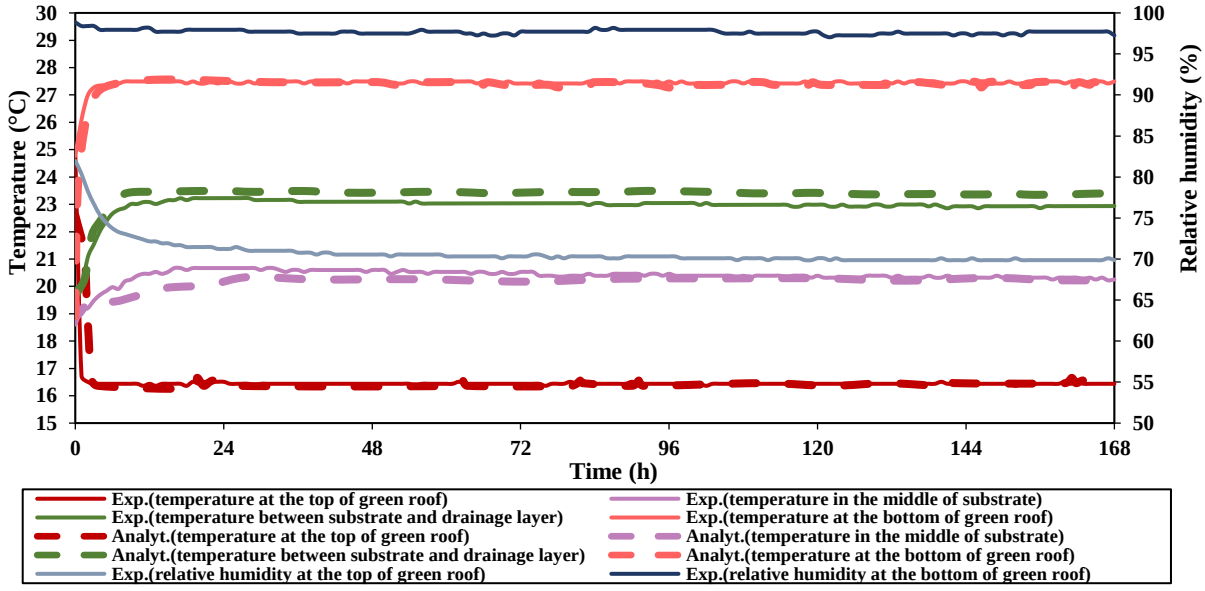

(b)

Fig. 5. 3. Results from experiments and models for green roofs with the drainage layer of IMSWA (a); and LECA (b).

5.3.2. Effect of weather conditions on green roof models

The effect of different weather scenarios on temperature and RH variations within the depth of green roof layers was assessed in this study. Also, the results of the water content of drainage and substrate layers under different weather conditions were presented. The outputs regarding heat flux transfer within different green roof models have been compared afterward.

5.3.2.1. Temperature and RH variations

Fig. 5.4 depicts the temperature and RH variations between the substrate and drainage layers during the 21st century. The temperature and RH fluctuations for green roofs with the SP and green roofs with the SC were nearly identical in each scenario. In scenario 1, the temperature and RH were in the 10.2-27.8 °C and 50-96.8 % ranges, respectively. The respective ranges for scenario 2 were 10.8-27.7 °C and 50-98 %. These ranges for scenario 3 were 11-27.8 °C and 50-94 %. Therefore, all scenarios had nearly the same maximum and minimum temperature and RH between the substrate and drainage layers.

According to Fig. 5.4(a), in scenario 1, the highest and lowest temperatures between substrate and drainage layers were obtained in August (summer) and March (beginning of spring), respectively. In scenarios 2 and 3 (Fig. 5.4(b) and 5.4(c)), the maximum temperatures were in the summer season (from June until August) and at the beginning of autumn (September), while the lowest temperatures were attained in December (beginning of winter). Concerning the RH, the reverse results were observed for all scenarios.

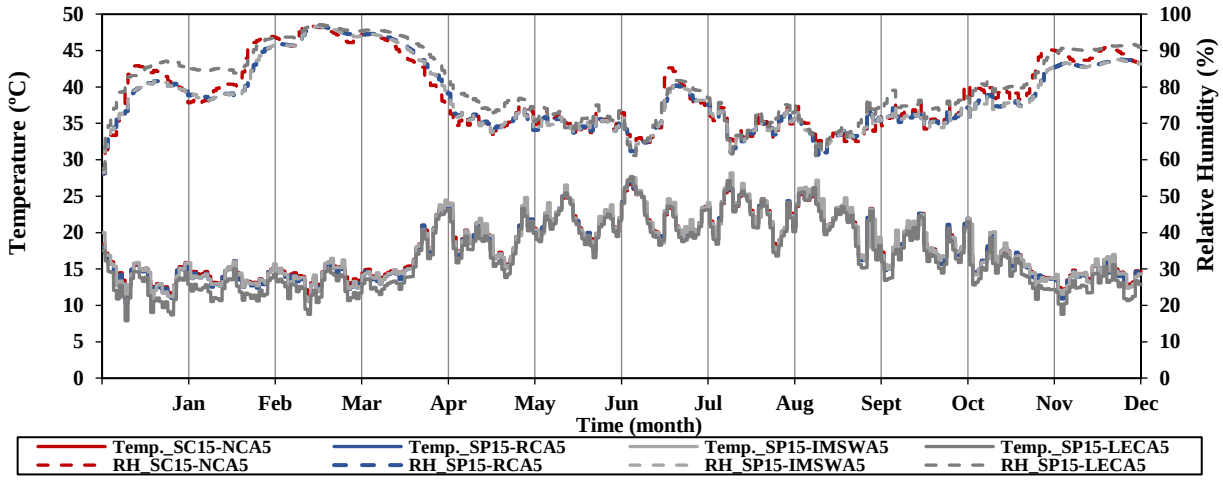

(a)

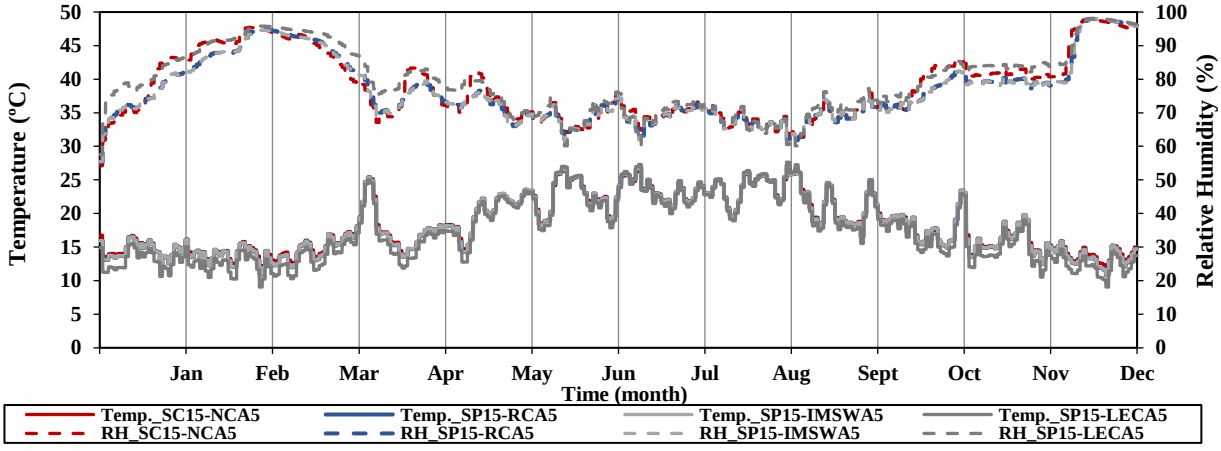

(b)

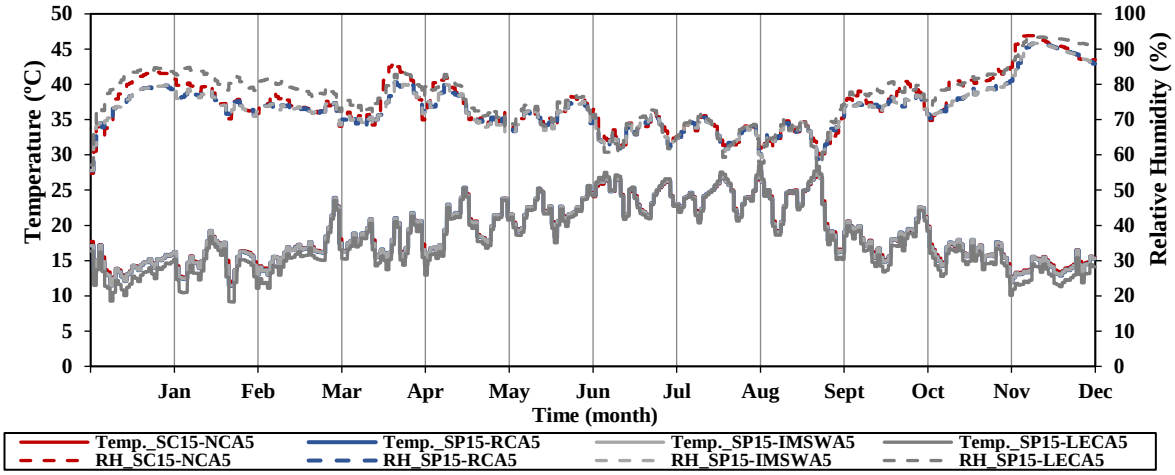

(c)

Fig. 5. 4. Temperature and RH variations between substrate and drainage layers at the beginning (a); middle (b); end of the 21st century (c).

Interior temperature and RH variations for all scenarios are shown in Fig. 5.5. For scenario 1, RH ranged from 48.2 to 73.1%, and temperature ranged from 17.9 to 25.6 °C, respectively. For scenario 2, the corresponding ranges were 49.9-73% and 18-25.6 °C. These ranges for scenario 3 were 47.5-74% and 18.1-25.8 °C. As recommended by Gilmore (Gilmore, 1972), the ideal internal RH range for comfort is between 30% and 70%. The results of all scenarios were nearly within the comfort range of RH given by Gilmore (Gilmore, 1972). To preserve the health of general populations during cold seasons, a safe and well-balanced indoor temperature is at least 18 °C according to the World Health Organization's 2018 recommendations (WHO, 2018). Also, healthy sedentary individuals living in an environment with an air temperature between 18 °C and 24 °C do not appear to be at risk for health problems (WHO, 2018). According to the results, the maximum and minimum range of interior temperatures for all scenarios were obtained near the comfort range given by World Health Organization (WHO, 2018).

In each scenario, nearly the same trends of interior temperature and RH were observed for green roofs with different types of materials. Also, the highest and lowest temperature and RH in the interior surface (Fig. 5.4(b)) occurred nearly during the same periods as observed between substrate and drainage layers (Fig. 5.4(a)). However, the fluctuation of temperature and RH was less in the interior surface than in between substrate and drainage layers. Similar results were found by Parizotto and Lamberts (Parizotto & Lamberts, 2011) in which the diurnal temperature variation at the lower layers of the green roof systems decreased.

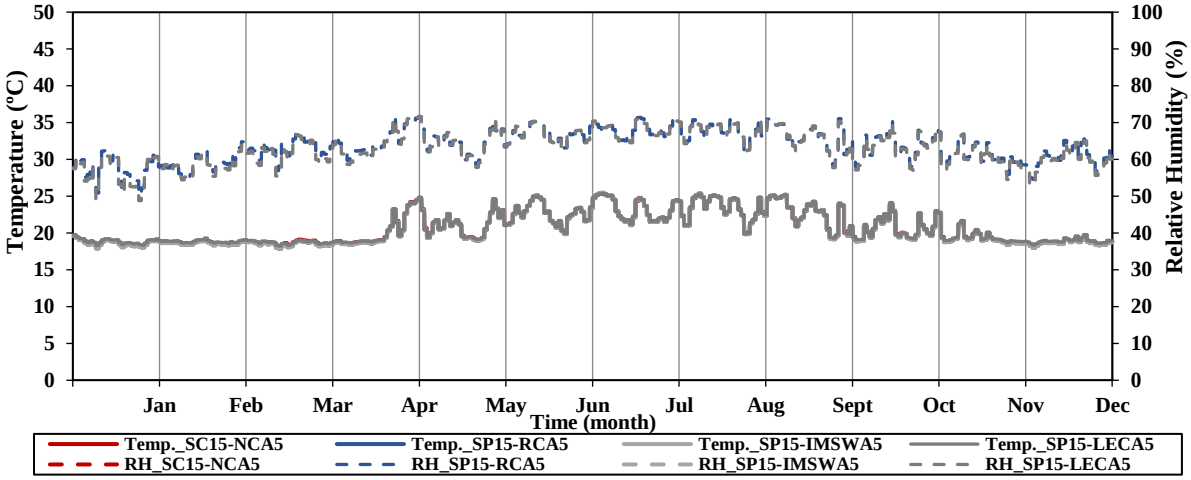

(a)

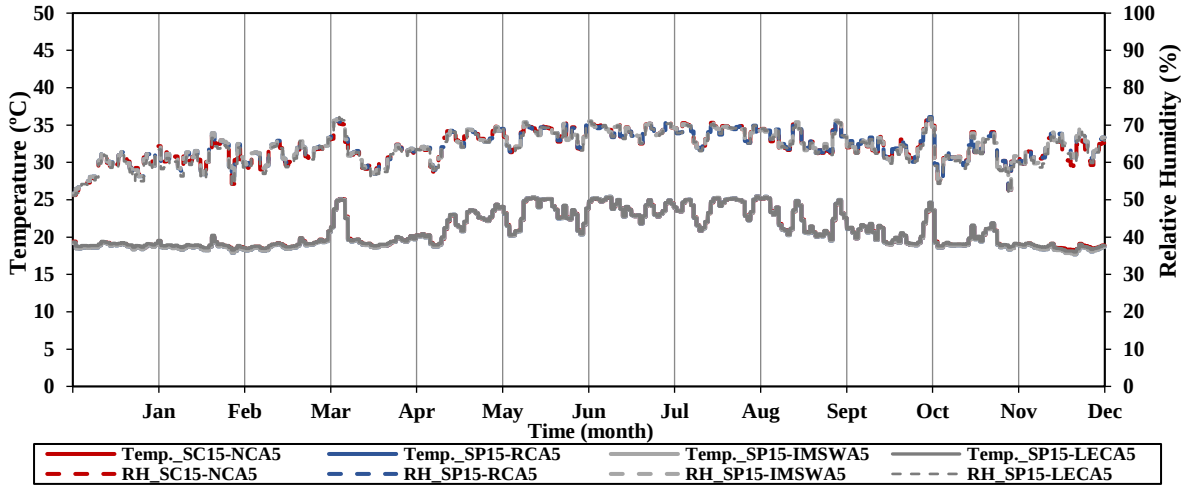

(b)

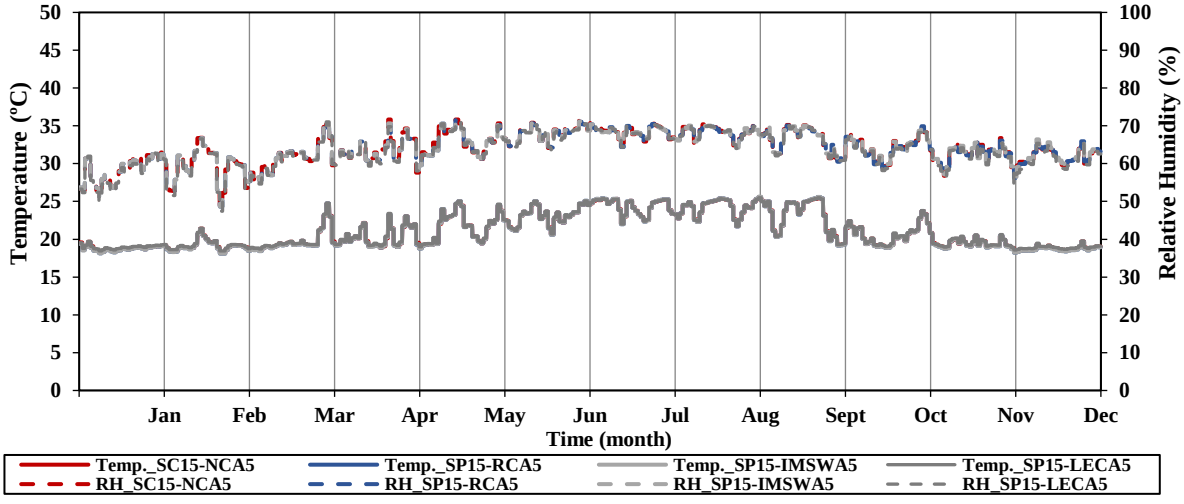

(c)

Fig. 5. 5. Temperature and RH variations at the bottom of green roof models at the beginning (a); middle (b); end of 21st century (c).

5.3.2.2. Water content

The water content values of green roof layers for each month were averagely presented in Fig. 5.6.

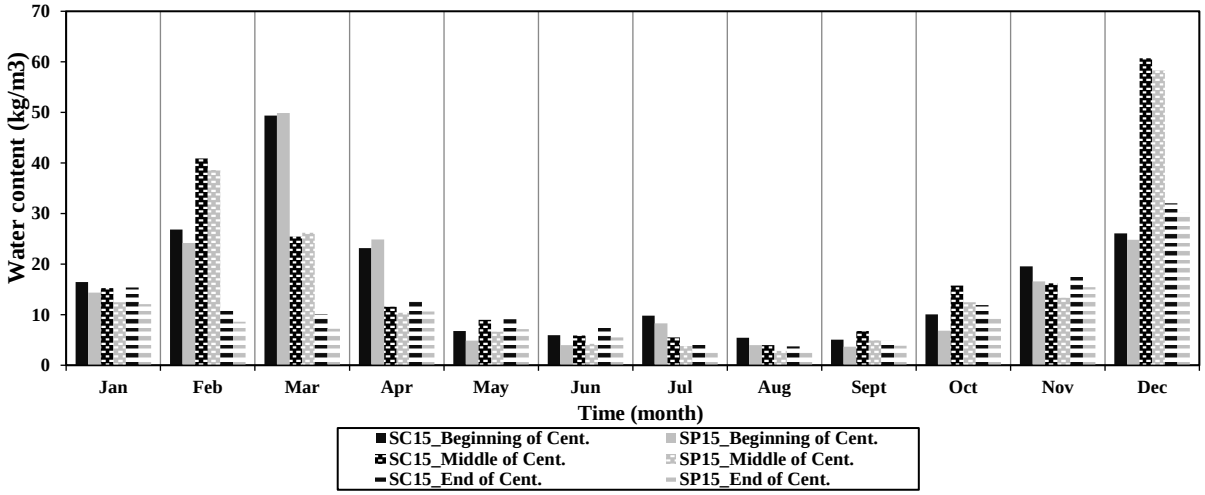

(a)

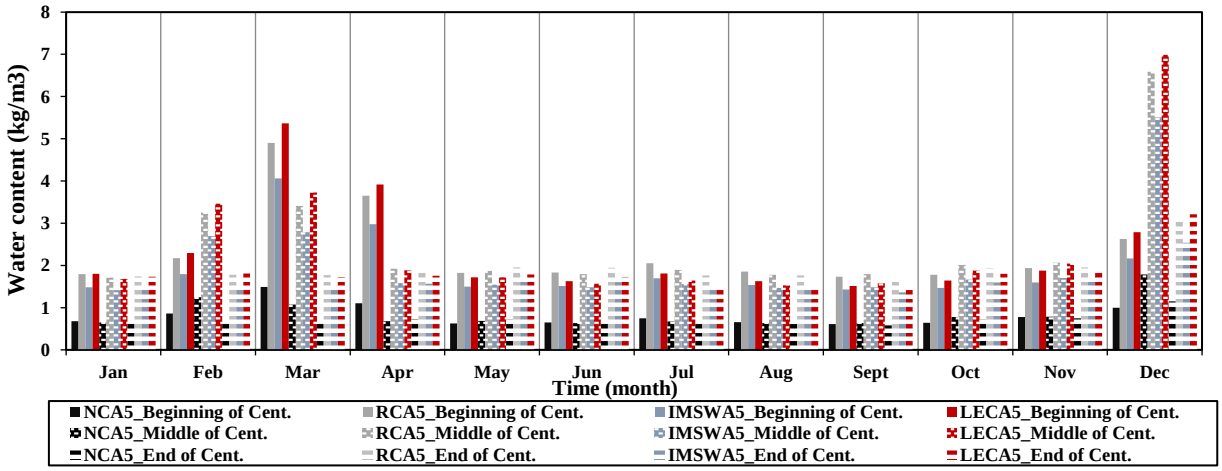

(b)

Fig. 5. 6. Water content of substrate layers (a); and drainage layers (b).

As shown in Fig. 5.6(a), the water content of SC and SP was averagely obtained at 17.05 and 15.53 kg/m^3, respectively, for scenario 1. The respective values for scenario 2 were 18.09 and 16.19 kg/m^3. The results for scenario 3 were 11.79 and 9.64 kg/m^3. Based on the above, the water content of SC was 13.5% more than that of SP. According to Fig. 5.6(b), the average water content values of NCA, RCA, IMSWA and LECA for scenario 1 were 0.8, 2.4, 2 and 2.4 kg/m^3, respectively. The corresponding values for scenario 2 were 0.9, 2.5, 2.1 and 2.5 kg/m^3. These values for scenario 3 were 0.7, 1.9, 1.6 and 1.9 kg/m^3. Therefore, the water content of RCA, IMSWA and LECA was obtained about 2.5 times more than that of NCA. Similar results were also attained by Kazemi et al. (M. Kazemi et al., 2023) regarding the water retention capacity of the aforementioned coarse granular aggregates.

The water contents of the substrate layer for scenarios 1, 2 and 3 were averagely obtained at about 16.3, 17 and 9.8 kg/m^3, respectively. The respective values for drainage materials were 1.9, 2 and 1.5 kg/m^3. Therefore, the water content of substrate layers was about nine times more

than that of drainage layers for scenarios 1 and 2. The corresponding difference for scenario 3 was 6.5 times.

According to Fig. 5.6(a), from January to February (winter), the water content of substrate materials increased for scenarios 1 and 2, while the reverse occurred for scenario 3. In March (beginning of spring), a decrease was observed for scenarios 2 and 3, while scenario 1 achieved the highest water content of substrate materials compared to other months. All scenarios experienced a decrease in the water content of substrate materials from March until May (spring). The lowest water content of substrate materials for all scenarios was in the summer season (from June until August) and at the beginning of autumn (September). Then, there was an incremental trend until the end of autumn (from September until November). This trend continued until December (the beginning of winter), when scenarios 2 and 3 had the highest water content of substrate materials compared to other months.

As shown in Fig. 5.6(b), for all scenarios, the lowest water content of drainage materials was from June until September, similar to what was revealed for substrate materials (Fig. 5.6(a)). For scenario 1, the highest water content of drainage materials was in March and then April (spring). An increase in the water content of drainage materials for scenario 2 was attained in February and March. Its highest water content was in December, as also observed for scenario 3.

5.3.2.3. Heat flux

The average values of heat flux in each month within the depth of green roof models are presented in Fig. 5.7.

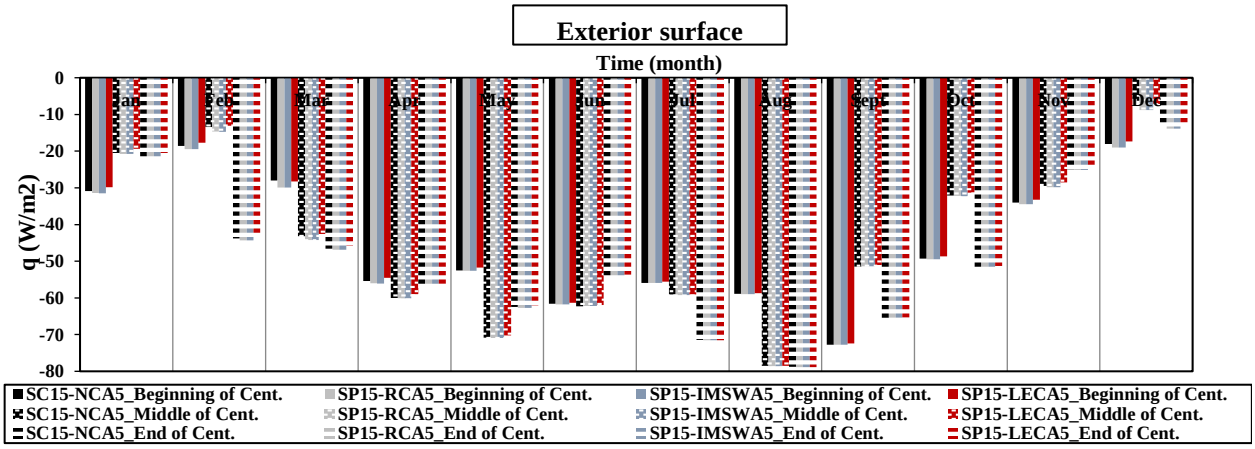

(a)

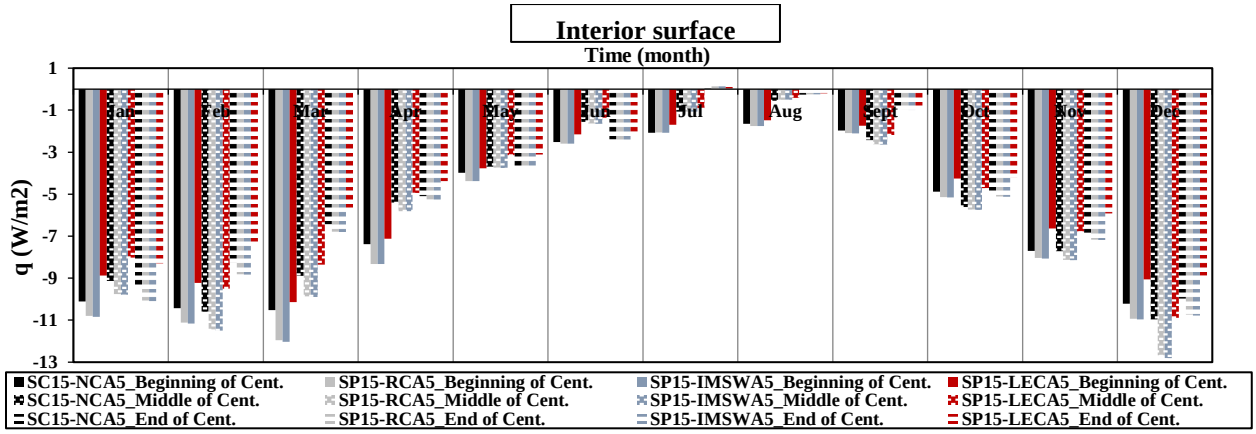

(b)

Fig. 5. 7. Heat flux on the top of green roof (a); at the bottom of green roof (b).

In the exterior surface (Fig. 5.7(a)), comparing different scenarios showed that there was a decrease in the heat flux value of scenarios 1 and 2 from January to February (winter), while the reverse was observed for scenario 3. In the spring season, the heat flux increment was experienced from March to May for scenarios 2 and 3, while this increment was observed for scenario 1 until April and then, there was a decrease in May. In the summer season, there was a fluctuation in heat flux values for scenario 1 from June to August. In the autumn season, scenarios 2 and 3 experienced a reduction in heat flux value from September to November. This trend was followed in December (winter). Generally, the highest and lowest exterior heat flux values of scenario 1 were averagely attained in September and December, respectively (72.5 W/m^2 and 18.5 W/m^2). For scenario 2, August and December had the highest and lowest exterior heat flux (78.5 W/m^2 and 7.5 W/m^2), similar to what was observed for scenario 3 (78.5 W/m^2 and 13.5 W/m^2).

The heat flux values in the interior surface of green roof models are presented in Fig. 5.7(b). The heat flux values for scenario 1 were averagely obtained at 6.1, 6.6, 6.6 and 5.5 W/m^2 for SC15-NCA5, SP15-RCA5, SP15-IMSWA5 and SP15-LECA5, respectively. The respective values for scenario 2 were 5.6, 6.1, 6.1 and 5.1 W/m^2. The results of scenario 3 were 4.85, 5.1, 5.1 and 4.2 W/m^2. Based on the aforementioned results, the green roof models with the drainage layer of RCA and IMSWA had the same thermal performance in the 21st century. Their heat flux values were 8.2%, 8.9% and 5.2% more than those of the control green roof model with the drainage layer of NCA in scenarios 1, 2 and 3, respectively. The same trend was observed by Kazemi et al. (M. Kazemi et al., 2023) when they compared the Rc-value of the green roof specimens, including the drainage layer of RCA and IMSWA, with the control green roof specimen in a wet state.

Therefore, this difference for scenario 1 (8.2%) was nearly the same as scenario 2 (8.9%), demonstrating that the control model with substrate layer of SC and NCA drainage layer moderately had better thermal resistance than green roof models with substrate layer of SP and the drainage layer of RCA and IMSWA. However, decreasing this difference to 5.2% for scenario 3 indicated the better thermal performance of the latter at the end of the 21st century than in other periods. The heat flux values of the green roof model with the drainage layer of

LECA were 9.8%, 8.9% and 13.4% less than those of the control green roof model in scenarios 1, 2 and 3, respectively. The same trend was observed by Kazemi et al. (M. Kazemi et al., 2023). Hence, the former outperformed the latter in providing thermal resistance for rooftops. Their heat flux differences in scenarios 1 and 2 were nearly the same (9.8% and 8.9%), and increasing this difference in scenario 3 (13.4%) showed better thermal performance of the green roof model with substrate layer of SP and LECA drainage layer at the end of 21st century, similar to what was obtained for green roof models with substrate layer of SP and the drainage layer of RCA and IMSWA.

As shown in Fig. 5.7(b), the highest and lowest interior heat flux values of scenario 1 were averagely attained in March and August, respectively (11.2 W/m^2 and 2 W/m^2). Scenario 2 had the highest and lowest interior heat fluxes in December and August (11.9 W/m^2 and 0.5 W/m^2). In scenario 3, the highest and lowest interior heat fluxes were obtained in December and July (10.1 W/m^2 and 0.1 W/m^2).

Generally, it can be stated that the interior surface had an incremental heat flux trend during the winter season (December, January and February) and the beginning of spring (March), while the reverse was observed in the exterior surface. Also, a decreasing heat flux tendency for the interior surface was obtained during the summer (June, July and August) and at the beginning of autumn (September), contrary to the exterior surface.

5.3.3. Sensitivity analysis

Since the maximum and minimum values of independent variables for materials of drainage and substrate layers were different, it was required to perform a separate sensitivity analysis for green roof layers as presented below:

5.3.3.1. Drainage layer

Figs. 5.8(a) to 5.8(d) show the heat flux histograms of the drainage layer for a single independent variable changed while keeping constant other independent variables. The heat flux histogram regarding the entire parameter change is shown in Fig. 5.8(e). The dispersion of heat flux (q) values had a symmetrical shape in all histograms, demonstrating that all data were well-distributed. Also, only 1% of q values exceeded the expected range. Therefore, there was greater than 99% confidence in the validity of the q values that were calculated using the values for the independent variables in Table 5.3.

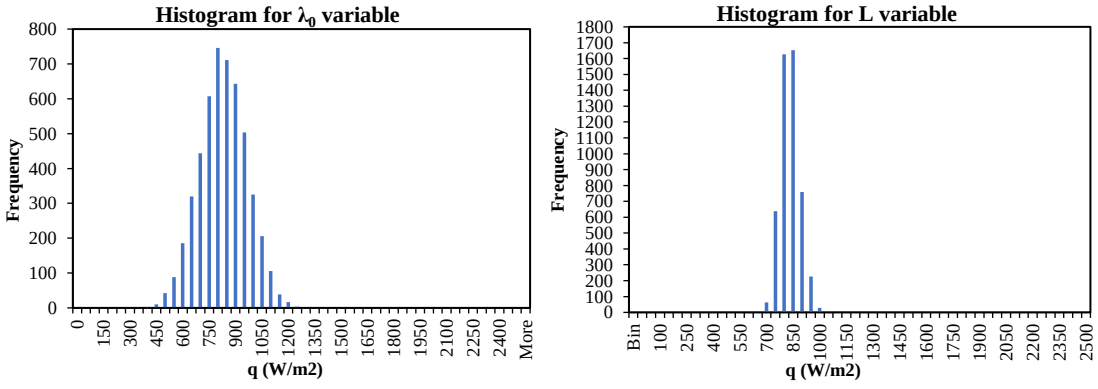

(a) (b)

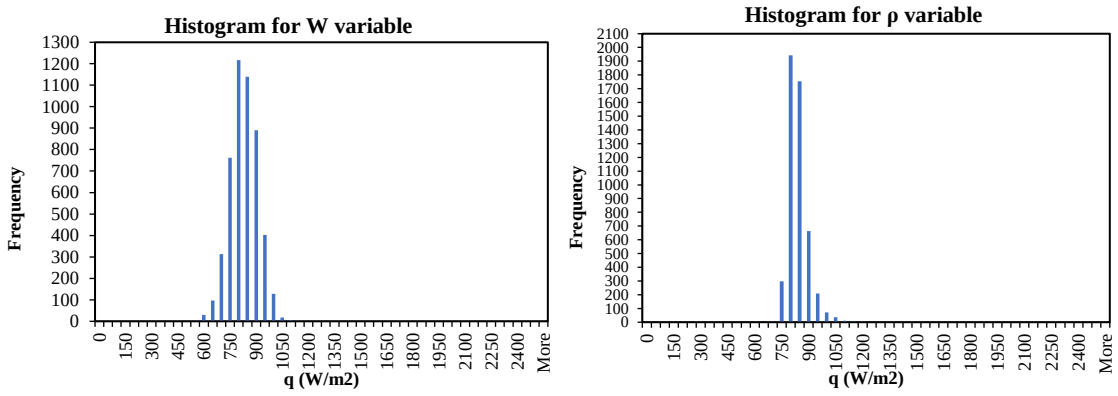

(c) (d)

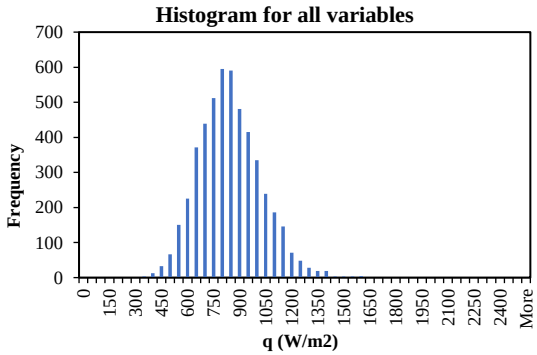

(e)

Fig. 5. 8. Heat flux histogram of drainage layer for λ_0 (a); L (b); W (c); ρ (d); and all variables (e).

To evaluate the sensitivity of the dependent variable (q) to the independent variables (λ_0, W, ρ and L), their COV values for the drainage layer were calculated in the first step. Then, the ratios of COV of q to COV of each independent variable were obtained for both local and global methods, as presented in Table 5.4. According to the results of the local method, the ratio above for λ_0 and L was about 1, showing that q was dispersed as much as they were scattered. However, the respective ratio for W and ρ was 0.29, indicating that q was less affected by their dispersion.

As per the results of the global method, the ratios of COV of q to COV of λ_0, L, W and ρ were 1.08, 2.69, 0.53 and 0.95. Therefore, the dispersion of q was more and less affected by λ_0 and W, respectively, similar to the results of the local method. However, due to the hidden interaction among independent variables, q was dispersed as much as ρ scattered in the global method, while the reverse was observed in the local method. Also, the scatter of L dispersed q more, and its effect in the global method was more than that in the local method.

Table 5. 4. COV values of dependent and independent variables for the drainage layer.

Sensitivity analysis method	Independent variables	COV of independent variables	COV of q	$\frac{\text{COV of dependent variable (q)}}{\text{COV of independent variables}}$
Local	λ_0	0.167	0.167	1
	L	0.067	0.067	0.97
	W	0.34	0.1	0.29
	ρ	0.19	0.055	0.29
Global	λ_0	0.167	0.18	1.08
	L	0.067		2.69
	W	0.34		0.53
	ρ	0.19		0.95

5.3.3.2. Substrate layer

The heat flux histograms of the substrate layer were obtained using local and global methods, as presented in Fig. 5.9. Their shapes were symmetrical, similar to what was observed for the drainage layer's histogram. The confidence of q values was high as well (99%).

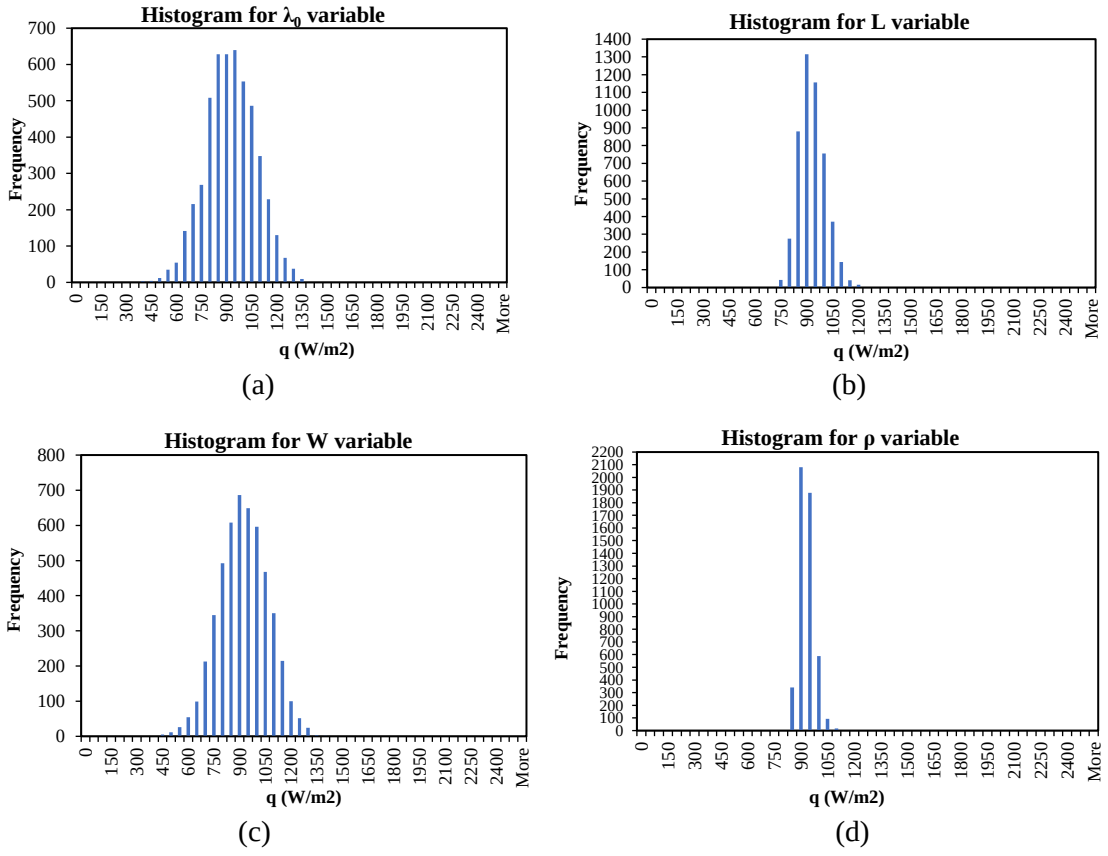

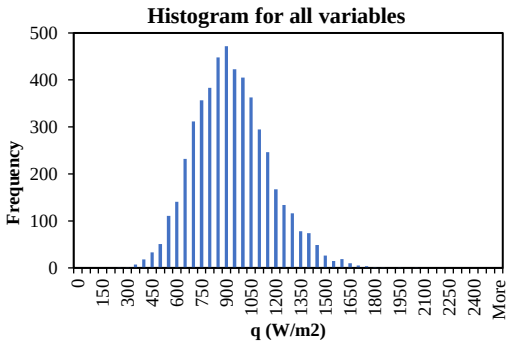

(e)

Fig. 5. 9. Heat flux histogram of substrate layer for λ_0 (a); L (b); W (c); ρ (d); and all variables (e).

Table 5.5 shows COV values of dependent and independent variables for the substrate layer. The ratios of COV of q to COV of λ_0, W, ρ and L were 1, 0.95, 0.48 and 0.48. Therefore, the scatter of λ_0 and L could be equally effective in the dispersion of q, while the influence of ρ and L was not significant, similar to what was observed for the drainage layer.

In the global method, the ratios of COV of q to COV of λ_0, L, W and ρ were 1.27, 2.53, 0.63 and 2.31. Therefore, the dispersion of q for the substrate layer was observed once L was scattered, as also occurred for the drainage layer. Also, the λ_0 was more effective in the global method than the local method. The W was not effectual in the global method as the local one. However, the hidden interaction among independent variables in the global method remarkably increased the influence of ρ on q scatter, contrary to the local one.

Table 5. 5. COV values of dependent and independent variables for substrate layer.

Sensitivity analysis method	Independent variables	COV of Independent variables	COV of q	$\frac{\text{COV of dependent variable (q)}}{\text{COV of independent variables}}$
Local	λ_0	0.165	0.165	1
	L	0.083	0.079	0.952
	W	0.333	0.161	0.48
	ρ	0.091	0.044	0.48
Global	λ_0	0.165	0.21	1.27
	L	0.083		2.53
	W	0.333		0.63
	ρ	0.091		2.31

5.4. Discussion

5.4.1. Main findings

The temperature and RH fluctuations between the substrate and drainage layers (Fig. 5.4) decreased compared to those in the exterior surface (Appendix 2). This could be due to the substrate's significant thermal mass generation near the top of the drainage layer, similar to what Lundholm et al. (Lundholm et al., 2014) observed. The RH values were obtained less than 100% in some cases between the substrate and drainage layers owing to air-voids among coarse drainage aggregates. Also, the temperature and RH in the interior surface of green roof models (Fig. 5.5) were less fluctuated than those between substrate and drainage layers (Fig. 5.4), so that the former's ranges were attained within the comfort ranges given by World Health Organization (WHO, 2018) and Gilmore (Gilmore, 1972). It may be because coarse granular

drainage materials had more pores, which created air voids in the drainage layer and increased its heat resistance against fluctuating exterior temperatures. This somewhat prevented the interior temperature from escaping through the green roof's exterior surfaces (Coma et al., 2016). Also, the drainage materials offered thermal resistance, preventing the exterior temperature from easily transferring to the interior surface. According to the modeling outputs, most of the time, as the temperature rose, the RH changed quickly. Similar to what Li and Zhu (Li & Zhu, 2016) reported, this process could be linked to the evaporation of water content in the substrate layer, which directly impacted heat transfer in the interior surface of green roof systems. As a result of the water in the substrate layer evaporating at high temperatures, the depth of the green roof system was somewhat protected from the transfer of outside temperature and solar radiation.

Due to the green roof layers' high water retention capacity, the interior RH decreased compared to the exterior one. SC's water content was an average of 13.5% higher than SP's (Fig. 5.6(a)), owing to a large amount of organic matter in the former, leading to slightly more water absorption of the substrate layer. Because of the higher porosity of artificial and recycled drainage aggregates (RCA, IMSWA and LECA), their water content was about 2.5 times more than that of NCA (Fig. 5.6(b)). The presence of fine particles in substrate materials caused their water content to be obtained 9 times more than drainage materials in scenarios 1 and 2. The respective difference in scenario 3 was 6.5 times. The lower difference in scenario 3 was due to less rainfall at the end of the 21st century (Appendix 2).

In comparison to green roof models with a substrate layer of SP and the drainage layer of RCA and IMSWA, the control green roof model with a substrate layer of SC and drainage layer of NCA marginally had greater thermal resistance for all scenarios (Fig. 5.7). The drainage layer of RCA, IMSWA and NCA nearly had the same thermal resistance (M. Kazemi et al., 2023). Therefore, the aforementioned difference could be that the soil's fine particles in SC moderately outperformed coarse recycled materials in SP to prevent heat flux transfer within green roof systems. However, compared to the green roof model with a substrate layer of SP and the drainage layer of LECA, the control green roof model's thermal resistance was lower. Due to the high porosity and low density of LECA as drainage material, its thermal resistance was better than that of NCA (M. Kazemi et al., 2023), similar to what other researchers obtained for other drainage aggregates (Coma et al., 2014; Pérez, Coma, et al., 2012). Therefore, in comparison to the substrate layer of SC, the drainage layer of LECA contributed more to providing thermal resistance for green roof systems in the 21st century. Note that the difference between the heat flux of the control green roof model and green roof models with the drainage layer of RCA and IMSWA decreased for scenario 3 compared to scenarios 1 and 2, while this difference between the former and green roof models with the drainage layer of LECA increased. The reason is that the rainfall and, subsequently, water content of green roof layers for scenario 3 (0.015 Ltr/m^2) were averagely lower than those for scenarios 1 and 2 (0.022 Ltr/m^2). Similar to what other researchers (Eskandarinia et al., 2022; Jahandari et al., 2021; Koushkbaghi et al., 2019; Rincón et al., 2014; Shadmani et al., 2018) reported, decreasing the amount of water content led to increasing air-voids and diffusion properties of artificial and recycled coarse aggregates with high porosity. That’s why the substrate layer enhanced the thermal performance of buildings when combined with a drainage layer with a large pore

volume, as revealed by Scharf and Zluwa (Scharf & Zluwa, 2017). Therefore, the drainage layer decreased temperature fluctuation and ultimately improved the green roof models' thermal resistance with less rainfall for scenario 3. As a result, since the thermal performance of green roofs with artificial and recycled materials was improved until end of 21st century against the temperate climate, they are recommended to be used for rooftops to apply lower weight to buildings owing to their lower density and higher porosity.

The value of heat flux on the interior surface (Fig. 5.7(b)) was lower than that on the exterior surface (Fig. 5.7(a)). This procedure showed that the drainage and substrate layers prevented temperature changes from transferring through the green roof systems, which decreased the diurnal temperature fluctuation at the lower layers of the green roof model (Parizotto & Lamberts, 2011), leading to decreasing the interior heat flux compared to the exterior one.

In contrast to the exterior surface (Fig. 5.7(a)), the summer months (June, July and August) and the beginning of fall (September) had a decreasing heat flow tendency in the interior surface (Fig. 5.7(b)). Increased temperature caused the water content in the substrate layer to evaporate once there was humidity in the various layers of the green roof during the summer. This evaporated water helped to absorb some of the solar light and temperature outdoors. Considering this, a thermal resistance layer was created in the green roof system due to the moisture in the drainage and substrate layers absorbing the outside temperature to attain a stable temperature (M. Kazemi & Courard, 2021b). Therefore, increasing solar radiation and air temperature and decreasing RH during the summer led to enhancing green roofs' passive cooling ability, resulting in less heat gain and heat flux (Jim & Peng, 2012). That's why the green roof decreased the cooling energy demand in places with temperate weather, as reported by Ávila-Hernández et al. (Ávila-Hernández et al., 2020).

The results of the local method (Tables 5.4 and 5.5) showed that the q value was scattered as much as the λ_0 and L dispersed. According to the results of the global method, the drainage and substrate layers' greatest q dispersion was attained once L was scattered, confirming that the thermal resistance of buildings was improved as the green roof construction became thicker, as revealed by Scharf and Zluwa (Scharf & Zluwa, 2017). The ratios of COV of q to COV of ρ showed that the effect of density on q dispersion for the substrate layer (2.31) was higher than that in the drainage layer (0.95). This difference may be because the ranges of maximum and minimum values of other independent variables (λ_0, W and L) for the substrate layer were greater than those for the drainage layer. This, in turn, increased the effect of hidden interaction among independent variables on the density parameter (ρ) to disperse q values more for the substrate layer.

5.4.2. Limitations

There were some limitations that could have affected the outcomes in this study. The influences of plants and their evapotranspiration phenomenon on the hygrothermal performance of green roof models were not considered. Moreover, the color of the soil that could affect the heat flux and the thermal behavior of the green roof layers was not taken into account in the analyses.

5.5. Conclusions

This study assessed the hygrothermal performance of green roof layers, including different coarse artificial and recycled materials, under three weather data scenarios of the 21st century. Sensitivity analysis on drainage and substrate layers made with artificial and recycled components was carried out as well. Based on the presented results, the following conclusions were extracted:

- In comparison to the exterior surface and the area between the substrate and drainage layers, the interior surface presented less temperature and relative humidity fluctuations. Also, for all scenarios, the interior temperature and relative humidity ranges were near to the comfort ranges, providing a healthy internal environment for buildings' occupants.
- Compared to the proposed substrate with coarse recycled materials, the control substrate without coarse recycled materials presented averagely 13.5% more water content by volume. In addition, RCA, IMSWA and LECA achieved around 2.5 times more water content than NCA. For scenarios 1 and 2, the substrate layers' water content was roughly nine times larger than the drainage layers. For scenario 3, the difference was 6.5 times larger owing to lower rainfall at the end of the 21st century.
- The lowest water content of green roof materials for all scenarios happened in the summer and at the beginning of autumn. For scenario 1, the highest water content of green roof materials happened in March and April (spring). With scenarios 2 and 3, the highest water content was observed in December (winter).
- The lowest interior heat flow values for scenarios 1 and 2 were observed in August. July experienced the same for scenario 3. March had the highest interior heat flow values for scenario 1. The same was observed in December for scenarios 2 and 3.
- During the summer months and the beginning of autumn, a decrease in the rainfall pattern until the end of the 21st century caused the heat resistance of green roof models with artificial and recycled materials to increase for scenario 3, compared to scenarios 1 and 2.
- Decreasing heat flow tendency in the interior surface during the summer months and the beginning of fall revealed the passive cooling ability of green roof models.
- The sensitivity to a single independent variable revealed that the highest dispersion of q for the green roof layers was attained when λ_0 and L changed. However, the former was less affected by the W and ρ scatter.
- The entire parameters change showed that the scatter of λ_0, ρ and L influenced the dispersion of q for the green roof layers. However, the scatter of ρ was more effective in the dispersion of q for the substrate layer than the drainage layer.

Therefore, using artificial and recycled components seems to improve the thermal performances of green roof systems against the temperate climate until the end of the 21st century and has a positive effect on buffering climate change for housing comfort.

Chapter 6: Conclusions and outlook

6.1. Conclusions

The main contribution of this thesis is assessing the possibility of using recycled and artificial materials for green roof layers. This thesis mainly focuses on substrate and drainage layers of green roof systems in which coarse recycled and artificial materials can be used. The findings of the thesis can provide valuable insights for researchers, green roof designers and professionals and constructors. This thesis consists of four main parts to address thesis objectives: 1) evaluation of water permeability, water retention capacity and thermal resistance of green roof layers made with recycled and artificial aggregates; 2) rainfall detention performance of green roof layers including coarse recycled materials; 3) modellisation of hygrothermal conditions of substrate and drainage layers for the thermal resistance assessment of green roof: effect of coarse recycled materials; 4) analysis of the sensitivity and the weather condition effects on hygrothermal performance of green roof models characterized by recycled and artificial materials' properties.

According to specific criteria, the materials were chosen for substrate and drainage layers of green roof systems:

- The substrate with recycled coarse materials (SP) was proposed for the substrate layer and results were compared with those of substrate without recycled coarse materials (SC).
- For the drainage layer, the results of Recycled Coarse Aggregate (RCA), Incinerated Municipal Solid Waste Aggregate (IMSWA) and Lightweight Expanded Clay Aggregate (LECA) were compared with those of Natural Coarse Aggregate (NCA).

The main objective of the thesis was to assess to what extent the presence of recycled and artificial materials can provide thermal resistance, water passing ability and water retention capacity for substrate and drainage layers compared to conventional green roof materials. Three leading indicators as dependent variables were measured and analyzed for green roof systems: Rc-value as heat resistance indicator, water permeability as water drainage indicator and water retention capacity as water holding indicator. According to the results, for the drainage layer, the water permeability of NCA was 1.5 times higher than that of LECA. The results of NCA, IMSWA and RCA were nearly the same. For the substrate layer, although the water permeability of SC was 1.5 times higher than that of SP, the results of both were within the range given by FLL guidelines (10^{-5} - 1.17×10^{-3} m/s). Concerning the water retention capacity, for the drainage layer, the results of IMSWA, RCA and LECA were more than NCA. For the substrate layer, although the water retention capacity of SC was 1.2 times higher than SP, the results of both were within the range of FLL guidelines (35% - 65%). Regarding thermal resistance measurement, for the drainage layer, LECA obtained the highest Rc-value. The results of NCA, IMSWA and RCA were nearly the same. For the substrate layer, Rc-value of SC was marginally more than that of SP. Also, the results of dry substrate were about twice of wet substrate.

These results clearly indicate that using coarse recycled and artificial materials can allow targeting minimum requirements for the water permeability, water retention capacity and thermal resistance in comparison with the conventional green roof materials.

A study by Rivière (Rivière, 2023) on green roofs including recycled materials under simulated rains with return periods of two years and 20 years showed that other factors such as the root type, aerial biomass and vegetation height could affect the water runoff quantity only for more intense precipitation events with higher runoff. More importantly, to regulate the water runoff under severe rain patterns, the type of substrate materials should be taken into account (Rivière, 2023). Considering this, another objective was to evaluate the rainfall detention performance of green roof layers including coarse recycled materials under high rainfall (100 mm/h) and low rainfall intensities (50 mm/h). A rainfall box was used to simulate two rainfall intensities on a lab-scale. Also, two thicknesses of 15 cm and 10 cm were considered for the substrate layer to assess the effect of substrate depth on the results. The results show that, whatever under low and high rainfall intensities, the rainfall detention performance of green roofs without coarse recycled materials was marginally higher than that of green roofs containing coarse recycled materials. Also, the rainfall detention performance of green roof systems marginally decreased either with or without coarse recycled materials by increasing the thickness of the substrate layer from 10 cm to 15 cm.

It can be consequently concluded that the use of coarse recycled materials can provide nearly the same rainfall detention performance for green roof layers as the conventional green roof materials.

Modelling the hygrothermal behaviour of green roof materials and optimize the thickness of substrate and drainage layers was also a major challenge. Green roofs with the substrate layer incorporating coarse recycled materials and the drainage layer of recycled coarse aggregate were firstly tested and assessed following ISO 9869-1. Then, the hygrothermal conditions of substrate and drainage layers were translated into the WUFI software. To validate the modeling outputs with experimental results, temperatures through green roof layers' depth were measured. Given that the thermal insulation performance was related to the temperature distribution through the depth of materials, the distribution of temperatures within green roof layers was evaluated. Also, to achieve an optimum design of the green roof system concerning its thermal performance, the thickness of drainage and substrate layers was changed (parametric study). According to the results, the thermal performance of the models with and without coarse recycled materials was accurately validated with that of roofing systems after translating green roof layers' initial hygrothermal properties into WUFI software. As per the results of the parametric study, a simultaneous change in the substrate and drainage layers' thickness revealed that 6-cm drainage layer and 18-cm unsaturated substrate layer were the best design to provide an adequate thermal resistance for the roofing systems.

The fifth objective was to assess the influence of using artificial or recycled materials on green roof performance under the temperate climate of Liège city till the end of the 21st century. Climate change influence is particularly important to be checked: the hygrothermal performance of green roof models characterized by recycled and artificial materials' properties was assessed under three weather data scenarios: beginning, middle and end of the 21st century. The effect of weather data scenarios on heat flux values and water content of green roof layers was evaluated and compared to each other. According to the results, for weather data scenarios at the beginning and middle of the 21st century, the substrate layers' water content was roughly

nine times larger than the drainage layers. For the weather data scenario at the end of the 21st century, the difference was 6.5 times larger owing to lower rainfall at the end of the 21st century. In comparison to scenarios at the beginning and middle of the 21st century, the summer and early fall periods of the 21st century experienced a drop in rainfall, which increased the heat resistance of green roof models made of artificial and recycled materials. It is worth mentioning that compact large low-rise and large low-rise archetypes, green roofs could be very useful in reducing surface and air temperatures as a study by Joshi (Joshi, 2024) on the local microclimate of Liège city demonstrated.

This can be concluded that green roof applications for rooftops of buildings can positively affect the microclimatic situation in Liège city and also, using alternative materials such as recycled concrete aggregates is favorable for the hygrothermal performance of green roof under the temperate climate of Liège city till the end of the 21st century.

Finally, the last objective of this thesis was to evaluate the heat flux sensitivity to the thickness and physical characteristics of green roofs with artificial and recycled materials. Both local and global sensitivity analyses were considered. In the local method, a single independent variable was changed, and others were assumed to be constant. The global method examined the sensitivity regarding the entire parameters change. As per the local method analysis, scattering thermal conductivity and layer thickness led to the highest dispersion of heat flux for the green roof layers. However, the latter was less affected by the water content and density scatter. Scattering thermal conductivity and layer thickness in the global method influenced the dispersion of heat flux for the green roof layers, similar to the local method. Contrary to the local method, the heat flux was scattered as much as density in the global method due to the hidden interaction among independent variables. Therefore, with the presence of recycled and artificial materials, the density effect on the thermal resistance of substrate materials should be taken into account more than that of drainage materials.

Green roof materials producers should avoid using fine aggregates (0-5 mm) for the drainage layer as they prevent dewatering of roofing systems. The drainage materials with a minimum size of 7 mm are recommended to be used as they can provide adequate rainfall detention performance for green roof systems. On the other hand, since the thickness of drainage layer is assumed to be thin (5 cm), the size of drainage aggregates should not be more than 15 mm.

Normally, the Rc-value of green roof systems should be about 4 m^2K/W to provide the thermal resistance for rooftops. In addition, the Rc-value of green roof with a 15-cm substrate layer of SP and a 5-cm drainage layer of recycled and artificial materials is 1 m^2K/W at the most. Therefore, although substrate and drainage layers cannot provide the required thermal resistance for rooftops (4 m^2K/W), they are able to contribute in providing thermal resistance for green roof systems.

To install green roof systems for some case studies in Liège city, the load-bearing capacity of 230 kg/m^2 should be taken into account for rooftops by green roof designers. The density of green roofs with a 10-cm saturated substrate layer of SP and a 5-cm drainage layer of all coarse artificial and recycled aggregates is less than 200 kg/m^2. Also, the corresponding value for 15-cm saturated substrate layer of SP and a 5-cm drainage layer of LECA is about 211 kg/m^2.

Therefore, the aforementioned configuration of substrate and drainage layers can be used in Liège city. The density of 15-cm saturated substrate layer of SP and a 5-cm drainage layer of RCA and IMSWA is about 240 kg/m^2 which is 4% more than the load-bearing capacity of some case studies in Liège city (230 kg/m^2). Since this difference is not remarkable, the possibility of 5-cm drainage layer of RCA and IMSWA can be taken into consideration. In any case, when there is more limitation with regard to load-bearing capacity of buildings, it is highly recommended to use the green roof drainage layer including coarse artificial and recycled materials. It is also advised to use a 10-cm substrate with coarse recycled materials as its rainfall detention performance is near to that without coarse recycled materials and its water retention capacity is within the required range given by FLL guidelines. However, the common thickness of extensive green roofs should not be more than 20 cm to prevent overloading rooftops. Considering this, 20-cm green roofs with a 15-cm substrate layer and a 5-cm drainage layer are recommended to be used for rooftops. The interior temperature and relative humidity ranges of these green roofs against the temperate climate of 21st century are near to the comfort ranges and a 15-cm substrate layer can provide an acceptable depth for a variety of plant growth. On the other hand, when the load bearing capacity of rooftops is high, the thickness of substrate and drainage layers can increase up to 18 cm and 6 cm, respectively, to provide the optimum thermal insulation for green roof systems (the optimum thicknesses based on interior and exterior temperatures). In general, due to the lower density and high porosity, green roofs made of coarse artificial and recycled materials are proposed to be used for rooftops to apply less weight to buildings as their thermal performance against the temperate climate will increase up until the end of 21st century.

Finally, this thesis allowed introducing commercial drainage and substrate materials as artificial and recycled production for green roof systems. It has been proved that these alternative materials can offer adequate hygrothermal performance for green roofs compared to the conventional green roof materials. Designing green roof systems with coarse artificial and recycled materials should allow to reduce the use of natural aggregates, to develop the recycling of wastes or by-products as secondary resources and to share opportunities of covering flat roof by means of green roof systems. Their design is based on hygrothermal properties that have been taken into account to optimize the thicknesses of substrate and drainage layers. Depending on climate change scenarios, this design method could be adapted and contribute to a optimize green roof system versus geographical local comfort requirements.

6.2. Perspectives

This thesis aimed to assess the possibility of using artificial and recycled materials for substrate and drainage layers of green roof systems.

Based on the findings of this thesis, the following are possible areas of research for the future:

1) This thesis assessed the hygrothermal performance of green roof layers without plants. However, the vegetation coverage at the top of the substrate layer can affect the evapotranspiration phenomenon within green roof systems. Therefore, it is of interest to

consider the effect of different types of plants on the hygrothermal performance of green roof layers including artificial and recycled materials.

2) Although the effect of using coarse recycled materials on the thermal performance of the green roof substrate layer was measured in this thesis, the color of the soil can also affect the thermal behavior of green roof systems. Considering this, further research needs to assess the effect of soil's color on the heat flux value within green roof systems.
3) This thesis mainly focused on using coarse recycled materials for the green roof substrate layer. Further research is needed to assess the effect of fine recycled and artificial materials on the hygrothermal performance of the green roof substrate layer.
4) In this thesis, the optimization of green roof layers' thickness was conducted based the temperature variations. However, other parameters can also affect the optimum thickness of green roof layers which can be taken into account in future studies.
5) The hygrothermal performance of green roof models under the temperate climate of Liège city was evaluated in this thesis. It is of interest to assess the performance of green roof models under other climate conditions in future studies.

6.3. List of journal and conference publications produced within this project

Kazemi, M., & Courard, L. (2021). Modelling hygrothermal conditions of unsaturated substrate and drainage layers for the thermal resistance assessment of green roof: Effect of coarse recycled materials. *Energy and Buildings*, *250*, 111315. https://doi.org/10.1016/j.enbuild.2021.111315

Kazemi, M., & Courard, L. (2021). Simulation of humidity and temperature distribution in green roof with pozzolana as drainage layer: Influence of outdoor seasonal weather conditions and internal ceiling temperature. *Science and Technology for the Built Environment*, *27*(4), 509–523. https://doi.org/10.1080/23744731.2021.1873658

Kazemi, M., & Courard, L. (2022). Modelling thermal and humidity transfers within green roof systems: Effect of rubber crumbs and volcanic gravel. *Advances in Building Energy Research*, *16*(3), 296–321. https://doi.org/10.1080/17512549.2020.1858961

Kazemi, M., & Courard, L. (2022). Selecting criteria and water permeability measurement of recycled and artificial materials for green roof layers. *CitiesAlive: 19th Annual Green Roof and Wall Conference, Philadelphia, USA*, 1–11.

Kazemi, M., & Courard, L. (2022). Thermal Resistance Measurement of Green Roof Layers with Coarse Artificial and Recycled Materials. *Doctoral Seminars on Sustainability Research in the Built Environment (DS^{2}BE), Ghent University, Ghent, Belgium*, 1–13.

Kazemi, M., Courard, L., & Attia, S. (2021). Hygrothermal modeling of green roof made with substrate and drainage layers of coarse recycled materials. *Building Simulation 2021 Conference, KU Leuven, Leuven, Belgium*, 1–8.

Kazemi, M., Courard, L., & Attia, S. (2023). Water permeability, water retention capacity, and thermal resistance of green roof layers made with recycled and artificial aggregates. *Building and Environment*, *227*, 109776. https://doi.org/10.1016/j.buildenv.2022.109776

Kazemi, M., Courard, L., & Hubert, J. (2021). Heat Transfer Measurement within Green Roof with Incinerated Municipal Solid Waste Aggregates. *Sustainability*, *13*(13), Article 13. https://doi.org/10.3390/su13137115

Kazemi, M., Courard, L., & Hubert, J. (2022). Coarse recycled materials for the drainage and substrate layers of green roof system in dry condition: Parametric study and thermal heat transfer. *Journal of Building Engineering*, *45*, 103487. https://doi.org/10.1016/j.jobe.2021.103487

Kazemi, M., Rahif, R., Courard, L., & Attia, S. (2023). Sensitivity analysis and weather condition effects on hygrothermal performance of green roof models characterized by recycled and artificial materials' properties. *Building and Environment*, *237*, 110327. https://doi.org/10.1016/j.buildenv.2023.110327

References

Abergel, T., Dean, B., & Dulac, J. (2017). Towards a zero-emission, efficient, and resilient buildings and construction sector. *Global Status Report*.

Akbarzadeh Bengar, H., Shahmansouri, A. A., Akkas Zangebari Sabet, N., Kabirifar, K., & W.Y. Tam, V. (2020). Impact of elevated temperatures on the structural performance of recycled rubber concrete: Experimental and mathematical modeling. *Construction and Building Materials*, *255*, 119374. https://doi.org/10.1016/j.conbuildmat.2020.119374

Allinson, D., & Hall, M. (2010). Hygrothermal analysis of a stabilised rammed earth test building in the UK. *Energy and Buildings*, *42*(6), 845–852. https://doi.org/10.1016/j.enbuild.2009.12.005

Almeida, R., Simões, N., Tadeu, A., Palha, P., & Almeida, J. (2019). Thermal behaviour of a green roof containing insulation cork board. An experimental characterization using a bioclimatic chamber. *Building and Environment*, *160*, 106179. https://doi.org/10.1016/j.buildenv.2019.106179

Ampim, P. A. Y., Sloan, J. J., Cabrera, R. I., Harp, D. A., & Jaber, F. H. (2010). Green Roof Growing Substrates: Types, Ingredients, Composition and Properties. *Journal of Environmental Horticulture*, *28*(4), 244–252. https://doi.org/10.24266/0738-2898-28.4.244

Ascione, F., De Masi, R. F., de Rossi, F., Ruggiero, S., & Vanoli, G. P. (2016). Optimization of building envelope design for nZEBs in Mediterranean climate: Performance analysis of residential case study. *Applied Energy*, *183*, 938–957. https://doi.org/10.1016/j.apenergy.2016.09.027

ASTM D4611 - 16. (2018). *Standard test method for specific heat of rock and soil*. ASTM International. https://doi.org/10.1520/D4611-16

Ávila-Hernández, A., Simá, E., Xamán, J., Hernández-Pérez, I., Téllez-Velázquez, E., & Chagolla-Aranda, M. A. (2020). Test box experiment and simulations of a green-roof: Thermal and energy performance of a residential building standard for Mexico. *Energy and Buildings*, *209*, 109709. https://doi.org/10.1016/j.enbuild.2019.109709

Awulachew, S. B., Lemperiere, P., & Tulu, T. (2009). *Training material on agricultural water management*. International Water Management Institute ; International Livestock Research Institute ; Adama University.

AzariJafari, H., Guest, G., Kirchain, R., Gregory, J., & Amor, B. (2021). Towards comparable environmental product declarations of construction materials: Insights from a probabilistic comparative LCA approach. *Building and Environment*, *190*, 107542. https://doi.org/10.1016/j.buildenv.2020.107542

Bahmani, M., Fatehi, H., Noorzad, A., & Hamedi, J. (2019). Biological soil improvement using new environmental bacteria isolated from northern Iran. *Environmental Geotechnics*, *40*(XXXX), 1–13.

Barnaby, C. S., & CRAWLEY, U. B. (2012). Weather data for building performance simulation. In *Building performance simulation for design and operation* (pp. 61–79). Routledge.

Bates, A. J., Sadler, J. P., Greswell, R. B., & Mackay, R. (2015). Effects of recycled aggregate growth substrate on green roof vegetation development: A six year experiment. *Landscape and Urban Planning*, *135*, 22–31. https://doi.org/10.1016/j.landurbplan.2014.11.010

Becker, D., & Wang, D. (2011). Green roof heat transfer and thermal performance analysis. *Unpublished Report), Civil and Environmental Engineering, Carnegie Mellon University, Pittsburgh, PA, USA*. https://www.cmu.edu/environment/campus-green-design/green-roofs/documents/heat-transfer-and-thermal-performance-analysis.pdf

Bellazzi, A., Barozzi, B., Pollastro, M. C., & Meroni, I. (2020). Thermal resistance of growing media for green roofs: To what extent does the absence of specific reference values potentially affect the global thermal resistance of the green roof? An experimental example. *Journal of Building Engineering*, *28*, 101076.

Berardi, U. (2019). The impact of aging and environmental conditions on the effective thermal conductivity of several foam materials. *Energy*, *182*, 777–794. https://doi.org/10.1016/j.energy.2019.06.022

Bianchini, F., & Hewage, K. (2012). How "green" are the green roofs? Lifecycle analysis of green roof materials. *Building and Environment*, *48*, 57–65. https://doi.org/10.1016/j.buildenv.2011.08.019

Bisceglie, F., Gigante, E., & Bergonzoni, M. (2014). Utilization of waste Autoclaved Aerated Concrete as lighting material in the structure of a green roof. *Construction and Building Materials*, *69*, 351–361. https://doi.org/10.1016/j.conbuildmat.2014.07.083

Bliss, D. J., Neufeld, R. D., & Ries, R. J. (2009). Storm Water Runoff Mitigation Using a Green Roof. *Environmental Engineering Science*, *26*(2), 407–418. https://doi.org/10.1089/ees.2007.0186

Brouwer, C., Goffeau, A., & Heibloem, M. (1985). Irrigation water management: Training manual no. 1-introduction to irrigation. *Food and Agriculture Organization of the United Nations, Rome, Italy*, 102–103.

BS 5250. (2011). Code of practice for control of condensation in buildings. *British Standards Institution*.

Cagnon, H., Aubert, J. E., Coutand, M., & Magniont, C. (2014). Hygrothermal properties of earth bricks. *Energy and Buildings*, *80*, 208–217. https://doi.org/10.1016/j.enbuild.2014.05.024

Carter, T., & Jackson, C. R. (2007). Vegetated roofs for stormwater management at multiple spatial scales. *Landscape and Urban Planning*, *80*(1), 84–94. https://doi.org/10.1016/j.landurbplan.2006.06.005

Cascone, S. (2019). Green Roof Design: State of the Art on Technology and Materials. *Sustainability*, *11*(11), Article 11. https://doi.org/10.3390/su11113020

Cascone, S., Catania, F., Gagliano, A., & Sciuto, G. (2018). A comprehensive study on green roof performance for retrofitting existing buildings. *Building and Environment*, *136*, 227–239.

Chan, A. L. S., & Chow, T. T. (2013). Energy and economic performance of green roof system under future climatic conditions in Hong Kong. *Energy and Buildings*, *64*, 182–198. https://doi.org/10.1016/j.enbuild.2013.05.015

Chenani, S. B., Lehvävirta, S., & Häkkinen, T. (2015). Life cycle assessment of layers of green roofs. *Journal of Cleaner Production*, *90*, 153–162.

Cirrincione, L., Marvuglia, A., & Scaccianoce, G. (2021). Assessing the effectiveness of green roofs in enhancing the energy and indoor comfort resilience of urban buildings to climate change: Methodology proposal and application. *Building and Environment*, *205*, 108198. https://doi.org/10.1016/j.buildenv.2021.108198

Coma, J., Pérez, G., Castell, A., Solé, C., & Cabeza, L. F. (2014). Green roofs as passive system for energy savings in buildings during the cooling period: Use of rubber crumbs as drainage layer. *Energy Efficiency*, *7*(5), 841–849. https://doi.org/10.1007/s12053-014-9262-x

Coma, J., Pérez, G., Solé, C., Castell, A., & Cabeza, L. F. (2016). Thermal assessment of extensive green roofs as passive tool for energy savings in buildings. *Renewable Energy*, *85*, 1106–1115. https://doi.org/10.1016/j.renene.2015.07.074

Daya, S. (2003). The t-test for comparing means of two groups of equal size. *Evidence-Based Obstetrics & Gynecology*, *5*(1), 4–5. https://doi.org/10.1016/S1361-259X(03)00054-0

Desogus, G., Mura, S., & Ricciu, R. (2011). Comparing different approaches to in situ measurement of building components thermal resistance. *Energy and Buildings*, *43*(10), 2613–2620.

De-Ville, S., Menon, M., Jia, X., & Stovin, V. (2018). A Longitudinal Microcosm Study on the Effects of Ageing on Potential Green Roof Hydrological Performance. *Water*, *10*(6), Article 6. https://doi.org/10.3390/w10060784

DIN 52 615. (1973). *Determination of water vapour (moisture) permeability of construction and insulating materials.*

Directive. (2010). *Directive 2010/31/eu of the European parliament and of the council of 19 May 2010 on the energy performance of buildings. Available from: Http://www.epbd-ca.eu. Accessed 5 Mar 2013.*

D'Orazio, M., Di Perna, C., & Di Giuseppe, E. (2012). Green roof yearly performance: A case study in a highly insulated building under temperate climate. *Energy and Buildings*, *55*, 439–451. https://doi.org/10.1016/j.enbuild.2012.09.009

Doutreloup, S., Fettweis, X., Rahif, R., Elnagar, E. A., Pourkiaei, M. S., Amaripadath, D., & Attia, S. (2022). Historical and Future Weather Data for Dynamic Building Simulations in Belgium using the MAR model: Typical & Extreme Meteorological Year and Heatwaves. *Earth System Science Data Discussions*, 1–19.

Dunnett, N., Nagase, A., Booth, R., & Grime, P. (2008). Influence of vegetation composition on runoff in two simulated green roof experiments. *Urban Ecosystems*, *11*(4), 385–398. https://doi.org/10.1007/s11252-008-0064-9

Dvorak, B. (2011). Comparative Analysis of Green Roof Guidelines and Standards In Europe and North America. *Journal of Green Building*, *6*(2), 170–191. https://doi.org/10.3992/jgb.6.2.170

Ebadati, M., & Ehyaei, M. A. (2020). Reduction of energy consumption in residential buildings with green roofs in three different climates of Iran. *Advances in Building Energy Research*, *14*(1), 66–93. https://doi.org/10.1080/17512549.2018.1489894

Eksi, M., & Rowe, D. B. (2016). Green roof substrates: Effect of recycled crushed porcelain and foamed glass on plant growth and water retention. *Urban Forestry & Urban Greening*, *20*, 81–88. https://doi.org/10.1016/j.ufug.2016.08.008

Eksi, M., Sevgi, O., Akburak, S., Yurtseven, H., & Esin, İ. (2020). Assessment of recycled or locally available materials as green roof substrates. *Ecological Engineering*, *156*, 105966. https://doi.org/10.1016/j.ecoleng.2020.105966

EN 1015-19. (1999). *Methods of test for mortar for masonry. Determination of water vapour permeability of hardened rendering and plastering mortars*.

EN 1925. (1999). *Natural stone test methods. Determination of water absorption coefficient by capillarity*. https://shop.bsigroup.com/ProductDetail?pid=000000000019973432

EN 12620. (2013). *Aggregates for concrete. European Committee for Standardization*. iTeh Standards Store. https://standards.iteh.ai/catalog/standards/cen/aef412e6-36ce-49d3-afaa-5200d721ff84/en-12620-2013

EN 15026. (2007). *Hygrothermal performance of building components and building elements. Assessment of moisture transfer by numerical simulation*.

Engineering ToolBox. (2003). *Specific Heat of some common Substances*. https://www.engineeringtoolbox.com/specific-heat-capacity-d_391.html

Eskandarinia, M., Esmailzade, M., Hojatkashani, A., Rahmani, A., & Jahandari, S. (2022). Optimized Alkali-Activated Slag-Based Concrete Reinforced with Recycled Tire Steel Fiber. *Materials*, *15*(19), Article 19. https://doi.org/10.3390/ma15196623

Fabiani, C., Coma, J., Pisello, A. L., Perez, G., Cotana, F., & Cabeza, L. F. (2018). Thermo-acoustic performance of green roof substrates in dynamic hygrothermal conditions. *Energy and Buildings*, *178*, 140–153. https://doi.org/10.1016/j.enbuild.2018.08.024

Fachinello Krebs, L., & Johansson, E. (2021). Influence of microclimate on the effect of green roofs in Southern Brazil – A study coupling outdoor and indoor thermal simulations. *Energy and Buildings*, *241*, 110963. https://doi.org/10.1016/j.enbuild.2021.110963

Fan, Y., & Xia, X. (2017). A multi-objective optimization model for energy-efficiency building envelope retrofitting plan with rooftop PV system installation and maintenance. *Applied Energy*, *189*, 327–335. https://doi.org/10.1016/j.apenergy.2016.12.077

Farrell, C., Ang, X. Qi., & Rayner, J. P. (2013). Water-retention additives increase plant available water in green roof substrates. *Ecological Engineering*, *52*, 112–118. https://doi.org/10.1016/j.ecoleng.2012.12.098

Fatehi, H., Abtahi, S. M., Hashemolhosseini, H., & Hejazi, S. M. (2018). A novel study on using protein based biopolymers in soil strengthening. *Construction and Building Materials*, *167*, 813–821. https://doi.org/10.1016/j.conbuildmat.2018.02.028

FLL guidelines. (2008). *Guidelines for the Planning, Construction and Maintenance of Green Roofing: Green Roofing Guideline*. Forschungsgesellschaft Landschaftsentwickung Landschaftsbau.

Getter, K. L., Rowe, D. B., Andresen, J. A., & Wichman, I. S. (2011). Seasonal heat flux properties of an extensive green roof in a Midwestern U.S. climate. *Energy and Buildings*, *43*(12), 3548–3557. https://doi.org/10.1016/j.enbuild.2011.09.018

Giada, G., Caponetto, R., & Nocera, F. (2019). Hygrothermal Properties of Raw Earth Materials: A Literature Review. *Sustainability*, *11*(19), Article 19. https://doi.org/10.3390/su11195342

Gilmore, C. P. (1972). More comfort for your heating dollar. *Popular Science*, *99*.

Gönen, M., Johnson, W. O., Lu, Y., & Westfall, P. H. (2005). The Bayesian Two-Sample t Test. *The American Statistician*, *59*(3), 252–257. https://doi.org/10.1198/000313005X55233

Graceson, A., Hare, M., Monaghan, J., & Hall, N. (2013). The water retention capabilities of growing media for green roofs. *Ecological Engineering*, *61*, 328–334. https://doi.org/10.1016/j.ecoleng.2013.09.030

Hamouz, V., Pons, V., Sivertsen, E., Raspati, G. S., Bertrand-Krajewski, J.-L., & Muthanna, T. M. (2020). Detention-based green roofs for stormwater management under extreme precipitation due to climate change. *Blue-Green Systems*, *2*(1), 250–266. https://doi.org/10.2166/bgs.2020.101

Hao, X., Ball, B. C., Culley, J. L. B., Carter, M. R., & Parkin, G. W. (2008). Soil density and porosity. *Soil Sampling and Methods of Analysis*, *2*, 179–196.

Hao, X., Xing, Q., Long, P., Lin, Y., Hu, J., & Tan, H. (2020). Influence of vertical greenery systems and green roofs on the indoor operative temperature of air-conditioned rooms. *Journal of Building Engineering*, *31*, 101373. https://doi.org/10.1016/j.jobe.2020.101373

He, Y., Yu, H., Dong, N., & Ye, H. (2016). Thermal and energy performance assessment of extensive green roof in summer: A case study of a lightweight building in Shanghai. *Energy and Buildings*, *127*, 762–773. https://doi.org/10.1016/j.enbuild.2016.06.016

He, Y., Yu, H., Ozaki, A., & Dong, N. (2020). Thermal and energy performance of green roof and cool roof: A comparison study in Shanghai area. *Journal of Cleaner Production*, *267*, 122205. https://doi.org/10.1016/j.jclepro.2020.122205

He, Y., Yu, H., Ozaki, A., Dong, N., & Zheng, S. (2017). Influence of plant and soil layer on energy balance and thermal performance of green roof system. *Energy*, *141*, 1285–1299. https://doi.org/10.1016/j.energy.2017.08.064

Holm, A., Krus, M., & Künzel, H. M. (1996). Feuchtetransport über Materialgrenzen im Mauerwerk/Moisture transport through interfaces in masonry. *Restoration of Buildings and Monuments*, *2*(5), 375–396.

Hu, F., Wu, S., & Sun, Y. (2019). Hollow-Structured Materials for Thermal Insulation. *Advanced Materials*, *31*(38), 1801001.

IES VE. (2018). *Thermal Conductivity, Specific Heat Capacity and Density*. https://help.iesve.com/ve2018/table_6_thermal_conductivity__specific_heat_capacity_and_density.htm

IRM. (2012). *Statistiques des précipitations extrêmes des communes belges Liège (ins 62063)—Google Search*. https://opendata.meteo.be/ftp/climate/extreme_precipitations/IDF_table_INS62063_fr.pdf

ISO 3301. (1975). *Statistical interpretation of data—Comparison of two means in the case of paired observations*. https://www.iso.org/cms/render/live/en/sites/isoorg/contents/data/standard/00/85/8540.html

ISO 9869-1. (2014). *Thermal insulation, Building elements, In-situ measurement of thermal resistance and thermal transmittance-Part 1: Heat flow meter method*. BSI: London, UK.

ISO 12572. (2001). *Hygrothermal performance of building materials and products—Determination of water vapour transmission properties*. https://www.iso.org/obp/ui/#iso:std:iso:12572:ed-1:v1:en

ISO 16586. (2003). *Soil quality—Determination of soil water content as a volume fraction on the basis of known dry bulk density—Gravimetric method*. ISO. https://www.iso.org/cms/render/live/en/sites/isoorg/contents/data/standard/03/23/32317.html

ISO 17892-11. (2019). *Geotechnical investigation and testing—Laboratory testing of soil—Part 11: Permeability tests*. ISO. https://www.iso.org/cms/render/live/en/sites/isoorg/contents/data/standard/07/20/72016.html

Jahandari, S., Mohammadi, M., Rahmani, A., Abolhasani, M., Miraki, H., Mohammadifar, L., Kazemi, M., Saberian, M., & Rashidi, M. (2021). Mechanical Properties of Recycled Aggregate Concretes Containing Silica Fume and Steel Fibres. *Materials*, *14*(22), Article 22. https://doi.org/10.3390/ma14227065

Jim, C. Y. (2014). Air-conditioning energy consumption due to green roofs with different building thermal insulation. *Applied Energy*, *128*, 49–59.

Jim, C. Y., & Peng, L. L. H. (2012). Weather effect on thermal and energy performance of an extensive tropical green roof. *Urban Forestry & Urban Greening*, *11*(1), 73–85. https://doi.org/10.1016/j.ufug.2011.10.001

Joshi, M. (2024). *City-scale Approaches to Assess the Role of a Realistic Roof Greening in Improving Urban Climate and Habitat* [PhD Thesis, University of Liège]. https://orbi.uliege.be/handle/2268/309088

Karczmarczyk, A., Baryła, A., & Kożuchowski, P. (2017). Design and Development of Low P-Emission Substrate for the Protection of Urban Water Bodies Collecting Green Roof Runoff. *Sustainability*, *9*(10), Article 10. https://doi.org/10.3390/su9101795

Kazemi, F., & Mohorko, R. (2017). Review on the roles and effects of growing media on plant performance in green roofs in world climates. *Urban Forestry & Urban Greening*, *23*, 13–26. https://doi.org/10.1016/j.ufug.2017.02.006

Kazemi, M., & Courard, L. (2021a). Modelling hygrothermal conditions of unsaturated substrate and drainage layers for the thermal resistance assessment of green roof: Effect of coarse recycled materials. *Energy and Buildings*, *250*, 111315. https://doi.org/10.1016/j.enbuild.2021.111315

Kazemi, M., & Courard, L. (2021b). Simulation of humidity and temperature distribution in green roof with pozzolana as drainage layer: Influence of outdoor seasonal weather conditions and internal ceiling temperature. *Science and Technology for the Built Environment*, *27*(4), 509–523. https://doi.org/10.1080/23744731.2021.1873658

Kazemi, M., & Courard, L. (2022). Modelling thermal and humidity transfers within green roof systems: Effect of rubber crumbs and volcanic gravel. *Advances in Building Energy Research*, *16*(3), 296–321. https://doi.org/10.1080/17512549.2020.1858961

Kazemi, M., Courard, L., & Attia, S. (2023). Water permeability, water retention capacity, and thermal resistance of green roof layers made with recycled and artificial aggregates. *Building and Environment*, *227*, 109776. https://doi.org/10.1016/j.buildenv.2022.109776

Kazemi, M., Courard, L., & Hubert, J. (2021). Heat transfer measurement within green roof with incinerated municipal solid waste aggregates. *Sustainability*, *13*(13), Article 13. https://doi.org/10.3390/su13137115

Kazemi, M., Courard, L., & Hubert, J. (2022). Coarse recycled materials for the drainage and substrate layers of green roof system in dry condition: Parametric study and thermal heat transfer. *Journal of Building Engineering*, *45*, 103487. https://doi.org/10.1016/j.jobe.2021.103487

Kazemi, M., Hajforoush, M., Talebi, P. K., Daneshfar, M., Shokrgozar, A., Jahandari, S., Saberian, M., & Li, J. (2020). In-situ strength estimation of polypropylene fibre reinforced recycled aggregate concrete using Schmidt rebound hammer and point load test. *Journal of Sustainable Cement-Based Materials*, 1–18.

Kazemi, M., Madandoust, R., & Brito, J. de. (2019). Compressive strength assessment of recycled aggregate concrete using Schmidt rebound hammer and core testing. *Construction and Building Materials*, *224*, 630–638. https://doi.org/10.1016/j.conbuildmat.2019.07.110

Kilmartin-Lynch, S., Roychand, R., Saberian, M., Li, J., & Zhang, G. (2022). Application of COVID-19 single-use shredded nitrile gloves in structural concrete: Case study from Australia. *Science of The Total Environment*, *812*, 151423. https://doi.org/10.1016/j.scitotenv.2021.151423

Kilmartin-Lynch, S., Saberian, M., Li, J., Roychand, R., & Zhang, G. (2021). Preliminary evaluation of the feasibility of using polypropylene fibres from COVID-19 single-use face masks to improve the mechanical properties of concrete. *Journal of Cleaner Production*, *296*, 126460. https://doi.org/10.1016/j.jclepro.2021.126460

Klein, P. M., & Coffman, R. (2015). Establishment and performance of an experimental green roof under extreme climatic conditions. *Science of The Total Environment*, *512–513*, 82–93. https://doi.org/10.1016/j.scitotenv.2015.01.020

Kordziel, S., Glass, S. V., Boardman, C. R., Munson, R. A., Zelinka, S. L., Pei, S., & Tabares-Velasco, P. C. (2020). Hygrothermal characterization and modeling of cross-laminated timber in the building envelope. *Building and Environment*, *177*, 106866. https://doi.org/10.1016/j.buildenv.2020.106866

Koushkbaghi, M., Alipour, P., Tahmouresi, B., Mohseni, E., Saradar, A., & Sarker, P. K. (2019). Influence of different monomer ratios and recycled concrete aggregate on mechanical properties and durability of geopolymer concretes. *Construction and Building Materials*, *205*, 519–528. https://doi.org/10.1016/j.conbuildmat.2019.01.174

Krus, M. (1996). *Moisture transport and storage coefficients of porous mineral building materials: Theoretical principles and new test methods*. Fraunhofer IRB Verlag Stuttgart.

Krus, M., & Künzel, H. M. (1995). *Flüssigtransport im Übersättigungsbereich*. Fraunhofer-Institut für Bauphysik.

Künzel, H. M. (1995). Simultaneous heat and moisture transport in building components. *One- and Two-Dimensional Calculation Using Simple Parameters. IRB-Verlag Stuttgart*, *65*.

La Roche, P., & Berardi, U. (2014). Comfort and energy savings with active green roofs. *Energy and Buildings*, *82*, 492–504. https://doi.org/10.1016/j.enbuild.2014.07.055

La Roche, P., Yeom, D. J., & Ponce, A. (2020). Passive cooling with a hybrid green roof for extreme climates. *Energy and Buildings*, *224*, 110243. https://doi.org/10.1016/j.enbuild.2020.110243

Ladani, H. J., Park, J.-R., Jang, Y.-S., & Shin, H.-S. (2019). Hydrological Performance Assessment for Green Roof with Various Substrate Depths and Compositions. *KSCE Journal of Civil Engineering*, *23*(4), 1860–1871. https://doi.org/10.1007/s12205-019-0270-4

Li, Y., & Zhu, Q. (2016). Simultaneous Heat and Moisture Transfer with Moisture Sorption, Condensation, and Capillary Liquid Diffusion in Porous Textiles. *Textile Research Journal*, *73*(6). https://journals.sagepub.com/doi/abs/10.1177/004051750307300609

Ling, H., Chen, C., Qin, H., Wei, S., Lin, J., Li, N., Zhang, M., Yu, N., & Li, Y. (2016). Indicators evaluating thermal inertia performance of envelops with phase change material. *Energy and Buildings*, *122*, 175–184. https://doi.org/10.1016/j.enbuild.2016.04.009

Liu, W., Engel, B. A., & Feng, Q. (2021). Modelling the hydrological responses of green roofs under different substrate designs and rainfall characteristics using a simple water balance model. *Journal of Hydrology*, *602*, 126786. https://doi.org/10.1016/j.jhydrol.2021.126786

Lu, J., Yuan, J., Yang, J., Chen, A., & Yang, Z. (2015). Effect of substrate depth on initial growth and drought tolerance of Sedum lineare in extensive green roof system. *Ecological Engineering*, *74*, 408–414. https://doi.org/10.1016/j.ecoleng.2014.11.018

Lundholm, J. T., Weddle, B. M., & MacIvor, J. S. (2014). Snow depth and vegetation type affect green roof thermal performance in winter. *Energy and Buildings*, *84*, 299–307. https://doi.org/10.1016/j.enbuild.2014.07.093

Ma'bdeh, S. N., Ali, H. H., & Rabab'ah, I. O. (2022). Sustainable assessment of using green roofs in hot-arid areas – Residential buildings in Jordan. *Journal of Building Engineering*, *45*, 103559. https://doi.org/10.1016/j.jobe.2021.103559

Madandoust, R., Kazemi, M., Talebi, P. K., & de Brito, J. (2019). Effect of the curing type on the mechanical properties of lightweight concrete with polypropylene and steel fibres. *Construction and Building Materials*, *223*, 1038–1052.

Mahar, W. A., Verbeeck, G., Reiter, S., & Attia, S. (2020). Sensitivity Analysis of Passive Design Strategies for Residential Buildings in Cold Semi-Arid Climates. *Sustainability*, *12*(3), Article 3. https://doi.org/10.3390/su12031091

Meddage, D. P. P., Chadee, A., Jayasinghe, M. T. R., & Rathnayake, U. (2022). Exploring the applicability of expanded polystyrene (EPS) based concrete panels as roof slab insulation in the tropics. *Case Studies in Construction Materials*, *17*, e01361. https://doi.org/10.1016/j.cscm.2022.e01361

Mehrabi, P., Shariati, M., Kabirifar, K., Jarrah, M., Rasekh, H., Trung, N. T., Shariati, A., & Jahandari, S. (2021). Effect of pumice powder and nano-clay on the strength and permeability of fiber-reinforced pervious concrete incorporating recycled concrete

aggregate. *Construction and Building Materials*, *287*, 122652. https://doi.org/10.1016/j.conbuildmat.2021.122652

Mickovski, S. B., Buss, K., McKenzie, B. M., & Sökmener, B. (2013). Laboratory study on the potential use of recycled inert construction waste material in the substrate mix for extensive green roofs. *Ecological Engineering*, *61*, 706–714.

Miller, C. (2003). Moisture management in green roofs. *Proc. Greening Rooftops for Sustainable Communities, 29–30 May, Chicago*, 1–6.

Miraki, H., Shariatmadari, N., Ghadir, P., Jahandari, S., Tao, Z., & Siddique, R. (2022). Clayey soil stabilization using alkali-activated volcanic ash and slag. *Journal of Rock Mechanics and Geotechnical Engineering*, *14*(2), 576–591. https://doi.org/10.1016/j.jrmge.2021.08.012

Mirrahimi, S., Mohamed, M. F., Haw, L. C., Ibrahim, N. L. N., Yusoff, W. F. M., & Aflaki, A. (2016). The effect of building envelope on the thermal comfort and energy saving for high-rise buildings in hot–humid climate. *Renewable and Sustainable Energy Reviews*, *53*, 1508–1519. https://doi.org/10.1016/j.rser.2015.09.055

Mohammadifar, L., Miraki, H., Rahmani, A., Jahandari, S., Mehdizadeh, B., Rasekh, H., Samadi, P., & Samali, B. (2022). Properties of Lime-Cement Concrete Containing Various Amounts of Waste Tire Powder under Different Ground Moisture Conditions. *Polymers*, *14*(3), Article 3. https://doi.org/10.3390/polym14030482

Molineux, C. J., Gange, A. C., Connop, S. P., & Newport, D. J. (2015). Using recycled aggregates in green roof substrates for plant diversity. *Ecological Engineering*, *82*, 596–604. https://doi.org/10.1016/j.ecoleng.2015.05.036

Nagase, A. (2020). Novel application and reused materials for extensive green roof substrates and drainage layers in Japan – Plant growth and moisture uptake implementation –. *Ecological Engineering*, *153*, 105898. https://doi.org/10.1016/j.ecoleng.2020.105898

Nagase, A., & Dunnett, N. (2012). Amount of water runoff from different vegetation types on extensive green roofs: Effects of plant species, diversity and plant structure. *Landscape and Urban Planning*, *104*(3), 356–363. https://doi.org/10.1016/j.landurbplan.2011.11.001

Navarro, L., de Garcia, A., Solé, C., Castell, A., & Cabeza, L. F. (2012). Thermal loads inside buildings with phase change materials: Experimental results. *Energy Procedia*, *30*, 342–349. https://doi.org/10.1016/j.egypro.2012.11.040

Nawaz, R., McDonald, A., & Postoyko, S. (2015). Hydrological performance of a full-scale extensive green roof located in a temperate climate. *Ecological Engineering*, *82*, 66–80. https://doi.org/10.1016/j.ecoleng.2014.11.061

Nematzadeh, M., & Baradaran-Nasiri, A. (2019). Mechanical performance of fiber-reinforced recycled refractory brick concrete exposed to elevated temperatures. *Computers and Concrete, An International Journal*, *24*(1), 19–35.

Nematzadeh, M., Baradaran-Nasiri, A., & Hosseini, M. (2019). Effect of pozzolans on mechanical behavior of recycled refractory brick concrete in fire. *Structural Engineering and Mechanics, An Int'l Journal*, *72*(3), 339–354.

Nematzadeh, M., Dashti, J., & Ganjavi, B. (2018). Optimizing compressive behavior of concrete containing fine recycled refractory brick aggregate together with calcium aluminate cement and polyvinyl alcohol fibers exposed to acidic environment.

Construction and Building Materials, *164*, 837–849. https://doi.org/10.1016/j.conbuildmat.2017.12.230

Nematzadeh, M., Nazari, A., & Tayebi, M. (2021). Post-fire impact behavior and durability of steel fiber-reinforced concrete containing blended cement–zeolite and recycled nylon granules as partial aggregate replacement. *Archives of Civil and Mechanical Engineering*, *22*(1), 5. https://doi.org/10.1007/s43452-021-00324-1

Nematzadeh, M., Shahmansouri, A. A., & Fakoor, M. (2020). Post-fire compressive strength of recycled PET aggregate concrete reinforced with steel fibers: Optimization and prediction via RSM and GEP. *Construction and Building Materials*, *252*, 119057. https://doi.org/10.1016/j.conbuildmat.2020.119057

Ngan, G. (2004). Green Roof Policies. *Landsc. Architecture Canada Foundation*.

Norouziasas, A., Pilehchi Ha, P., Ahmadi, M., & Rijal, H. B. (2022). Evaluation of urban form influence on pedestrians' wind comfort. *Building and Environment*, *224*, 109522. https://doi.org/10.1016/j.buildenv.2022.109522

Oberndorfer, E., Lundholm, J., Bass, B., Coffman, R. R., Doshi, H., Dunnett, N., Gaffin, S., Köhler, M., Liu, K. K., & Rowe, B. (2007). Green roofs as urban ecosystems: Ecological structures, functions, and services. *BioScience*, *57*(10), 823–833.

Ochs, F., Heidemann, W., & Müller-Steinhagen, H. (2008). Effective thermal conductivity of moistened insulation materials as a function of temperature. *International Journal of Heat and Mass Transfer*, *51*(3–4), 539–552.

Olszewski, M. W., & Young, C. A. (2011). Physical and Chemical Properties of Green Roof Media and Their Effect on Plant Establishment. *Journal of Environmental Horticulture*, *29*(2), 81–86. https://doi.org/10.24266/0738-2898-29.2.81

Ouldboukhitine, S.-E., & Belarbi, R. (2015). Experimental Characterization of Green Roof Components. *Energy Procedia*, *78*, 1183–1188. https://doi.org/10.1016/j.egypro.2015.11.099

Ouldboukhitine, S.-E., Belarbi, R., & Djedjig, R. (2012). Characterization of green roof components: Measurements of thermal and hydrological properties. *Building and Environment*, *56*, 78–85. https://doi.org/10.1016/j.buildenv.2012.02.024

Ouldboukhitine, S.-E., Belarbi, R., Jaffal, I., & Trabelsi, A. (2011). Assessment of green roof thermal behavior: A coupled heat and mass transfer model. *Building and Environment*, *46*(12), 2624–2631. https://doi.org/10.1016/j.buildenv.2011.06.021

Palla, A., Gnecco, I., & Lanza, L. G. (2012). Compared performance of a conceptual and a mechanistic hydrologic models of a green roof. *Hydrological Processes*, *26*(1), 73–84. https://doi.org/10.1002/hyp.8112

Papafotiou, M., Pergialioti, N., Tassoula, L., Massas, I., & Kargas, G. (2013). Growth of Native Aromatic Xerophytes in an Extensive Mediterranean Green Roof as Affected by Substrate Type and Depth and Irrigation Frequency. *HortScience*, *48*(10), 1327–1333. https://doi.org/10.21273/HORTSCI.48.10.1327

Parizotto, S., & Lamberts, R. (2011). Investigation of green roof thermal performance in temperate climate: A case study of an experimental building in Florianópolis city, Southern Brazil. *Energy and Buildings*, *43*(7), 1712–1722. https://doi.org/10.1016/j.enbuild.2011.03.014

Peng, C., & Wu, Z. (2008). In situ measuring and evaluating the thermal resistance of building construction. *Energy and Buildings*, *40*(11), 2076–2082. https://doi.org/10.1016/j.enbuild.2008.05.012

Pérez, G., Coma, J., Solé, C., Castell, A., & Cabeza, L. F. (2012). Green roofs as passive system for energy savings when using rubber crumbs as drainage layer. *Energy Procedia*, *30*, 452–460. https://doi.org/10.1016/j.egypro.2012.11.054

Pérez, G., Vila, A., Rincón, L., Solé, C., & Cabeza, L. F. (2012). Use of rubber crumbs as drainage layer in green roofs as potential energy improvement material. *Applied Energy*, *97*, 347–354. https://doi.org/10.1016/j.apenergy.2011.11.051

Pérez-Bella, J. M., Domínguez-Hernández, J., Cano-Suñén, E., del Coz-Díaz, J. J., & Álvarez Rabanal, F. P. (2015). A correction factor to approximate the design thermal conductivity of building materials. Application to Spanish façades. *Energy and Buildings*, *88*, 153–164. https://doi.org/10.1016/j.enbuild.2014.12.005

Peri, G., Licciardi, G. R., Matera, N., Mazzeo, D., Cirrincione, L., & Scaccianoce, G. (2022). Disposal of green roofs: A contribution to identifying an "Allowed by legislation" end–of–life scenario and facilitating their environmental analysis. *Building and Environment*, *226*, 109739. https://doi.org/10.1016/j.buildenv.2022.109739

Perini, K., & Rosasco, P. (2016). Is greening the building envelope economically sustainable? An analysis to evaluate the advantages of economy of scope of vertical greening systems and green roofs. *Urban Forestry & Urban Greening*, *20*, 328–337. https://doi.org/10.1016/j.ufug.2016.08.002

Pettersson, K., Maggiolo, D., Sasic, S., Johansson, P., & Sasic-Kalagasidis, A. (2020). On the impact of porous media microstructure on rainfall infiltration of thin homogeneous green roof growth substrates. *Journal of Hydrology*, *582*, 124286. https://doi.org/10.1016/j.jhydrol.2019.124286

Pianella, A., Clarke, R. E., Williams, N. S. G., Chen, Z., & Aye, L. (2016). Steady-state and transient thermal measurements of green roof substrates. *Energy and Buildings*, *131*, 123–131. https://doi.org/10.1016/j.enbuild.2016.09.024

Qin, M., Walton, G., Belarbi, R., & Allard, F. (2011). Simulation of whole building coupled hygrothermal-airflow transfer in different climates. *Energy Conversion and Management*, *52*(2), 1470–1478.

Rahif, R., Hamdy, M., Homaei, S., Zhang, C., Holzer, P., & Attia, S. (2022). Simulation-based framework to evaluate resistivity of cooling strategies in buildings against overheating impact of climate change. *Building and Environment*, *208*, 108599. https://doi.org/10.1016/j.buildenv.2021.108599

Rahif, R., Norouziasas, A., Elnagar, E., Doutreloup, S., Pourkiaei, S. M., Amaripadath, D., Romain, A.-C., Fettweis, X., & Attia, S. (2022). Impact of climate change on nearly zero-energy dwelling in temperate climate: Time-integrated discomfort, HVAC energy performance, and GHG emissions. *Building and Environment*, *223*, 109397. https://doi.org/10.1016/j.buildenv.2022.109397

Raji, B., Tenpierik, M. J., & van den Dobbelsteen, A. (2015). The impact of greening systems on building energy performance: A literature review. *Renewable and Sustainable Energy Reviews*, *45*, 610–623.

Rincón, L., Coma, J., Pérez, G., Castell, A., Boer, D., & Cabeza, L. F. (2014). Environmental performance of recycled rubber as drainage layer in extensive green roofs. A comparative Life Cycle Assessment. *Building and Environment*, *74*, 22–30. https://doi.org/10.1016/j.buildenv.2014.01.001

Rivière, L. (2023). *Concevoir des toitures vertes analogues aux pelouses sèches indigènes pour la biodiversité et l'hydrologie* [PhD Thesis, University of Liège]. https://orbi.uliege.be/handle/2268/309237

Rodler, A., Guernouti, S., & Musy, M. (2019). Bayesian inference method for in situ thermal conductivity and heat capacity identification: Comparison to ISO standard. *Construction and Building Materials*, *196*, 574–593.

Rohon, S. (2017). *Rénovation énergétique: Potentiel de végétalisation des toitures de la rive Est de Liège* [Masters Thesis, University of Liège]. https://matheo.uliege.be/handle/2268.2/2585

Rowe, D., Clayton, R., Van Woert, N., Monterusso, M., & Russell, D. (2003). Green roof slope, substrate depth and vegetation influence runoff. Greening Rooftops for Sustainable Communities. *Proceedings of the First North American Green Roofs Conference, Chicago, IL*.

Saadatian, O., Sopian, K., Salleh, E., Lim, C. H., Riffat, S., Saadatian, E., Toudeshki, A., & Sulaiman, M. Y. (2013). A review of energy aspects of green roofs. *Renewable and Sustainable Energy Reviews*, *23*, 155–168.

Sadineni, S. B., Madala, S., & Boehm, R. F. (2011). Passive building energy savings: A review of building envelope components. *Renewable and Sustainable Energy Reviews*, *15*(8), 3617–3631. https://doi.org/10.1016/j.rser.2011.07.014

Sailor, D. J., & Hagos, M. (2011). An updated and expanded set of thermal property data for green roof growing media. *Energy and Buildings*, *43*(9), 2298–2303. https://doi.org/10.1016/j.enbuild.2011.05.014

Sandoval, V., Bonilla, C. A., Gironás, J., Vera, S., Victorero, F., Bustamante, W., Rojas, V., Leiva, E., Pastén, P., & Suárez, F. (2017). Porous Media Characterization to Simulate Water and Heat Transport through Green Roof Substrates. *Vadose Zone Journal*, *16*(4), vzj2016.10.0101. https://doi.org/10.2136/vzj2016.10.0101

Schade, J., Lidelöw, S., & Lönnqvist, J. (2021). The thermal performance of a green roof on a highly insulated building in a sub-arctic climate. *Energy and Buildings*, *241*, 110961. https://doi.org/10.1016/j.enbuild.2021.110961

Schafaczek, B., & Zirkelbach, D. (2013). *Ermittlung von Materialeigenschaften und effektiven Übergangsparametern von Dachbegrünungen zur zuverlässigen Simulation der hygrothermischen Verhältnisse in und unter Gründächern bei beliebigen Nutzungen und unterschiedlichen Standorten:[Abschlussbericht]*. Fraunhofer-IRB-Verlag.

Scharf, B., & Zluwa, I. (2017). Case study investigation of the building physical properties of seven different green roof systems. *Energy and Buildings*, *151*, 564–573. https://doi.org/10.1016/j.enbuild.2017.06.050

Schirmer, R. (1938). *Die Diffusionszahl von Wasserdampf-Luft-Gemischen und die Verdampfungsgeschwindigkeit* [PhD Thesis]. VDI-Verlag.

Scolaro, T. P., & Ghisi, E. (2022). Life cycle assessment of green roofs: A literature review of layers materials and purposes. *Science of The Total Environment*, *829*, 154650. https://doi.org/10.1016/j.scitotenv.2022.154650

Shadmani, A., Tahmouresi, B., Saradar, A., & Mohseni, E. (2018). Durability and microstructure properties of SBR-modified concrete containing recycled asphalt pavement. *Construction and Building Materials*, *185*, 380–390. https://doi.org/10.1016/j.conbuildmat.2018.07.080

Shafique, M., Azam, A., Rafiq, M., Ateeq, M., & Luo, X. (2020). An overview of life cycle assessment of green roofs. *Journal of Cleaner Production*, *250*, 119471. https://doi.org/10.1016/j.jclepro.2019.119471

Shahmansouri, A. A., Akbarzadeh Bengar, H., & AzariJafari, H. (2021). Life cycle assessment of eco-friendly concrete mixtures incorporating natural zeolite in sulfate-aggressive environment. *Construction and Building Materials*, *268*, 121136. https://doi.org/10.1016/j.conbuildmat.2020.121136

Shahmansouri, A. A., Yazdani, M., Hosseini, M., Akbarzadeh Bengar, H., & Farrokh Ghatte, H. (2022). The prediction analysis of compressive strength and electrical resistivity of environmentally friendly concrete incorporating natural zeolite using artificial neural network. *Construction and Building Materials*, *317*, 125876. https://doi.org/10.1016/j.conbuildmat.2021.125876

Simões, N., Almeida, R., Tadeu, A., Brett, M., & Almeida, J. (2020). Comparison between cork-based and conventional green roof solutions. *Building and Environment*, *175*, 106812. https://doi.org/10.1016/j.buildenv.2020.106812

Sleiman, M., Ban-Weiss, G., Gilbert, H. E., François, D., Berdahl, P., Kirchstetter, T. W., Destaillats, H., & Levinson, R. (2011). Soiling of building envelope surfaces and its effect on solar reflectance—Part I: Analysis of roofing product databases. *Solar Energy Materials and Solar Cells*, *95*(12), 3385–3399. https://doi.org/10.1016/j.solmat.2011.08.002

Sleiman, M., Kirchstetter, T. W., Berdahl, P., Gilbert, H. E., Quelen, S., Marlot, L., Preble, C. V., Chen, S., Montalbano, A., Rosseler, O., Akbari, H., Levinson, R., & Destaillats, H. (2014). Soiling of building envelope surfaces and its effect on solar reflectance – Part II: Development of an accelerated aging method for roofing materials. *Solar Energy Materials and Solar Cells*, *122*, 271–281. https://doi.org/10.1016/j.solmat.2013.11.028

Soudani, L., Fabbri, A., Woloszyn, M., Grillet, A.-C., & Morel, J.-C. (2018). Hydric characterisation of rammed earth samples for different lime concentrations. *IOP Conference Series: Earth and Environmental Science*, *143*(1), 012010.

Soulis, K. X., Ntoulas, N., Nektarios, P. A., & Kargas, G. (2017). Runoff reduction from extensive green roofs having different substrate depth and plant cover. *Ecological Engineering*, *102*, 80–89. https://doi.org/10.1016/j.ecoleng.2017.01.031

Squier, M., & Davidson, C. I. (2016). Heat flux and seasonal thermal performance of an extensive green roof. *Building and Environment*, *107*, 235–244. https://doi.org/10.1016/j.buildenv.2016.07.025

Stella, P., & Personne, E. (2021). Effects of conventional, extensive and semi-intensive green roofs on building conductive heat fluxes and surface temperatures in winter in Paris.

Building and Environment, *205*, 108202. https://doi.org/10.1016/j.buildenv.2021.108202

Stovin, V., Poë, S., & Berretta, C. (2013). A modelling study of long term green roof retention performance. *Journal of Environmental Management*, *131*, 206–215. https://doi.org/10.1016/j.jenvman.2013.09.026

Stovin, V., Poë, S., De-Ville, S., & Berretta, C. (2015). The influence of substrate and vegetation configuration on green roof hydrological performance. *Ecological Engineering*, *85*, 159–172. https://doi.org/10.1016/j.ecoleng.2015.09.076

Strzałkowski, J., Sikora, P., Chung, S.-Y., & Abd Elrahman, M. (2021). Thermal performance of building envelopes with structural layers of the same density: Lightweight aggregate concrete versus foamed concrete. *Building and Environment*, *196*, 107799. https://doi.org/10.1016/j.buildenv.2021.107799

Suleiman, B. M., Larfeldt, J., Leckner, B., & Gustavsson, M. (1999). Thermal conductivity and diffusivity of wood. *Wood Science and Technology*, *33*(6), 465–473.

Sumner, D. M., & Jacobs, J. M. (2005). Utility of Penman–Monteith, Priestley–Taylor, reference evapotranspiration, and pan evaporation methods to estimate pasture evapotranspiration. *Journal of Hydrology*, *308*(1–4), 81–104.

Sun, T., Bou-Zeid, E., & Ni, G.-H. (2014). To irrigate or not to irrigate: Analysis of green roof performance via a vertically-resolved hygrothermal model. *Building and Environment*, *73*, 127–137. https://doi.org/10.1016/j.buildenv.2013.12.004

Sun, T., Bou-Zeid, E., Wang, Z.-H., Zerba, E., & Ni, G.-H. (2013). Hydrometeorological determinants of green roof performance via a vertically-resolved model for heat and water transport. *Building and Environment*, *60*, 211–224. https://doi.org/10.1016/j.buildenv.2012.10.018

Szota, C., Fletcher, T. D., Desbois, C., Rayner, J. P., Williams, N. S. G., & Farrell, C. (2017). Laboratory Tests of Substrate Physical Properties May Not Represent the Retention Capacity of Green Roof Substrates In Situ. *Water*, *9*(12), Article 12. https://doi.org/10.3390/w9120920

Tabares-Velasco, P. C., Zhao, M., Peterson, N., Srebric, J., & Berghage, R. (2012). Validation of predictive heat and mass transfer green roof model with extensive green roof field data. *Ecological Engineering*, *47*, 165–173. https://doi.org/10.1016/j.ecoleng.2012.06.012

Tams, L., Nehls, T., & Calheiros, C. S. C. (2022). Rethinking green roofs- natural and recycled materials improve their carbon footprint. *Building and Environment*, *219*, 109122. https://doi.org/10.1016/j.buildenv.2022.109122

Tariku, F., & Hagos, S. (2022). Performance of green roof installed on highly insulated roof deck and the plants' effect: An experimental study. *Building and Environment*, *221*, 109337. https://doi.org/10.1016/j.buildenv.2022.109337

Teemusk, A., & Mander, Ü. (2009). Greenroof potential to reduce temperature fluctuations of a roof membrane: A case study from Estonia. *Building and Environment*, *44*(3), 643–650.

Toghroli, A., Mehrabi, P., Shariati, M., Trung, N. T., Jahandari, S., & Rasekh, H. (2020). Evaluating the use of recycled concrete aggregate and pozzolanic additives in fiber-

reinforced pervious concrete with industrial and recycled fibers. *Construction and Building Materials*, *252*, 118997. https://doi.org/10.1016/j.conbuildmat.2020.118997

Togkalidou, T., Karoglou, M., Bakolas, A., Giakoumaki, A., & Moropoulou, A. (2013). Correlation of water vapor permeability with microstructure characteristics of building materials using robust chemometrics. *Transport in Porous Media*, *99*(2), 273–295.

Torres, M. I. M., & de Freitas, V. P. (2001). *Modelling of rising damp in historical buildings*. 381–390.

UEPG. (2021). *European Aggregates Association Annual Review 2020-2021*. Brussels.

Van Mechelen, C., Dutoit, T., & Hermy, M. (2015). Adapting green roof irrigation practices for a sustainable future: A review. *Sustainable Cities and Society*, *19*, 74–90. https://doi.org/10.1016/j.scs.2015.07.007

Van Renterghem, T., Hornikx, M., Forssen, J., & Botteldooren, D. (2013). The potential of building envelope greening to achieve quietness. *Building and Environment*, *61*, 34–44. https://doi.org/10.1016/j.buildenv.2012.12.001

Veas, L. (2006). *Development and application of a methodological model that allows evaluate and compare the behaviour of external walls exposed to moisture phenomenons* [PhD Thesis]. UCLouvain.

Vertal', M., Zozulák, M., Vašková, A., & Korjenic, A. (2018). Hygrothermal initial condition for simulation process of green building construction. *Energy and Buildings*, *167*, 166–176.

Vesuviano, G., & Stovin, V. (2013). A generic hydrological model for a green roof drainage layer. *Water Science and Technology*, *68*(4), 769–775.

Vijayaraghavan, K. (2016). Green roofs: A critical review on the role of components, benefits, limitations and trends. *Renewable and Sustainable Energy Reviews*, *57*, 740–752. https://doi.org/10.1016/j.rser.2015.12.119

Vila, A., Pérez, G., Solé, C., Fernández, A. I., & Cabeza, L. F. (2012). Use of rubber crumbs as drainage layer in experimental green roofs. *Building and Environment*, *48*, 101–106. https://doi.org/10.1016/j.buildenv.2011.08.010

Vilar, M. L., Tello, L., Hidalgo, A., & Bedoya, C. (2021). An energy balance model of heterogeneous extensive green roofs. *Energy and Buildings*, *250*, 111265. https://doi.org/10.1016/j.enbuild.2021.111265

Vo, D.-H., Yehualaw, M. D., Hwang, C.-L., Liao, M.-C., Tran Thi, K.-D., & Chao, Y.-F. (2021). Mechanical and durability properties of recycled aggregate concrete produced from recycled and natural aggregate blended based on the Densified Mixture Design Algorithm method. *Journal of Building Engineering*, *35*, 102067. https://doi.org/10.1016/j.jobe.2020.102067

Wanielista, M., Kelly, M., & Hardin, M. (2008). A Comparative analysis of greenroof designs including depth of media, drainage layer materials, and pollution control media. *Florida Department of Environmental Protection: Tallahassee, FL, USA.*

Wei, T., Jim, C. Y., Chen, A., & Li, X. (2021). A random effects model to optimize soil thickness for green-roof thermal benefits in winter. *Energy and Buildings*, *237*, 110827. https://doi.org/10.1016/j.enbuild.2021.110827

White, I., & Alarcon, A. (2009). Planning Policy, Sustainable Drainage and Surface Water Management: A Case Study of Greater Manchester. *Built Environment*, *35*(4), 516–530. https://doi.org/10.2148/benv.35.4.516

WHO. (2018). *WHO housing and health guidelines*.

Wilcox, S., & Marion, W. (2008). *Users manual for TMY3 data sets*.

Wong, G. K. L., & Jim, C. Y. (2014). Quantitative hydrologic performance of extensive green roof under humid-tropical rainfall regime. *Ecological Engineering*, *70*, 366–378. https://doi.org/10.1016/j.ecoleng.2014.06.025

Yang, J., & Wang, Z.-H. (2014). Physical parameterization and sensitivity of urban hydrological models: Application to green roof systems. *Building and Environment*, *75*, 250–263. https://doi.org/10.1016/j.buildenv.2014.02.006

Yang, M., Dong, W., Cheng, R., Wang, H., Zhao, Z., Wang, F., & Wang, Y. (2022). Effect of highly efficient substrate modifier, super-absorbent polymer, on the performance of the green roof. *Science of The Total Environment*, *806*, 150638. https://doi.org/10.1016/j.scitotenv.2021.150638

Yang, Y., Davidson, C. I., & Zhang, J. (2021). Evaluation Of Thermal Performance Of Green Roofs Via Field Measurements And Hygrothermal Simulations. *Energy and Buildings*, 110800. https://doi.org/10.1016/j.enbuild.2021.110800

Zhang, K., Garg, A., Mei, G., Jiang, M., Wang, H., Huang, S., & Gan, L. (2022). Thermal performance and energy consumption analysis of eight types of extensive green roofs in subtropical monsoon climate. *Building and Environment*, *216*, 108982. https://doi.org/10.1016/j.buildenv.2022.108982

Zhang, Y., Zhang, L., Ma, L., Meng, Q., & Ren, P. (2019). Cooling Benefits of an Extensive Green Roof and Sensitivity Analysis of Its Parameters in Subtropical Areas. *Energies*, *12*(22), Article 22. https://doi.org/10.3390/en12224278

Zhao, M., & Srebric, J. (2012). Assessment of green roof performance for sustainable buildings under winter weather conditions. *Journal of Central South University*, *19*(3), 639–644. https://doi.org/10.1007/s11771-012-1050-1

Zhao, Z., Courard, L., Groslambert, S., Jehin, T., Léonard, A., & Xiao, J. (2020). Use of recycled concrete aggregates from precast block for the production of new building blocks: An industrial scale study. *Resources, Conservation and Recycling*, *157*, 104786. https://doi.org/10.1016/j.resconrec.2020.104786

Zheng, X., Yang, Z., Yang, J., Tang, M., & Feng, C. (2022). An experimental study on the thermal and energy performance of self-sustaining green roofs under severe drought conditions in summer. *Energy and Buildings*, *261*, 111953. https://doi.org/10.1016/j.enbuild.2022.111953

Zhou, X., Zheng, F., Li, H., & Lu, C. (2010). An environment-friendly thermal insulation material from cotton stalk fibers. *Energy and Buildings*, *42*(7), 1070–1074. https://doi.org/10.1016/j.enbuild.2010.01.020

Zirkelbach, D. (2017). *Green roofs − hygrothermal simulation of moisture and energy performance*. 6.

Zirkelbach, D., Mehra, S.-R., Sedlbauer, K.-P., Künzel, H.-M., & Stöckl, B. (2017). A hygrothermal green roof model to simulate moisture and energy performance of building components. *Energy and Buildings*, *145*, 79–91.

Zölch, T., Henze, L., Keilholz, P., & Pauleit, S. (2017). Regulating urban surface runoff through nature-based solutions – An assessment at the micro-scale. *Environmental Research*, *157*, 135–144. https://doi.org/10.1016/j.envres.2017.05.023

Appendix 1: Green roof materials

Recycled Coarse Aggregate (RCA) produced by Tradecowall

GRANULATS RECYCLÉS BÉTON

LE PRODUIT

Soigneusement sélectionnés au versage, nos granulats recyclés béton sont issus du recyclage des matériaux de déconstruction de chantiers locaux. Ils sont produits par opérations de triage, concassage, criblage et recomposition.

Grave (0/D) ou sable (0/d) ou gravillon (d/D).

0/6,3 – 0/10 – 0/20 – 0/31,5 – 0/63 – 31,5/63.

AVANTAGES

> S'inscrit dans l'économie circulaire
> Economise nos gisements et ressources naturelles
> Excellent rapport qualité / prix
> Transformation d'un déchet en un produit de qualité
> Traitement et réutilisation en milieu urbain
> Moins de transport, gain de temps, moins de CO_2
> Traçabilité totale du produit fini grâce à la maîtrise des flux et à la sélection des matériaux entrants

SPÉCIFICATIONS TECHNIQUES

> Conformes à la législation environnementale (Contrôles toutes les 5000 tonnes par tests suivant l'annexe 2 de l'AGW du 28 février 2019 – Sortie de Statut de Déchet)
> Conformes au cahier des charges Qualiroutes (suivant nos fiches techniques)
> Conformes à la norme NBN EN 13242 et certifiés CE2+
> Le marquage CE2+ fait l'objet d'un audit annuel par un organisme indépendant

DOMAINES D'APPLICATION

> Chantiers publics et chantiers privés
> Voiries, trottoirs, giratoires, bâtiments...
> En couche de forme ou couche de propreté
> Sous-fondations, fondations, couches drainantes
> Composant centrale à béton
> Remblais d'assainissement, réseaux, tranchées
> Gabions à usage décoratif et paysager

CONSEILS DE MISE EN OEUVRE

> Choix de la granularité en fonction du cahier des charges ou du dimensionnement de l'ouvrage
> Eviter la ségrégation des graves après livraison sur chantier – réhomogénéiser
> Corriger si nécessaire le taux d'humidité qui doit être à l'Optimum Proctor pour garantir les meilleures performances du produit
> Compactage par couches de 30 cm maximum
> Eviter le passage de véhicules vibrants après compactage
> Eviter la mise en œuvre par temps de gel
> Procéder à des contrôles réguliers de la portance par essais à la plaque

La présente fiche produit ne vise qu'à l'information et ne saurait être interprétée comme un engagement contractuel.

Valorem
info@valorem-recyclage.be

Recynam
commercial@tradecowall.be

Recymex
info@recymex.be

Des filiales du groupe: Tradecowall
commercial@tradecowall.be
www.tradecowall.be

CE 4 - CE 2+ - QR - SSD

Incinirated Municipal Solid Waste Aggregate (IMSWA) produced by Thumaide waste proccessing centre

(1) Fiche technique (2012), Mémorandum technique pour l'utilisation des mâchefers de l'unité de valorisation par incinération de Thumaide, 1-36.

Caractéristiques géométriques des mâchefers d'incinérateur de Thumaide mesurées sur 54 échantillons depuis 2007.

Caractéristiques	Norme	Indice	Unité	Valeurs moyennes	Valeurs extrêmes (*min – max*)	Exigences QUALIROUTES	Commentaires
Granularité	NBN EN 933-1	**d/D**	---	**0/14**		**0/14**	0/20 selon ancien cahier des charges et manuel d'utilisation
Passant à 28 mm			%	100		100	
Passant à 20 mm			%	99,9 - 100	99,8 – 100		
Passant à 14 mm			%	96	88,0 – 99,0	75 – 99	
Passant à 10 mm			%	90,8	73,0 – 97,3		
Passant à 7,1 mm			%	72	52 - 86		
Passant à 2 mm (*sable grossier*)			%	41,2	26,6 – 52,8		
Passant à 63 µm (*particules fines*)		**f**	%	11,9	8,3 – 16,2	≤ 15	
Tolérance sur la granularité						**GT_{A20}**	
Grave 0/14							
Tamis à 14 mm				± 8		± 5	Légère diversion
Tamis à 7,1 mm				± 20		± 20	
Tamis à 0,063 mm				± 4,3		± 4	
Qualité des fines	NBN EN 933-9	***MB***	gr/kg MS	0,21		≤ 2,5	Peu représentatif

Caractéristiques physiques des mâchefers de l'incinérateur de Thumaide

Caractéristiques	Norme	Indice	Unité	Valeurs (2010)	Nombre échantillons	Critères QUALIROUTES	Commentaires
Résistance à la fragmentation Essai Los Angeles	EN 1097-2	L_A	%	28 – 31	4		Faible résistance à la fragmentation
Résistance à l'usure Essai micro-Deval en présence d'eau	EN 1097-1	M_{DE}	%	18 – 21	4		Résistance moyenne à l'usure
Masse volumique sèche en vrac	EN 1097-3		t/m^3	1,197 – 1,309	4	> 1,00	

Lightweight Expanded Clay Aggregate (LECA) produced by Intratium

Physical characteristics of LECA

Application	Fraction (mm)	Colour	Weight (kg/liter)
drainage layer	5-15	grey, white	0.4

Substrate with coarse recycled materials (SP) produced by ZinCO

Information produit
Substrat léger pour toiture verte Extensif

Art.-Nr. 6171 / 6172 / 6173

Substrat de matériel recyclé léger pour une végetalisation extensive.

Recycling for a better environment

Données techniques

Substrat léger pour toiture verte Extensif

Substrat sur base Zincolit® Plus (mélange de tuile et briques recyclées, matériel céramique et adjuvant sélectionnés) additionné à du matériel organique, Zincohum®.

Applicable comme substrat pour végétalisation extensive sur un système de toit vert et plusieurs couches. Selon les plantes désirées, on peut choisir entre des plantes en godet de ZinCo® multitops, des boutures ou semences ou des tapis de sedum pré cultivés.

Pour le bon développement des multi tops, boutures ou semences, il est important d'utiliser notre engrais durable spécialement développé ZinCo Plantzenfit® 4 M.

Le substrat est disponible en Big Bags de 1 m³, en vrac et en silo.

Le substrat léger pour toiture verte Extensif a un taux de tassement d'environ 20 %.

Livrable en:	Art.-Nr.
Big Bags de 1.0 m³	6171
En vrac (camion)	6172
Camion silo	6173

Caractéristiques

- Produit recyclé de haute qualité
- Haute capacité de rétention d'eau
- Haut volume d'air même à saturation d'eau
- Résistant à l'humidité et de structure stable
- Soufflage possible
- La qualité de matière première Zincolit® est sous contrôle constant de l' Université de Hohenheim

Caractéristiques chimiques et physiques

Paramètres	Valeurs
Poids du volume - sec - à saturation d'eau	 800 g/l (+/- 100 g/l) 1200 g/l (+/- 100 g/l)
Capacité d'eau maximale	env. 40 vol. %
Ecoulement de l' eau mod. K_f	0,6–70 mm/min
Valeur pH- (en $CaCl_2$)	6.5–8.0
Taux de sel (extrant d'eau)	< 2.5 g/l
Substances organiques	< 65 g/l
Tassement	env. 20 %

Appendix 2: Weather data

Weather data: solar radiation (a); air temperature (b); RH (c); Rainfall (d).

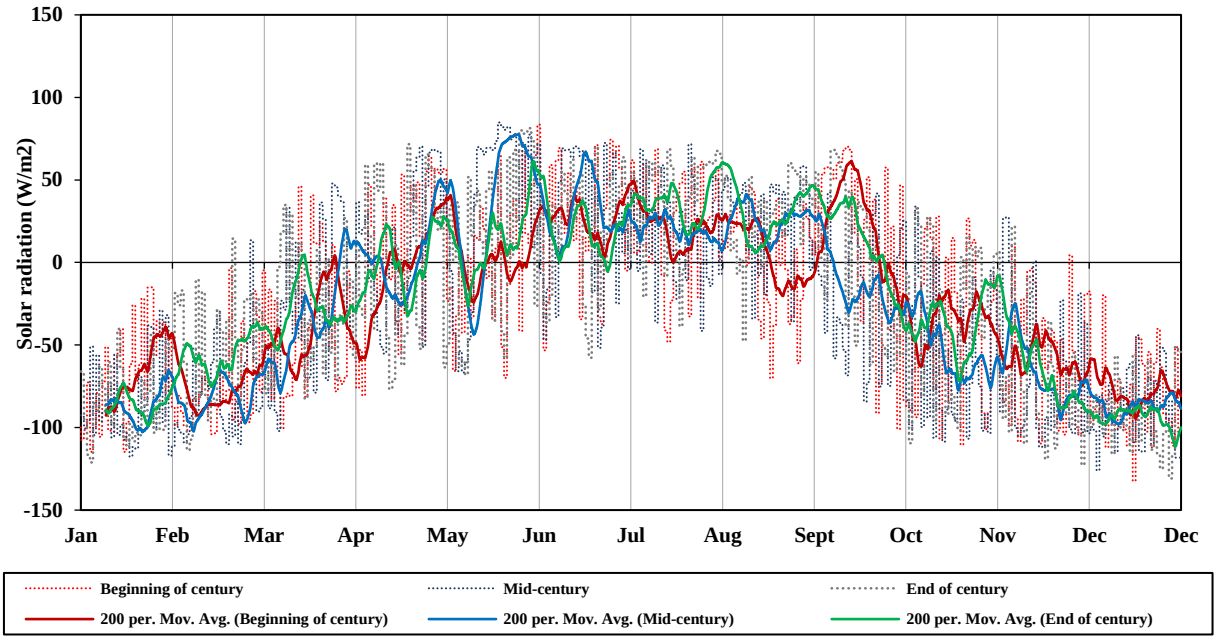

(a)

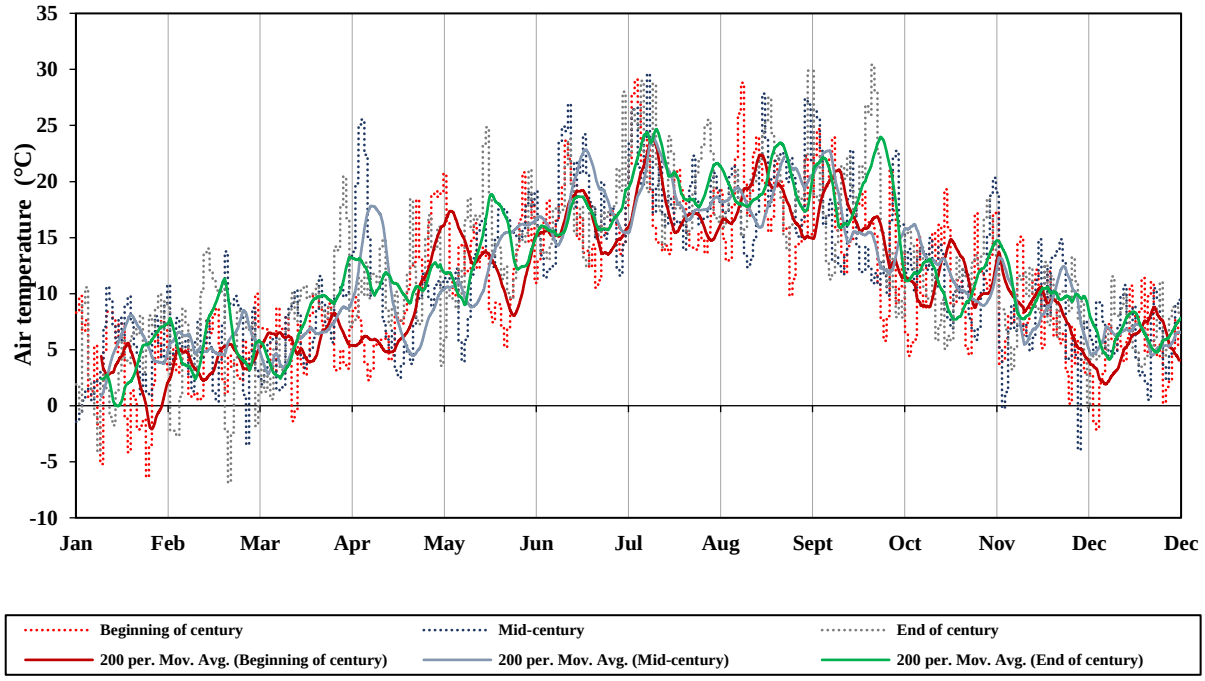

(b)

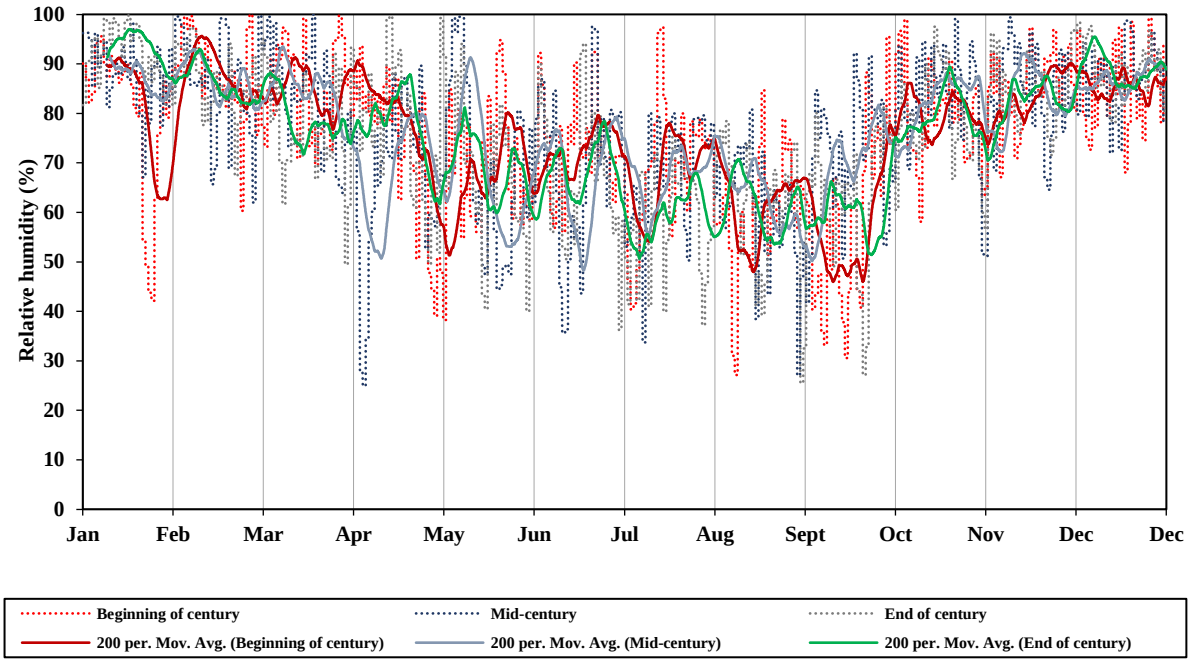
Relative humidity (%)
100
90
80
70
60
50
40
30
20
10
0
Jan
Feb
Mar
Apr
May
Jun
Jul
Aug
Sept
Oct
Nov
Dec
Dec
Beginning of century
Mid-century
End of century
200 per. Mov. Avg. (Beginning of century)
200 per. Mov. Avg. (Mid-century)
200 per. Mov. Avg. (End of century)

(c)

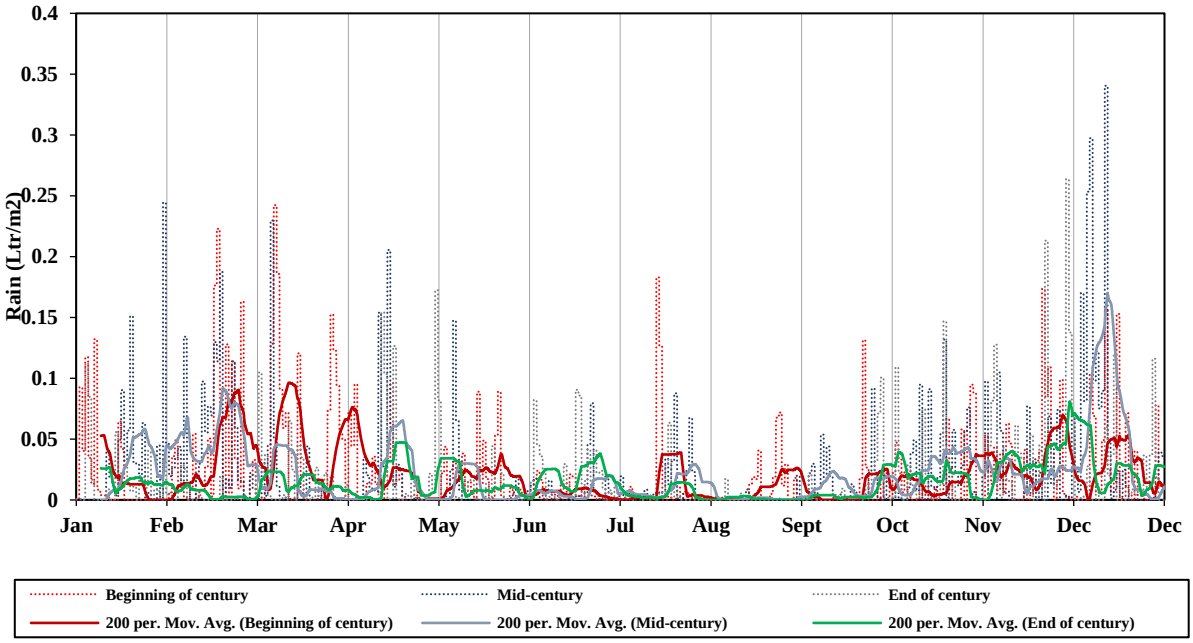
Rain (Ltr/m2)
0.4
0.35
0.3
0.25
0.2
0.15
0.1
0.05
0
Jan
Feb
Mar
Apr
May
Jun
Jul
Aug
Sept
Oct
Nov
Dec
Dec
Beginning of century
Mid-century
End of century
200 per. Mov. Avg. (Beginning of century)
200 per. Mov. Avg. (Mid-century)
200 per. Mov. Avg. (End of century)

(d)

ABSTRACT

The thesis presents alternative materials for substrate and drainage in green roof layers. Comparison between substrate with recycled coarse materials (SP) and substrate without recycled coarse materials (SC) has been studied. For the drainage layer, the results of Recycled Coarse Aggregate (RCA), Incinerated Municipal Solid Waste Aggregate (IMSWA) and Lightweight Expanded Clay Aggregate (LECA) were compared with those of Natural Coarse Aggregate (NCA). Three leading indicators as dependent variables are measured for green roof systems: Rc-value, water permeability and water retention capacity. Further experimental research on the rainfall detention performance as well as hygrothermal performance of green roof models including recycled coarse materials is presented. Further modeling research on the hygrothermal performance of green roof models under the temperate climate of Liège city is then presented, according to 3 weather scenarios: beginning, middle and end of the 21st century, corresponding to variable temperatures and rainfall. The heat flux sensitivity to the thickness and physical characteristics of green roofs with artificial and recycled materials is assessed. According to the results, using coarse recycled and artificial materials can allow targeting minimum requirements for the water permeability, water retention capacity and thermal resistance. Also, the heat resistance of green roof models produced with artificial and recycled materials increased for scenario 3 in comparison to scenarios 1 and 2 during the summer and the beginning of autumn due to a drop in the rainfall pattern till the end of the 21st century. The parameters change in the sensitivity analysis showed that the scatter of the thermal conductivity, layer thickness and density affect the dispersion of heat flux for the green roof layers.

RÉSUMÉ

La thèse présente des matériaux alternatifs pour les couches de substrat et de drainage dans les toitures vertes. La comparaison entre le substrat avec des matériaux grossiers recyclés (SP) et le substrat sans matériaux grossiers recyclés (SC) a été étudiée. Pour la couche de drainage, les résultats du granulat grossier recyclé (RCA), du granulat de déchets solides municipaux incinérés (IMSWA) et du granulat d'argile expansé léger (LECA) ont été comparés à ceux du granulat grossier naturel (NCA). Trois indicateurs principaux sont mesurés en tant que variables dépendantes pour les systèmes de toitures vertes: résistance thermique Rc, perméabilité à l'eau et capacité de rétention d'eau. D'autres recherches expérimentales sur les performances de rétention des précipitations et les performances hygrothermiques des modèles de toitures vertes comprenant des matériaux grossiers recyclés sont présentées. Une modélisation des performances hygrothermiques des modèles de toitures vertes dans le climat tempéré de la ville de Liège est ensuite présentée, selon 3 scénarios météorologiques : début, milieu et fin du 21ème siècle, correspondant à des températures et des précipitations variables. La sensibilité du flux de chaleur à l'épaisseur et aux caractéristiques physiques des toitures vertes avec des matériaux artificiels et recyclés est évaluée. D'après les résultats, l'utilisation de matériaux recyclés et artificiels grossiers permet de répondre aux exigences minimales en matière de perméabilité à l'eau, de capacité de rétention d'eau et de résistance thermique. En outre, la résistance thermique des modèles de toitures vertes produits avec des matériaux artificiels et recyclés a augmenté pour le scénario 3 par rapport aux scénarios 1 et 2 pendant l'été et le début de l'automne en raison d'une baisse du régime des précipitations jusqu'à la fin du 21e siècle. La modification des paramètres dans l'analyse de sensibilité a montré que la dispersion de la conductivité thermique, l'épaisseur de la couche et la densité affectent la dispersion du flux de chaleur pour les couches des toitures vertes.